INFOMAR Report December 2012

Dublin City University

Carbon Cycling in Dunmanus Bay pockmarks

Contributors: Shane O' Reilly, Brian Kelleher (DCU)[1]
Michal Szpak (DCU)[1] and Xavier Monteys (GSI)[2]

1. *School of Chemical Sciences, Dublin City University, Glasnevin, Dublin 9*
2. *Geological Survey of Ireland, Beggars Bush, Haddington Road, Dublin 4*

** Correspondence to brian.kelleher@dcu.ie*

Marine Institute
Foras na Mara

GSI
Geological Survey of Ireland
Suirbhéireacht Gheolaíochta Éireann
www.gsi.ie

INFOMAR
Integrated Mapping for the Sustainable Development of Ireland's Marine Resource

DCU

Preface

Overall the project has been going very well and we have exceeded our targets. This report begins with a preliminary background geophysical and geochemical report on the Dunmanus pockmarks that will form the basis for the first publication from this work. Chapter two includes geochemical and geomicrobial work that we have carried out in the Irish Sea. This is similar to research currently being written up for publication for the Dunmanus Bay pockmarks. This paper will report on an unprecedented chemical and microbiological characterisation of the Dunmanus pockmarks. The data will include:

- A thorough geochemical analysis including gas and nutrient dynaimcs,
- Biomarker analysis down the cores that include paleoenvironmental data,
- Isotope ratio analysis including both compound specific and bulk carbon,
- Nuclear Magnetic Resonance (NMR) on organic matter extracts and porewater,
- Quantitative PCR analysis down the cores,
- In the process of acquiring pyrosequencing data down cores and
- Hydrocarbon degradation studies that look at the genes responsible for hydrocarbon decomposition.

Also attached are two papers that have recently been submitted to "Marine Chemistry" (*Sources and transportation of organic matter on the Malin Shelf, NW of Ireland*) and "FEMS Ecology" (*Microbial diversity at a low-activity pockmark on the Malin Shelf, N.W. Ireland*) and one paper in preparation for "Limnology and Oceanography" (*Sources and distribution of organic matter in surface marine sediments in the western Irish Sea*). This work was supported by the INFOMAR 2012 research funding.

Chapter 1
Geophysical and benthos survey of a small pockmark field in Dunmanus Bay, Ireland.

Introduction

Fluid flow in the marine subsurface is a known but rather poorly understood and difficult to observe phenomenon (Hovland and Judd, 1988). Pockmarks, usually sub-circular, shallow depressions, which are believed to be geo-morphological indications of fluid seepage (namely CH_4, H_2S, hydrocarbons, groundwater) through the seabed (King and MacLean, 1970), are often used to identify sites where fluid flow is intensified (Link, 1952; Hedberg, 1980). Contribution of these marine seepages to the food web (Straugham, 1982; Danto, 2001), nutrient cycles and carbon cycle in particular (Lambert and Schmidt, 1993; Judd, 2003; Judd 2004) remains elusive.

Dunmanus Bay is located in the west of Ireland in the County Cork, south of the larger and better known Bantry Bay. The bay is 7 km wide from Sheep's Head to Three Castle Head and 25 km long from its mouth to Four Mile Water head. It is a fjord-like setting with only one small river, Durrus, and several streams draining into the bay. Water depth in bay does not exceed 20 m and reaches over 70 m at its mouth (Figure 1). The area experiences strong influences from coastal upwelling but tidal activity is low as Dunmanus Bay is out of the main tidal flow.

Favourable thermal fronts and adequate nutrient concentrations support high levels of phytoplankton production in these waters and seasonal blooms are common (Raine et al. 1990). Notably, blooms of *Gyrodinium aureolum* (dinoflagellate responsible for the so called '*red tides*') are frequent in these waters affecting the aquaculture of the region (Jenkinson and Connors, 1980; Roden et al. 1980, 1981). Benthic fauna of the Dunmanus Bay remains largely unstudied however in waters close to shore and rocky outcrops frequent sightings of sea lettuce (*U. lactuca*), snails (*N. lapillus*), barnacles (*B. balanoides*, *C. montagui*), mussles (*Mytilus* spp.) and limpets (*P. vulgate*, *P. aspera*) have been reported (Cross and Southgate, 1983).

The bedrock geology of Dunmanus Bay was not studied *per se* but inferred from the geology of bordering landmasses in the 1850s by Jukes, 1864 and Jukes et al. 1861 and more recently by Naylor, 1975, Naylor and Sevastopulo, 1993 and MacCarthy, 2007. Both Bantry and Dunmanus Bays lie in the South Munster Basin separated by the Sheeps Head anticline. The major, sedimentation controlling fault in this area is the Dunmanus Fault (DF) crossing the entire bay parallel to the landmass (Figure 1). Two major branchings of this fault occur in the vicinity of the pockmark field area: the Gortavallig Fault (GVF) and the Letter Fault (LF). Moreover there are several minor faults in the northern part of the Dunmanus syncline separate from the DF, notably the Rossmore Fault (RF) and the Glanlough Fault (GF). Faults are often associated with fluid migration provided that source rocks are present and thermal conditions favour hydrocarbon generation (e.g. Kutas et al. 2004). Early Carboniferous formations abundant in the area contain in places organic-rich shales, so called '*marine bands*' and "*Alluvium, Peat-bog*" is present in the Dunmanus and Bantry area (Jukes, 1864 and Hunt, 1859). The surface sediments in Dunmanus Bay are predominantly muddy sands with a small gravel component.

Surveying efforts of INFOMAR (Integrated Mapping For Sustainable Development of Ireland's Marine Resources) and its predecessor INSS (Irish National Seabed Survey) in the past 10 years have revealed pockmarks and other seepage related structures in numerous locations in Irish waters, i.e. on the Malin Shelf (Monteys et al., 2008; Monteys et al., 2009) and in the Irish Sea (Croker and Garica Gil, 2002; Croker et al., 2005). The most recent bathymetric survey of Dunmanus Bany, SW Ireland revealed another, previously unknown small pockmark field (Monteys et al., 2010). In this paper we report findings of this survey, assess the activity and nature of pockmarks and investigate their influence on benthic communities.

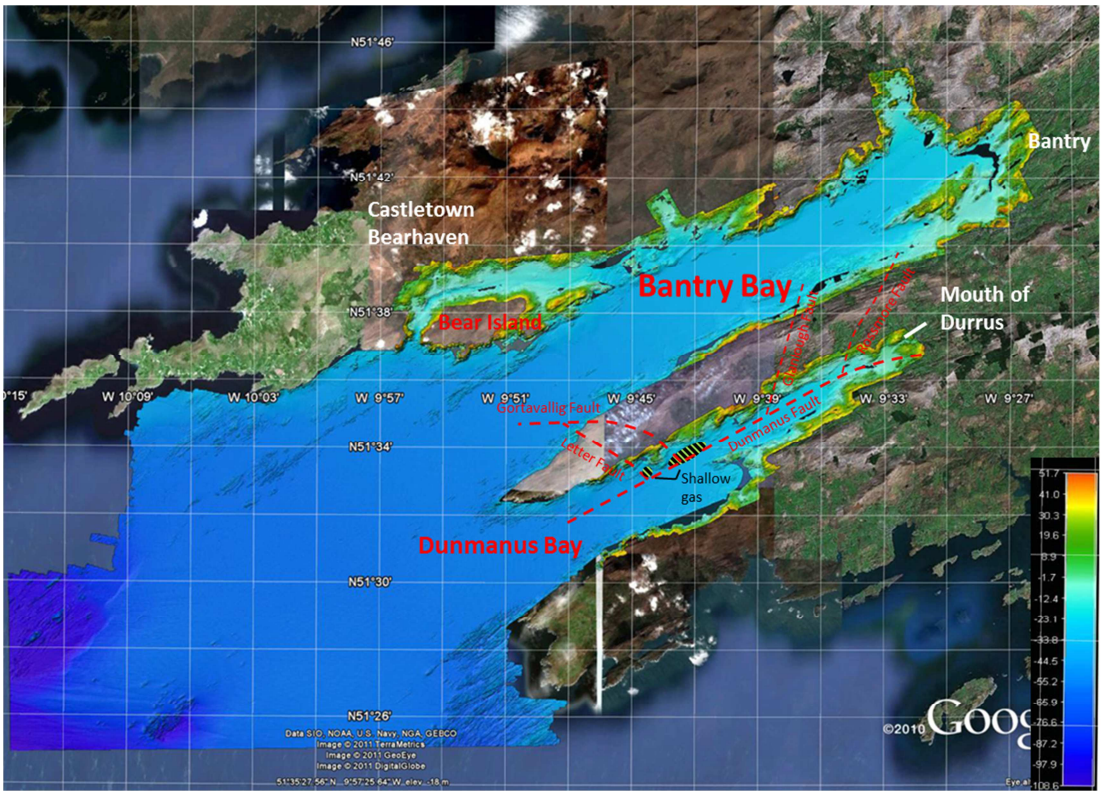

Figure 1 Area of study.

Materials and methods

Bathymetry

Pockmarks in Dunmanus Bay were identified in 2007 during a multibeam survey carried out by the RV Celtic Voyager as a part of the INFOMAR program. Bathymetric data of Dunmanus Bay was acquired in 2006 during a Tenix Lidar survey (shallow water) and on board the RV Celtic Explorer (mouth and outer part of the bay). Although data acquired during these surveys permitted identification of the pockmark field, low resolution of the data limited insight into the morphology of these features. In April 2009 the RV Celtic Voyager acquired very high resolution data that permitted further insight into morphology and distribution of the Dunmanus

Bay pockmarks (Szpak et al. 2009 and Monteys et al., 2010) Data were acquired onboard the R.V. Celtic Explorer and R.V. Celtic Voyager using a Kongsberg-Simrad EM1002 multibeam echosounder, with an operational frequency of 93-98 kHz and pulse length of 0.7 ms and low survey speed (2-3 knots). Resulting bathymetric terrain models were gridded at 5x5 m. High resolution bathymetry was crucial in identifying these relatively small seabed features.

Sub-bottom profiler

Sub-bottom profile data were acquired using a heave-corrected SES Probe 5000 3.5 kHz transceiver in conjunction with a hull-mounted 4°x4° transducer array. Acquisition parameters, data logging and interpretation were carried out using the CODA Geokit suite. Both Raw Navigation string and Heave Compensation string are fed into the Coda DA200 system (from the Seapath 200). An average estimated acoustic velocity of 1650 m/s was used to calculate the thickness of the sedimentary units. Acoustic penetration in some areas was in the order of 60 m below seabed with approximately 0.4 m vertical resolution (I think this needs adjustment).

Water column sampling

Water column samples were collected (Fig. 1) with Niskin bottles mounted on a SBE 32 Carousel Water sampler (Sea-Bird Electronics Inc., USA). During descent the Conductivity, Temperature and Depth (CTD) profiles were recorded to identify oceanographic background conditions and allow sampling water column in a more informative manner. Upon retrieval samples were transferred immediately to 125 ml serum bottles and crimp sealed with gas-tight thick butyl rubber septum. All water samples were poisoned with saturated mercuric chloride ($HgCl_2$) solution to inhibit microbial activity and stored at 2-4^{o}C until analysis. Samples were analyzed according to modified head-space method with salting out as described by Gal'chenko et al., 2004. Briefly samples were boiled in water bath for 1 h on the day of analysis to ensure full desorption of methane. Due to the breakdown of portable gas chromatograph (Model 312, PID Analyzers) the methane content from head-space was determined on shore after the cruise on Carlo Erba gas chromatograph equipped HP-PLOT Q capillary column (30 m × 0.32 mm i.d., 20 µm film thickness) and flame ionization detector (GC-FID). The detector temperature was set to 225^{o}C and He was used as carrier gas. Samples were quantified based on the methane gas standard response as described in Gal'chenko et al., 2004. Method robustness was tested with methane standards across range of concentrations and yielded with precision of ± 0.5 nM, n=4 for concentrations <25 nM.

METS sensor

The METS sensor (Franatech GmbH, Germany) was mounted on the Sea-Bird 911 CTD (Sea-Bird Electronics Inc., USA) unit. The CTD's water pump feeding tubes were modified to ensure that both sensors analyze the same representative water sample. Sensor was calibrated by the manufacturer for methane concentrations ranging from 2 to 200 nmol/l in temperature range from 2 to 20^{o}C. The METS type sensors have relatively slow response time, therefore an equilibration test was performed to assess minimal time necessary to reach baseline signal after saturation. Lag time varied between 200 and 300 s depending on saturation conditions (350 and

700 nmol/l respectively).Sensor was deployed with the CTD and held 5 m above the seabed until signal stabilized. Between deployments sensor was kept powered on and immersed in running surface water to minimize humidity and temperature variability.

Sediment sampling

Sediment samples were collected with use of box and gravity corers. Upon retrieval samples were transferred to Argon purged glove box and redox potential (E_h) measurement was taken with the use of temperature compensated push-in Pt electrode with Ag/AgCl reference junction (SCHOTT). Electrode was routinely checked for sulfide poisoning and tested for reproducibility between measurement series with saturated quinhydrone pH buffer solutions (pH = 4.0 and 7.0, with expected ΔE_h = 172±4 mV). Sediment cores (10 cm^3) for interstitial gas analysis were collected with cut-off syringes and transferred to head-space vials and processed similarly to water samples. Pore water sulphate and chloride concentrations were determined on shore by ion chromatography according to standard methodology.

Benthos survey

Day Grab sampler (0.1 m^2) was used to collect benthos samples. Five replicate samples were taken per site (Fig. 1) A Perspex core was taken from each sample for on shore meiofaunal assemblage analysis, remaining sample was sieved on a 1 mm mesh sieve and retained macrofaunal assemblage was preserved in 10% buffered formalin solution. All meiofaunal and macrofaunal assemblages were sorted under a microscope into four main groups: Polychaeta, Mollusca, Crustacea and Others which consisted of echinoderms, nematodes, nemerteans, cnidarians and other lesser phyla. The taxa were identified to a species level where possible. Additionally granulometric analysis was performed on dried sediment from each benthos station. Approximately 100 g of sediment was sieved through series of Wenthworth graded sieves (McMahon et al., 1996). Chlorophyll *a* concentrations were derived from fluorescence measurements recorded during all CTD casts. Fluorescence sensor was calibrated for Chlorophyll *a* concentrations ranging from 0.04 to 200 µg/l.

Univariate and multivariate statistical analyses were carried out on the combined replicate station-by-station faunal data. The following diversity indices were calculated: Margalef's species richness index (D), (Margalef, 1958), Pielou's Evenness index (J), (Pielou, 1977) and Shannon-Wiener diversity index (H'), (Pielou, 1977). The PRIMER ® programme (Clarke and Warwick, 2001) was used to carry out multivariate analyses. All species/abundance data were fourth root transformed and used to prepare a Bray-Curtis similarity matrix in PRIMER ®. The fourth root transformation was used in order to down-weigh the importance of the highly abundant species and to allow the mid-range and rarer species to play a part in the similarity calculation. The Bray-Curtis similarity matrix was subjected to a non-metric multi-dimensional scaling (MDS) algorithm and cluster analysis (Kruskal and Wish, 1978).

Sediment profile images were taken in five replicates at the same locations as benthic samples with Sediment Profile Imagery camera (SPI; AQUAFACT International Services Ltd., Ireland). SPI cameras permit *in situ* images of the undisturbed sediment water interface to be obtained which is impossible to obtain *ex situ* mainly due to sediment disruption and compaction during sampling with use of conventional apparatus (Somerfieled and Clarke, 1997). SPI cameras mounted on a

frame are slowly lowered on to the seabed to minimize sediment disruption and then hydraulic or gravity based system is triggered from the vessel to insert the prism into the seabed.

Results and discussion

Hydrology and seabed bulk parameters. (this paragraph will be restructured or incorporated into paragraphs below)

Thermo and haloclines were well defined on an average depth of 11 m (data not shown) The average surface water temperature was 10.6 ^{o}C and 10.2 ^{o}C below the thermocline and 9.6 ^{o}C at near bottom. Dunmanus Bay with only few streams is more marine than estuarine environment with little freshwater influence. The salinity reaches average open ocean values and generally follows the thermocline fronts with surface water reaching salinity of 34.92 psu increasing to 35.05 psu below the pycnocline and 35.08 psu in near bottom waters. Effects of weak coastal upwelling could be observed in the water column but generally tidal activity is low as Dunmanus Bay is out of the main tidal flow (Cross and Southgate, 1983). Uniform water column structure was expected as the survey area is only approximately 2 km long but also because significant variability in the water column characteristics can also affect benthos community structure (Clarke and Green, 1988).

Chlorophyll *a* (Chl *a*) concentrations were similar in all stations and varied between 3.33 - 2.33 µg/l. Chl *a* maximum was present on average depth of 17 m. The concentration of phytoplankton started to increase just after the pycnocline, with the lower boundary located around 30 m. A slight decline in concentrations (R^2=0.41, n=9) can be observed across the transect. These values are consistent with previously reported for sister Bantry Bay (Gribble et al., 2007) as there is no plankton data published on Dunmanus Bay.

Sediment in all stations was similar across all size classes a comprised mainly of sands with small percentage of gravel and with significant but not dominant silt/clay component (Table 1). Percentage of gravel varied from 6 to 19.2% and more gravel was found in the stations located in the vicinity of rock outcroppings suggesting erosional origin rather than typical dropstones. Sands were almost evenly distributed across their size classes (mean 11.3%, n=10) with the finer facies being slightly more abundant (11-31%). Silt and clay comprised of approximately a third (mean 32.8%, n=10) of the total volume of the sediment. With the sedimentary matrix being relatively uniform across all stations grain size changes should have negligible effect on the benthos community structure (Clarke and Green, 1988).

	Grain size (µm)									
Site	>2000	>1000	>500	>250	>125	>63	<63	Gravel	Sand	Silt/Clay
17	14.9	13	10.4	8.9	8.9	11.2	32.7	14.9	52.4	32.7
18	7.4	9.9	9.7	8.1	9.2	17.1	38.6	7.4	54	38.6
41	19.2	10.2	10.2	9.4	9	15.6	26.4	19.2	54.4	26.4
19	6.3	12.3	14.1	11.7	10.8	12.5	32.3	6.3	61.4	32.3
20	12.3	9.8	8.7	7.9	6.9	15.7	36	12.3	49	36
21	15.1	10.9	9.1	7.6	9.3	14	33.8	15.1	50.9	33.8
22	6	12.1	12.4	11	10.8	13.6	34.1	6	59.9	34.1

39	5.3	6.9	39	5.1	6.9	12.1	24.7	5.3	70	24.7
16	2.2	5.5	5.8	4.7	14.3	31.1	36.4	2.2	61.4	36.4
40	15.4	12.8	9.7	8.4	9.3	11.6	32.8	15.4	51.8	32.8

Table 2

Pockmark distribution and morphology

Dunmanus Bay pockmark field contains 125 sub-circular pockmarks. Majority of these pockmarks range from 0.2 to 0.7m in depth and have average diameter between 8 and 10m (Table 2). There is also a group of very small (1-3m) and very shallow (<0.2m) satellite pockmarks scattered across the field. Majority of pockmarks occur in parallel clusters and only few individual units are observed outside of these pockmark groups. Larger units are often merged forming composite pockmarks however their individual sub-circular units are usually distinguishable. The field shows clear NE-SW orientation limited by two rock outcrops.

Pockmark group	No of units	Estimated total area [km^2]	Estimated pockmark density [units/km^2]	Dimensions [m]			Depth [m]	
				Max	Min	Average	Max	Min
I	14			15	5	9	0.2	0.6
II	14			17	5	10	0.2	0.6
III	20			11	6	8	0.2	0.7
IV	22			10	4	7	0.3	0.6
V	7			13	5	8	0.2	0.6
Ungrouped	19			11	5	9	0.2	0.6
Satellite	25						<0.2	0.6

Pockmark formation

Pockmarks are seabed features associated with fluid expulsion through the seabed. The fluid involved in the formation of most marine pockmarks, discovered in areas not adjacent to landmass and therefore devoid of a potential aquifer influence, is hydrocarbon gas (Judd and Hovland, 2007). Nevertheless exceptions to this generalisation have been reported. In areas of the Florida Escarpment which is a part of the Florida Platform freshwater seeps occurs at depths exceeding 3000 m (Paull et al. 1984). Another example is Black Ridge located ca. 200 km offshore at 600 m depth (Judd and Hovland, 2007). However in general estuarine, lacustrine and coastal settings groundwater escape is a viable mechanism of pockmark formation. Pockmarks formed by this mechanisms have been widely reported (e.g. Christodoulou et al. 2003; Judd and Hovland, 2007). Since Dunmanus Bay pockmarks are located

just 650 m away from the landmass freshwater expulsion is a potential and probable formation mechanism of these features.

There was no evidence of salinity changes similar to that reported by Christodoulou et al. 2003 and others that would imply active flow of freshwater into the water column. The salinity in the last 10 m of the water column shows a gentle increasing trend in all stations to reach an average value of 35.07 psu (We can produce a Figure here if needed). Unfortunately the CTD carousel due to weather conditions had to be kept approximately 5 m above the seabed to compensate for the swell induced rocking of the vessel and protect the instrument from contacting the seabed. Interestingly the salinity decrease reported by Christodoulou et al. 2003 was observed in the 3 m water layer above the seabed and the water column above was not affected. It is therefore possible that moderate freshwater flow was not recorded in the above mentioned experimental conditions. Detailed video surveying of these pockmarks with a fly-by camera during a recent research cruise (2011 CE11_017) did not reveal any visible freshwater flow. This finding however does not necessarily eliminate the possibility of freshwater expulsion which might occur periodically. The western coast of Ireland is known for high precipitation and the Dunmanus Bay area is one of the two locations in the entire country (the other being west of Connaught) where annual mean rainfall exceeds 2800 mm/year (Met Eireann, 1961-1990 annual mean, www.met.ie/climate/rainfall.asp). Moreover there is little vegetation that could assimilate at least a portion of the rainfall, and permeable rocks such as limestone and sandstone are the dominant rock type in the area (Naylor, 1975). According to Burnett et al. 2003 these are the main factors along with groundwater abstraction and topography that control the likelihood of a groundwater discharge in a coastal setting. Given the above it could be expected that periodically, particularly after heavy rainfall, the amount of freshwater in unconfined aquifers will increase. This can result in a pressure gradient that can potentially result in pore fluid displacement and/or freshwater expulsion (Judd and Hovland, 2007). This hypothesis is however not supported by the pore fluid data from the collected sediment core, although profiles show some interesting features (Figure 2). Concentration of chloride in the entire core shows typical seawater values with no evidence for pore water freshening which would be expected if ground water was migrating through the seabed. Similarly, reduction of sulphate is observed without any evidence of freshwater dilution. The sulphate profiles show an initial decrease and then at around 1.5 mbsf the trend is reversed possibly by re-oxidation of sulphite. A sharp decrease would be expected in the case of intrusion and for a diffusive/advective scenario a linear or concave profile would be expected (Schulz and Zabel, 2005). Therefore we find no evidence of pore water freshening of both water column and the sediment and we conclude that freshwater expulsion is not a likely mechanism for the formation of Dunmanus Bay pockmarks.

Since freshwater is rather unlikely the fluid involved in the formation of these features alternatively hydrocarbon gas can be responsible. The sub bottom data contain multiple signals that are commonly interpreted as associated with shallow gas and gas venting into the water column (Figure 3). Numerous and extensive areas of acoustic turbidity (AT) as well as hyperbolic reflectors (HR) in the water column in the vicinity of the AT are visible (middle panel). AT is a strong indicator of shallow gas accumulation, similarly as observed in the Malin Shelf (Szpak et al, 2011). The AT appears to be extended over a relatively wide area and yet also confined to a particular sedimentary facies as there is clearly less turbidity above and below the main feature. Moreover acoustic blanking (AB) typically observed below the gas front

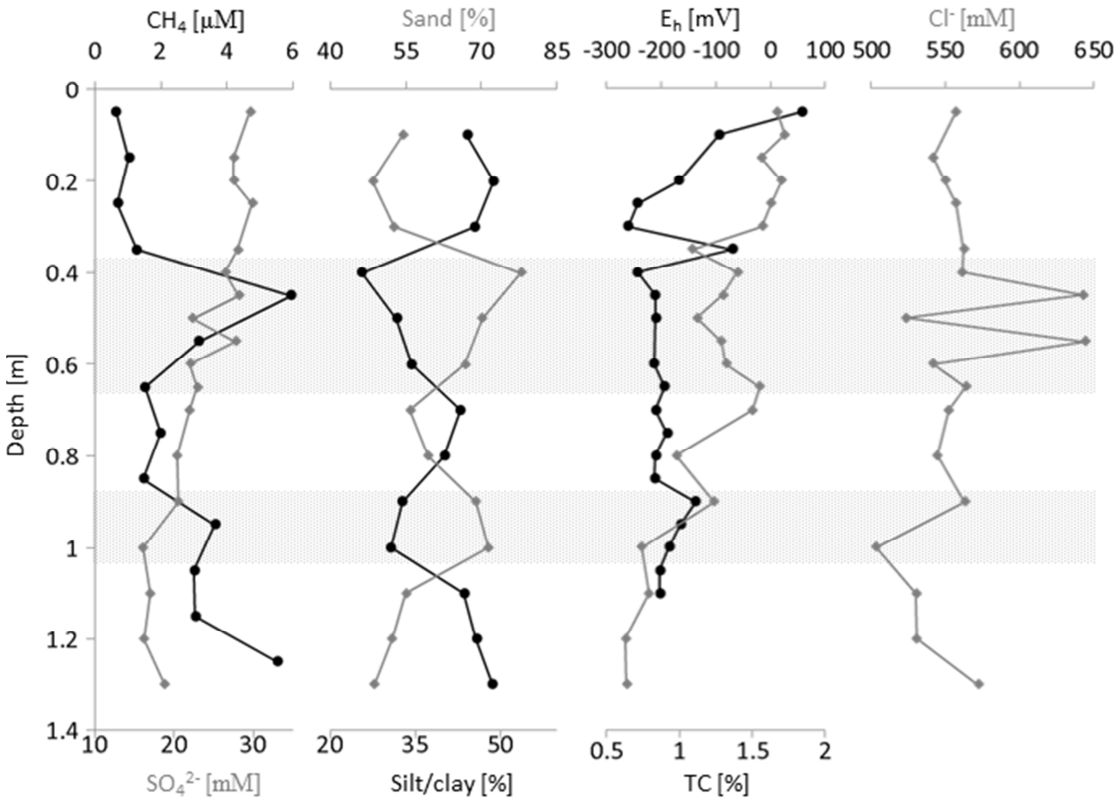

Figure 2. Pore fluid profiles from the collected sediment cores.

is virtually absent in this setting. Only one visible amplitude decrease is observed below one of the pockmarks that could be ascribed to weak AB (Figure, bottom panel). Although it is not as apparent as in the Malin Shelf area however weakening and partial discontinuity of the bedrock reflector below this feature is clearly visible. In this area gas appears to be more dispersed and more evenly distributed in the sediment. Moreover the AT is less profound than in the area to the north-west which might be related to grain size distribution and compaction of the sediment, however the latter is of a less importance composed almost exclusively of young, non-consolidated sediments. These two parameters control the porosity of the sediment and indirectly size of the pore space available for the gas to occupy. As discussed previously the weaker AT signal might not necessarily mean that there is less gas in the sediment as signal attenuation is related to bubble diameter rather than concentration. Therefore it is impossible to infer gas concentrations from seismic data alone and ground-truthing is necessary. An important feature of these seismic profiles is the lack of AB signals below the prominent AT area. This suggests that gas might be generated in this lateral facies rather than vented from faults in the bedrock, except for the location discussed above where a deeper source cannot be ruled out. Assuming that gas is continuously vented from a deeper source, namely bedrock fault, signals such as AB or AT connecting with the bedrock are to be expected. However this is only true for a continuous gas supply scenario. Periodic gas migration caused by successive cycles of seal failure-renewal could still be a viable scenario particularly given the vicinity of Gortavallig and Dunmanus Faults. Importantly the Gortavallig Fault crosses directly underneath the area where weak AB and discontinuity of bedrock reflector were observed. The acoustic signals in the water column (HR) can

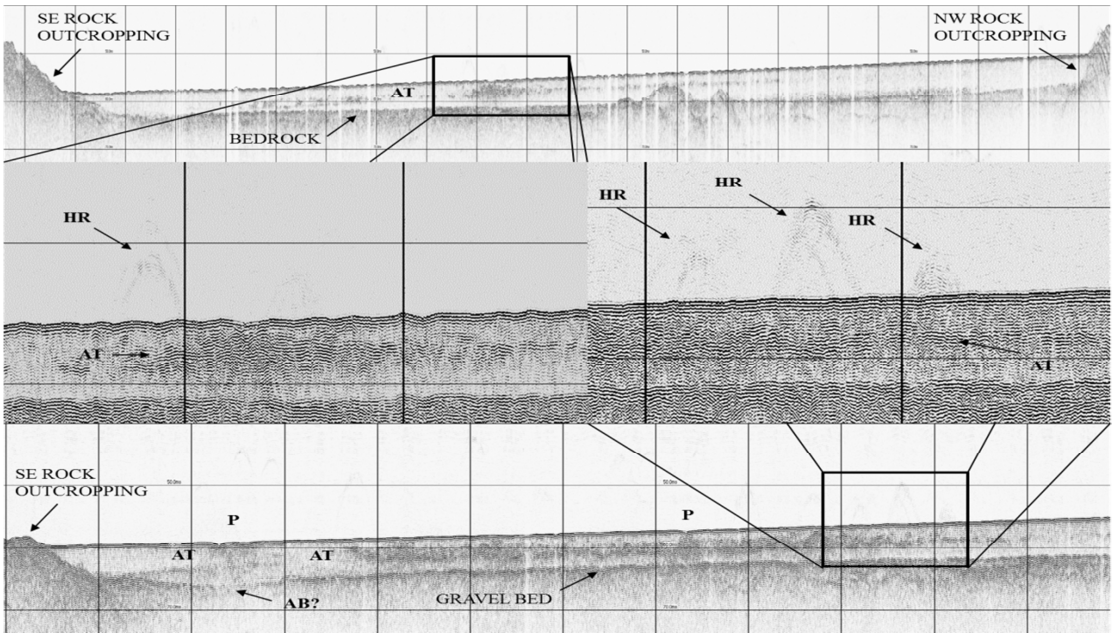

Figure 3. Sub bottom data

easily be mixed up with fish swim bladders. Shape and migration patterns are two means of distinguishing between the two (Judd and Hovland, 2007). Fish shoals according to Judd et al. 1997 are more diffuse and horizontally extended whereas seeping gas will have more columnar, vertically extended characteristics. The shape of hyperbolic reflectors observed in pinger data (Figure 3) is both horizontally and vertically extended and thus ambiguous and difficult to interpret. However MBES data also contains very narrow and exclusively vertical signals that are most likely caused by ascending bubbles. (Figure 4). These signals do not appear to be artefacts since they occur in multiple places (not all of such signatures detected are shown on Figure in different areas and more importantly the same verticals signals are observed in different lines in the same seabed area (e.g. Figure 3, middle panel). We therefore propose that venting mechanism based on successive cycles of seal failure-renewal. There was no evidence of water freshening in the any of the CTD cast as well as in the sediment core pore water chloride data therefore fresh water expulsion is not a viable formation mechanism of these pockmarks.

Pockmark activity

Detection of active venting can be troublesome according to current pockmark formation models (e.g. Cathles et al. 2010) and field data (Judd and Hovland, 2007). Periodic gas expulsion, particularly after initial violent pockmark formation, is typical for most pockmarks and they are considered settings where moderate fluid migration is dominant. Nevertheless active venting has been reported. Newman et al. 2008 demonstrated methane concentrations reaching 100 nM in pockmarks along the US mid-Atlantic shelf break. Christodoulou et al. 2003 reported both freshwater and gas related active pockmarks systems in the Patras and Corinth gulfs, Greece. In both of these studies the METS sensor (Garcia and Masson, 2004) was used to measure methane concentrations in the water column above and in the vicinity of pockmarks. We have employed the same instrument in Dunmanus Bay.

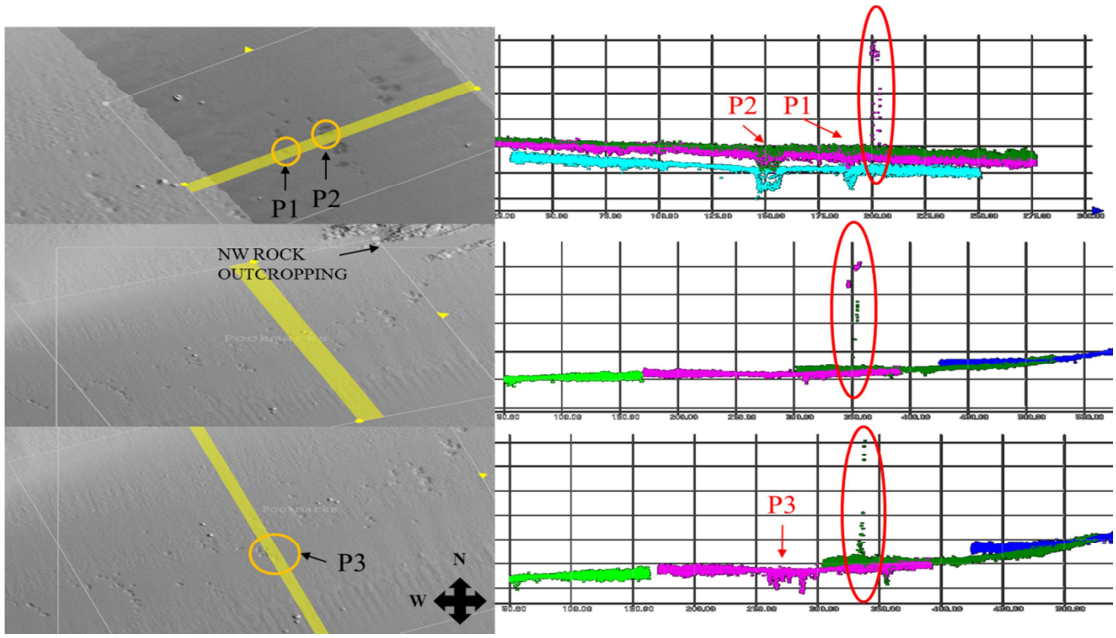

Figure 4. MBES data

Methane concentrations recorded by the METS sensor along the SE to NW transect ranged from 5.1 to 14.2 nM (Table 2). Slightly higher values were consistently recorded in the western part of the pockmark field however overall variability of the data is low and the highest concentrations only slightly exceed typical marine water methane values (Holmes et al. 2000).

Cast	Lat	Long	CH_4 [nM]
CV0923_03	51.55817	-9.71867	14.2
CV0923_01	51.55700	-9.71667	12.1
CV0923_02	51.55767	-9.71567	13.1
CV0923_15	51.55967	-9.71517	10.2
CV0923_08	51.55933	-9.71383	9.5
CV0923_14	51.55633	-9.71150	8.6
CV0923_3_1	51.56183	-9.71033	5.7
CV0923_11	51.55983	-9.70850	10.2
CV0923_12	51.56133	-9.70783	6.5
CV0923_3_2	51.55950	-9.70700	5.1

Table 2

Methane concentrations in the water column above the Dunmanus Bay pockmark were typical for open ocean values (Holmes et al., 2000). Although acoustic evidence of gas plumes in the water column was acquired this was not reflected in the methane concentrations. Discrete samples collected across the water column show similar concentrations which ranged from 12.2 to 22.9 nM in the photic zone (3-5 m) and were dropping with depth where they ranged from 2.2 to 6.4 nM. Although it was disappointing to find such low methane concentrations despite

acoustic evidence of seepage this is not uncommon even in areas where shallow gas accumulation and venting is more vigorous. Dando et al. 1991 reported methane concentrations from a large active pockmark in the North Sea and only in two of six stations these concentrations exceeded 25 nM, in half of them methane was below 15 nM. They found higher concentrations exceeding 50 nM only in areas where an echo sounder showed gas bubbles in the water column. The water column methane data indicates that we were unable to capture any of the plumes recorded previously. The data suggest discreet and periodic seepage that requires a more targeted approach with use of instruments that are not confined to location but can cover a larger area and are quick to deploy to the active area. With the absence of an SUV we could not verify the concentrations throughout entire water column with the METS sensor as gathering remote data with the use of CTD would require very long deployments time and therefore increase the risk of equipment loss due to weather conditions. The bottom water methane concentrations recorded by METS sensor were slightly higher than these from head-space method but overall are in good agreement with the head-space data. Gradual decrease in concentrations was along the W-E transect. In the first three stations (03, 01 and 02) highest CH_4 concentrations were recorded (14.2, 12.2 and 13.3 nM respectively) followed by drop to very low values ranging from 5.1 to 6.6 nM (stations 3_2 and 13 respectively). The concentration of methane in the sediment cores (ie Figure 2) shows a general increasing trend with depth. The values range from < 1.0 μM to 6 μM in the deeper sections. Higher hydrocarbons C_{2+} (mostly C2) were present in trace amounts therefore the gas can be considered dry and lack of higher homologs implies microbial origin (Faber and Stahl, 1984; Floodgate and Judd, 1992). In a normal setting where shallow gas is absent, methane generation is only possible after sulphate has been depleted and methane is not present in the sediment above the sulphate depletion depth (Schulz and Zabel., 2005). The sulphate is far from depleted yet methane presence was recorded in the sediment. This suggests that the methane is migrating upward from the AT area observed in the sub bottom profile. The in-situ generation of methane in the sediment analysed is not possible since the optimal conditions for microbial methanogenesis were not met. Moreover the conditions in the sediment must be anaerobic since all methanogens are strict anaerobes and contain typically more than 0.5% of organic carbon available to the microbes. The redox potential measurements suggest that conditions in the sediment are indeed anoxic (Figure 2) although sediment was not fully reduced (black). This is an interesting finding given that low redox potential (< 150mV) marking the beginning of anoxic zone is usually, however not always, coupled with depletion of sulphate which we do not observe. Nevertheless given that sulphate is not depleted the microbial generation of methane, if it occurs must be take place deeper.

Dunmanus Bay pockmarks are clearly features created by gas expulsion. The acoustic data confirms presence of shallow, lateral gas accumulation and bubbles in the water column however the water column sampling did not provide solid evidence that these bubbles are methane gas. Judging from the pockmark size and the acoustic signals in the subsurface, gas venting may be moderate in nature. The pockmarks are relatively small and they are accompanied by scattered small satellite features. Hovland et al. 2010 suggested that small satellite unit-pockmarks represent most recent and most active local seepage locations. Methane concentrations across the water column measured from discrete samples (Figure, right panel) as well as by METS sensor show no evidence of drastically elevated methane concentrations typically observed in sites where vigorous venting takes place.

Pockmarks and benthic communities

The variety and abundance of marine life associated with seepages can be astounding across all trophic levels. Dynamic, energetic venting systems are known to support unique ecosystems (Kiel, 2010). There is evidence that pockmarks on a smaller scale can support local communities however the debate on that matters continuous. To examine if local communities from Dunmanus Bay are affected by these features a benthic survey was conducted over the pockmark area (Figure 1).

The benthic infauna taxonomic identification revealed a total of 122 species, comprising 8865 individuals, ascribed to 12 phyla present in the surface sediments. The most abundant organisms were ascribed to polychaetes (57 species), crustaceans (25 speices), molluscsc (13 species) and echinoderms (8 species). Eight phyla were grouped as others; this group consisted of cnidarians, plathyhelminthes, nemerteans, nematodes, priapulids, sipunculids, oligochaetes and phoronids. Species numbers ranged from 23 to 77 (station 21 and 16 respectively). Numbers of individuals ranged from 382 to 1878 (station 20 and 19 respectively). The 5 most abundant species were *Leptopentacta elongata* (Cucumariidae, Duben and Koren), *Amphiura filiformis* (Amphiuridae, Muller), *Tubificoides amplivasatus* (Annelida, Erséus), *Scalibregma inflatum* (Annelida, Rathke) and *Magelona alleni* (Annelida, Wilson) and accounted for over 80% of individuals. Highest species richness was found in the control site and ranged from 3.47 to 11.16 (station 21 and 16 respectively). Evenness index ranged from 0.35 to 0.61 (station 21 and 20 respectively). Diversity ranged from 1.6 to 3.66 (station 21 and 16 respectively). Detailed data are given in Table.

Classification and cluster analysis was performed to find “natural groupings’ of samples, i.e. samples within a group that are more similar to each other, than they are similar to samples in different groups (Figure 5). A highest similarity of 73.9 % was observed between stations 18 and 19. In these stations 53 species were found with three species accounting for 90% of the whole assemblage: sea cucumber *Leptopentacta elongata* (52.7%), polychaete *Scalibregma inflatum* (31.9%) and polychaete *Diplocirrus glaucus* (5.4%). These species accounted for 28% similarity within this group. Because of the dominance of the three species these stations had low richness (5.21 – 5.57), evenness (0.37) and diversity (1.96 - 2.01). Stations 17 and 41 grouped at a similarity level of 71.2 %. These stations contained 57 species with four species accounting for 78.5% of total assemblage: brittlestar *Amphiura filiformis* (25.8%), sea cucumber *Leptopentacta elongata* (24%), polychaete *Diplocirrus glaucus* (14.7%) and polychaete *Scalibregma inflatum* (14%). These four species also accounted for 28% of similarity in this group. The dominance of these species was not as significant as in other stations as shown by higher diversity indices (Table 4).

Station	Species	Individuals	Richness	Evenness	Diversity
16	77	908	11.16	0.58	3.66
17	46	632	6.98	0.57	3.14
18	39	1462	5.21	0.37	1.96
19	43	1878	5.57	0.37	2.01
20	34	382	5.55	0.61	3.09
21	23	568	3.47	0.35	1.60
22	43	786	6.30	0.36	1.94
39	35	929	4.98	0.42	2.17
40	32	741	4.69	0.40	2.02

41	41	579	6.29	0.60	3.19

Table 4

All four of these stations grouped at a similarity level of 70.33%. The next most similar stations were 20 and 22 grouping at a similarity level of 69.1 %. A total of 51 species were found in these stations of which three accounted for 80.4% of the whole assemblage: sea cucumber *Leptopentacta elongata* (53.3%), polychaete *Scalibregma inflatum* (21.9%) and polychaete *Diplocirrus glaucus* (5.2%). Because of low numbers of individuals station 20 had the highest evenness and moderate richness and diversity. Station 22 on the other had moderate richness and low evenness and diversity. All six of these stations grouped at a similarity level of 66.4 %. Station 39 grouped with these stations at a similarity level of 65.4 %. In this station 35 species were observed with three accounting for 88.9% of the whole assemblage: sea cucumber *Leptopentacta elongata* (46.9%), polychaete *Scalibregma inflatum* (34.6%) and polychaete *Diplocirrus glaucus* (7.4%). Dominance of three species was reflected in low diversity indices. Next station 40 joined the previously discussed stations with 59.9 % similarity. A total of 32 species with three species accounting for 87.6% of the whole assemblage: polychaete *Scalibregma inflatum* (58.7%), sea cucumber *Leptopentacta elongata* (25%), and polychaete *Diplocirrus glaucus* (3.9%). This station was characterized by low richness, evenness and diversity. Station 21 had a 55.5% similarity with previous stations. A total of 23 species were observed in this station and three species accounted for 89% of individuals: sea cucumber *Leptopentacta elongata* (74.5%), polychaete *Scalibregma inflatum* (11.4%) and oligochaete *Tubificoides amplivasatus* (3.2%). This station was characterized by low richness, evenness and diversity. Finally station 16 had a 47.4 % similarity with 77 species of which four accounted for 75% of all individuals: polychaete *Scalibregma inflatum* (27.9%), sea cucumber *Leptopentacta elongata* (16.2%), brittlestar *Amphiura filiformis* (25.8%) and polychaete *Diplocirrus glaucus* (15%). In this station the highest species number was observed which resulted with high richness and diversity. These delineations were also preserved in the MDS analysis (stress value <0.05). Control station 16 grouped separately from the other stations. Stations 18, 19, 17, 41, 20 and 22 formed a central group with stations 39, 40 and 21 at varying distances from the central group (Figure 6).

Images taken from the sediment water interface with the SPI camera show numerous burrows, mainly vertical but lateral are also present, and in places infauna can be spotted (Figure 7). The substrate on the images comprises mainly of very fine sand with a few patches of coarser sand. Progression of natural geochemical zonation is visible in most images in a form of colour change. However in most images the transition is not sharp (i.e image 19) and marked with abundant dark streaks. This might be indicative of bioturbation and/or bioirrigation given the high count of actively burrowing species. The images are in good agreement with the redox potential profiles taken on undisturbed box cores (data not shown). The oxygenated sediment (with typical values > +200 mV) was found to be present only in the very top layer of the sediment. This layer comprised of photodetrital drift and loose sands therefore measurement of redox potential in such mobile and unconsolidated substrate was not possible in most cases. This is a natural finding as the penetration of oxygen in marine sediments usually does not exceed a few cm and in areas with high organic input from the water column (high productivity) it can be as low as a few mm or be absent (Schulz and Zabel, 2005). The post oxic zone (with typical values from -150 to

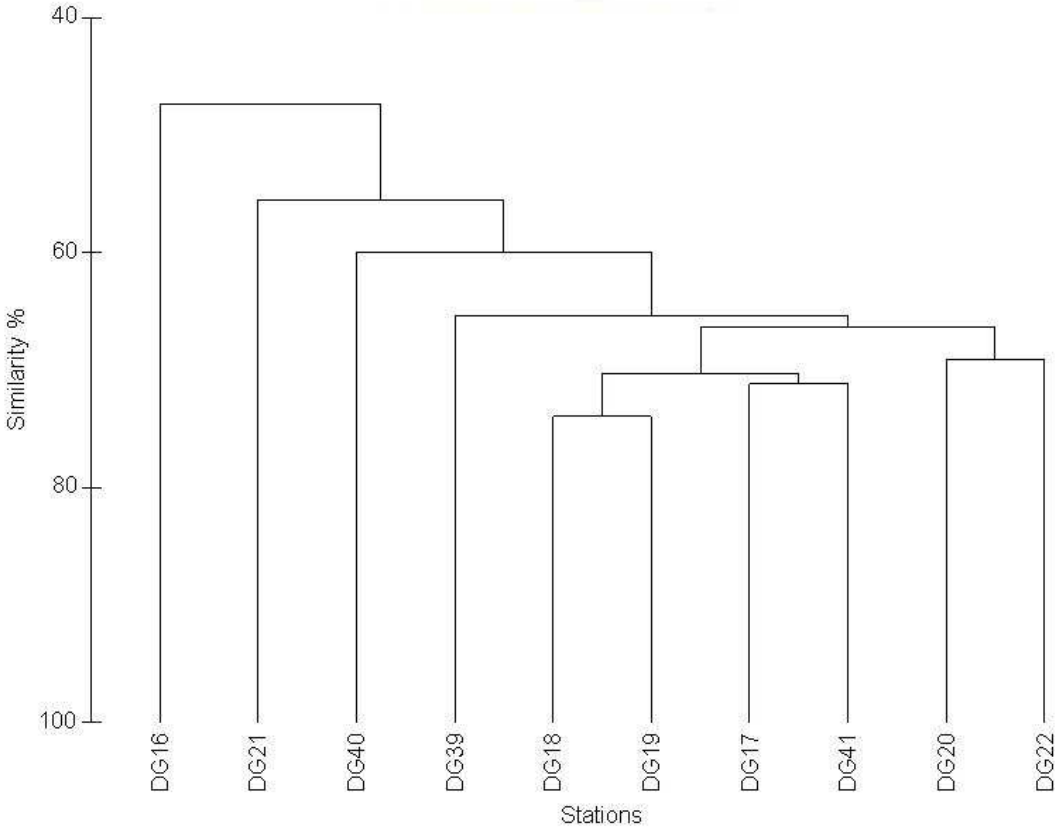

Figure 5. Classification and cluster analysis

+200 mV) depth ranged from a shallow 4 cm to more than 15 cm in most stations. Anoxic conditions (typically < -200 mV) were detected only in one station.

Benthic communities in the Dunmanus Bay pockmark field were dominated by four species: sea cucumber *Leptopentacta elongata* (43.6%), polychaete *Scalibregma inflatum* (28.9%), polychaete *Diplocirrus glaucus* (7.5%) the brittlestar *Amphiura filiformis* (6.1%). The *Leptopentacta elongate* is a burrowing sea cucumber often found in U-shaped burrows. It prefers muddy sands or mud and shallow waters. This species is widespread around Great Britain and Ireland. *Scalibregma inflatum* is a segmented worm, an active burrower, often found buried deep in sand or mud. It feeds on organic detritus and this species is widespread around Great Britain, but not that frequently encountered around Ireland. *Diplocirrus glaucus* is also a segmented worm, detritus feeder, often found in sandy and muddy bottoms. This species is widespread in the Northern Atlantic. *Amphiura filiformis* is a small brittle star with very long arms living buried in the sediment with arms extended into the water current to catch suspended matter. This species is also widespread around Ireland and Great Britain. None of these species has been reported in abundance in active pockmarked areas. The dominant species in the observed benthic community structure are typical representatives of sublittoral benthos around Ireland. The lack of species that are known to be abundant in methane venting settings (e.g. Dando et al. 1991; Jensen et al. 1992; Kiel, 2010) suggests that benthic communities do not benefit nor rely on the occasionally released hydrocarbon gas. Benthic counts indicate a pristine and healthy habitat. Community structure in the pockmark area compared to controls had on avergage lower richness, eveness but higher diversity of species. Reference station however, show only 47.4% similarity with others. Considering negligible

influence of sediment particle size this suggest that other factors such as seabed morphology might affect differences in distribution of macrobenthos in the pockmark scarred and unaffected seabed.

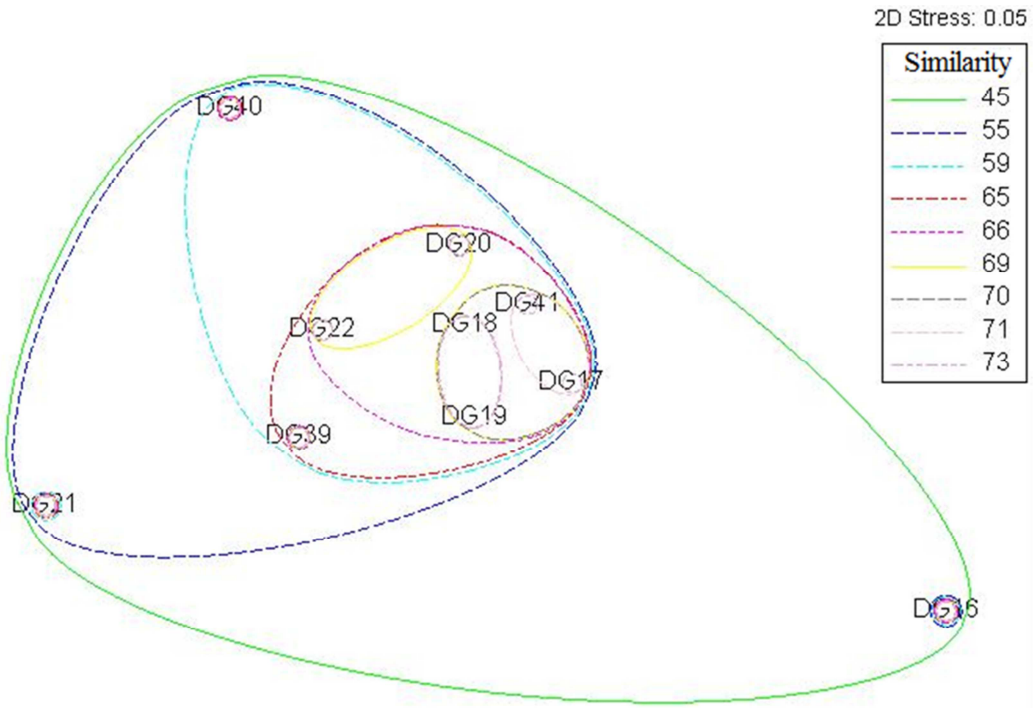

Figure 6.

Conclusions

The survey of the Dunmanus Bay pockmarks revealed gas related features and that an active fluid system is present in the subsurface. The shallow gas accumulation was laterally extended and in most areas did not reach the bedrock. Although penetration of suspected gas accumulation was not achieved based on the methane analysis and pore water profiles we can assume that the gas below is likely to be mainly methane. The pockmarks appear to periodically vent accumulated gas however the scale of these events is small. The origin of the gas remains unknown. The sediment in Dunmanus Bay comprised mainly of sands mixed with gravel and finer fractions. The benthic communities were dominated by four common species and overall show structures typical for the sublittoral environment around Ireland. Organisms frequently encountered in areas with methane gas seepages were not observed and thus we conclude that benthic communities do not rely on methane as food source.

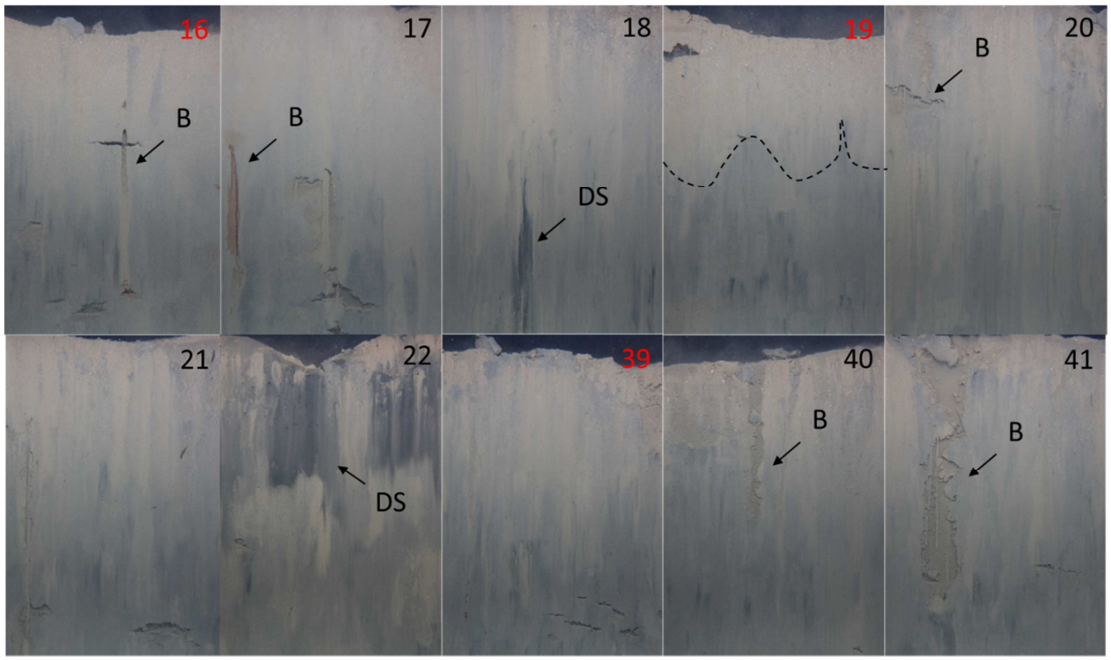

Figure 7. SPI camera images.

Chapter 2.

Multidisciplinary characterization of seabed fluid seepage features in Irish waters

Introduction

Significant improvements in remote and geophysical investigation and mapping technology since the 1960's has revealed regions of significant gas and fluid seepage to the water column characterize the ocean's seafloor. The most dramatic examples of this include hydrothermal vents or 'black smokers' at the mid Atlantic ridge and pockmarks on the Scotian shelf. It is now evident that this seabed fluid flow is of fundamental importance to the geological, chemical and biological composition of the marine environment and also the composition of the atmosphere (Judd 2007). Today the investigation of the marine seabed and fluid flow processes requires the integration of a variety of fields such as marine geology, geophysics, oceanography, aquatic chemistry, geochemistry, organic geochemistry and geomicrobiology. As such this project has reflected this need and is a multidisciplinary approach. This masters thesis shall cover an up-to-date review of the literature pertinent to marine biogeochemistry and seabed fluid flow (Chapter 1), a multidisciplinary study of gas seepage features in the Irish Sea by seismic profiling, underwater video investigations, geochemical profiling of pore water sedimentary phases at these features and also lipid biomarker analysis (Chapter 2), a metagenomic study of microbial diversity of a large pockmark in the Malin Deep, off N.W. Ireland (Chapter 3), and will finish with a brief chapter on future work to be carried out for the award of the PhD thesis (Chapter 4). Chapters 2 and 3 are considered complete studies and publication-ready. These chapters will be submitted to peer-reviewed journals, with Chapter 2 submitted intended to be submitted to *Marine Geology* and Chapter 3 being submitted to the *ISME (International Society for Microbial Ecology)* journal. The data presented in Chapter 5 comprises a brief overview of current results from a recent expedition (May 2011 – *RV Celtic Explorer* expedition CE11_017), and future work that shall be the primary focus for the remainder of the research project.

Literature Review

2.1 The extent and importance of the marine seabed environment

The oceans cover 71% of the earth's surface, with about two thirds of the earth's land located in the northern hemisphere, as shown in Figure 1A. While the ocean seafloor is geologically distinct from the continents, it is intimately linked with their geological processes. Due to plate tectonics the seafloor is in a perpetual cycle of formation and destruction. Over geological timescales mantle convection causes spreading from the mid ocean ridges towards the continents, the oceanic plate is subducted into the mantle and the continental plate is pushed up to form mountains (Figure 1B.). The oceans are a natural depository for the dissolved and particulate matter arising from continental weathering, riverine and aeolian transport, and also from marine inputs (Hedges and Keil 1995, Hedges, Keil and Benner 1997). Upon input to the oceans dissolved matter is consolidated by biological and geochemical processes and is deposited with particulate matter over geological timescales as marine sediments on the ocean floors. In this way the ocean floor is invaluable for understanding the earth's history and for reconstructing past environmental conditions of continents and oceans (Futterer 2006). Figure 1C. shows an idealized diagram of the structure of continental margins, and is composed of the continental shelf, the slope and the rise. The abyssal plains of the oceans commence after the continental rise.

However, this perspective of the ocean's seafloor is a limited. Improvements in remote seabed mapping technology and remotely operated submersibles have resulted in a distinct shift away from the perception of the marine environment a flat, unchanging expanse as shown in Figure 1. to that of one including diverse geological settings such as canyons, cold seeps, deep-water coral reefs, mud volcanoes, pockmarks, carbonate mounds, ridges and trenches (Jorgensen and Boetius 2007). Thus it is evident that although the oceans cover the majority of the earth's surface, are highly diverse both physically and biologically, and are intimately related to processes and life on the continents where humankind exists, there are vast regions yet to explore and much yet to discover and understand.

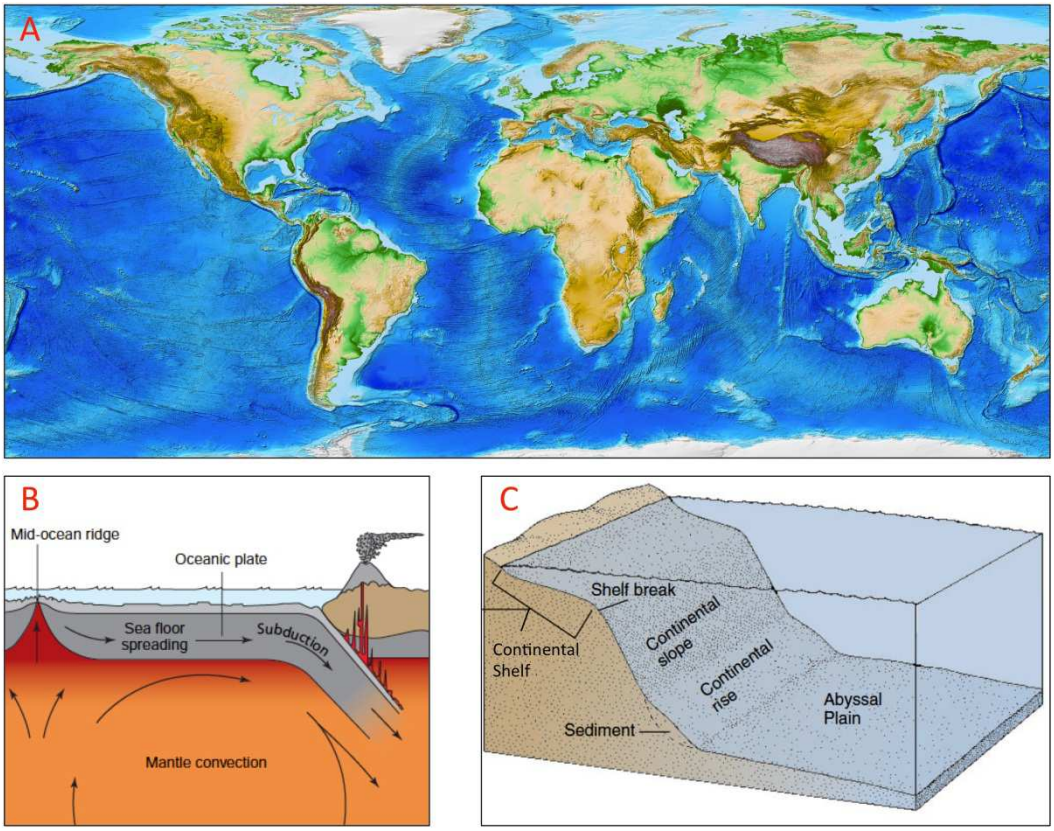

Figure 1: (A) Surface of the earth, showing seafloor bathymetry and terrestrial elevation (NOAA) (B) Schematic diagram showing plate subduction, seafloor spreading and mountain building (Wallace and Hobbs, 2006) (C) Idealized diagram showing the components of the continental margin (the shelf, the slope, the rise) and the abyssal plain (Castro, 2003)

2.2 Carbon cycling and the role played by the marine sedimentary environment

Chemical cycling on earth is of utmost importance and consists of complex reversible and irreversible fluxes between the geo-, hydro-, atmo- and biosphere. Many chemical cycles are strongly influenced by organisms, particularly plants and microbes. These are termed biogeochemical cycles and the major cycles are carbon, nitrogen, oxygen, phosphorus and sulphur (Manahan 2005). The focus of this review shall be on carbon cycling, as this is quantitatively the most important. A schematic outline of the global carbon cycle is given in Figure 2. The earth's natural C reservoirs consist of fossil fuels (~3700 GtC), vegetation, soil and detritus (~2300 GtC), the atmosphere (597 GtC), the surface ocean (900 GtC), the intermediate and deep ocean (37,100 GtC) and surface sediments (150 GtC). CO_2 is removed from the atmosphere via weathering by silicate rocks (0.2 GtC yr^{-1}) and also fixed as organic C (OC) (120 GtC yr^{-1}) by plants and microbes, with most of this CO_2 being returned to the atmosphere by respiration

(119.6 GtC yr^{-1}) (Denman et al. 2007). It is noteworthy that globally more OC occurs in soil humus (~1600 GtC), recently deposited marine sediments (~1000 GtC) and dissolved in seawater (~700 GtC) than in all land plants (~600 GtC) and marine organisms (~3 GtC) combined (Hedges, et al. 2000). Accordingly these vast deposits of organic molecules play major roles in global temperature modulation, in weathering processes, in supporting life, and also in composing precursors for coal and petroleum (Hedges, et al. 2000).

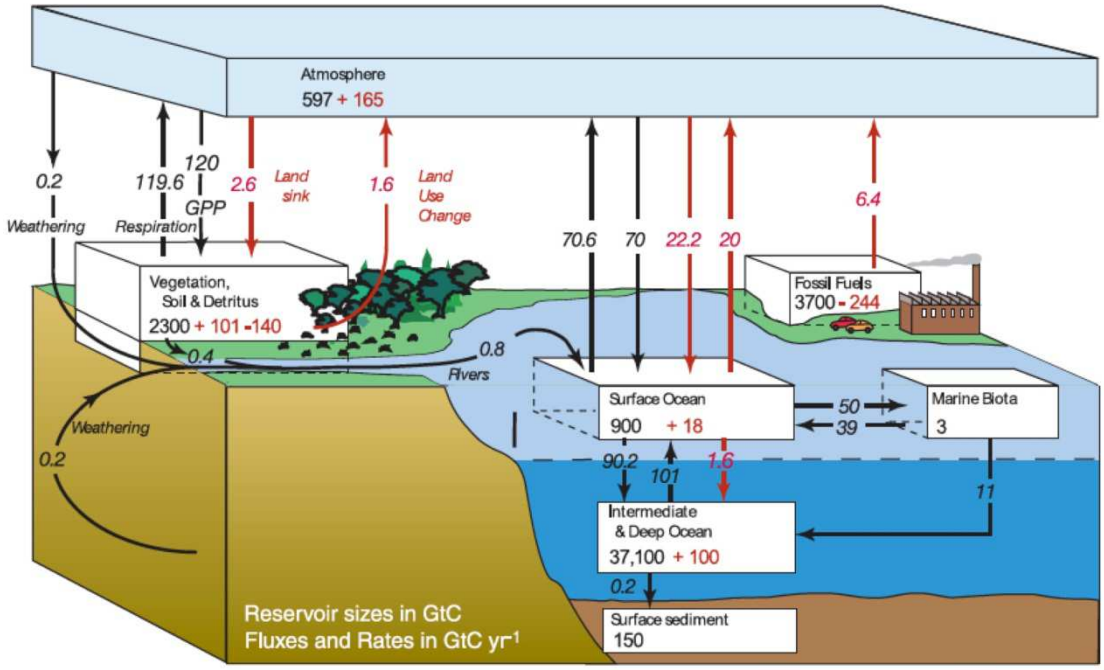

Figure 2: The global C cycle for the 1990's, showing annual fluxes in Gt C yr^{-1}. Pre-industrial fluxes are shown in black, anthropogenic fluxes are shown in red. GPP is annual gross primary production. (Denman et al. 2007, and references therein.)

Continental weathering and biomass degradation delivers 0.8 GtC yr^{-1} to the surface oceans via rivers (Hedges and Oades 1997, Benner 2004). Oceanic C exists is several forms: dissolved inorganic carbon (DIC), dissolved organic carbon (DOC), particulate organic carbon (POC) with ratios of approximately 2000:38:1 DIC:DOC:POC (Denman et al. 2007). CO_2 is exchanged between the atmosphere and the ocean (70Gt C yr^{-1} to the oceans and 70.6 GtC yr^{-1} to the atmosphere), and this exchange, (which varies considerably due to factors such as wind speed, precipitation, heat flux, sea ice and the presence of surfactants), is determined by the partial pressure of CO_2 (pCO_2). While atmosphere-ocean CO_2 exchange is considerably altered by advection and mixing processes, this exchange is also altered through what

are termed the 'solubility pump', the 'organic carbon pump' (also called the 'biological pump') and the '$CaCO_3$ pump' (Denman et al. 2007). The solubility pump concerns changes in solubility of gaseous CO_2, whereby on dissolution CO_2 reacts with water to form HCO_3^- and CO_3^{2-} (making up DIC). The OC pump concerns changes in carbon fixation to POC by phytoplankton via photosynthesis (50 GtC yr^{-1}), at the surface waters (39 GtC yr^{-1}) and export transport to deeper waters. The $CaCO_3$ pump concerns changes in CO_2 release through formation of planktonic shells ($CaCO_3$) (Volk and Hoffert 1985). DOC is primarily sourced from terrestrial environments via rivers or from marine planktonic water column metabolism, and residence time can vary significantly from days to 10kyr (Loh and Bauer 2004). Mineralization and remineralization of OC occurs primarily in the upper 1000m of the ocean water column (90.2 GtC yr^{-1} and 101 Gt yr^{-1}), with the remainder of the particle flux entering marine sediments (0.2 GtC yr^{-1}). The organic carbon content of sedimentary deposits can range from zero to up to 100% in coals, but is typically less than 2% in freshly deposited marine sediments and averaged over the entire ocean floor is less than 0.25% (Pedersen and Calvert 1990). A more detailed discussion of the composition and cycling of organic matter in marine sediments will be given in section 1.3.

The Gaia hypothesis, which was first proposed in the 1970's, contends that all organisms and their inorganic surroundings on Earth's are intimately integrated in one complex self-regulating system that maintains the fragile conditions that support life (Lovelock 1979). The effects of anthropogenic activity on the Earth are illustrated in Figure 2 and demonstrate this concept clearly. The red figures and arrows highlight how anthropogenic processes, in particular the burning of fossil fuels such as coal and petroleum, since the industrial revolution, c. 1750, has resulted in enhanced concentrations of atmospheric CO_2, which according to ice core records are the highest in 650 kyr (Denman et al. 2007). $[CO_2]_{atm}$ was stable for c. 10 kyr pre-1750, at 260-280 ppm, and in about 150 yr has increased to 380 ppm in 2005. While CO_2 is the primary causal factor in current climate change, atmospheric CH_4, has increased from 770 ppb in 1750 to 1775 ppb in 2005 (Fluckiger, et al. 2002) and per mole has a radiative forcing 25 times greater than CO_2 (Denman et al. 2007). The primary cause of this increase is agriculture (changing land usage and ruminant animals), waste production and disposal, fossil fuel use and biomass burning, while major natural causes include wetlands, oceans, vegetation and CH_4 hydrates (Denman et al. 2007).

Additionally CH_4 is the most abundant reactive trace gas in the troposphere and has a significant impact on tropospheric and stratospheric chemistry (Wuebbles and Hayhoe 2002).

2.3 Early diagenesis of sedimentary organic matter

Diagenesis is the sum total of processes, whether physical, chemical and/or biological that bring about changes in a sediment or sedimentary rock subsequent to deposition in water. Early diagenesis concerns the changes that occur during deposition and burial to a few hundred metres where elevated temperatures are not encountered (Berner 1980). There are a plethora of processes and phenomena, which fall under the heading of early diagenesis and include compaction, cementation, crystallization and desiccation. However the most studied and most important is the diagenesis of organic matter (OM). As illustrated in Figure 2. above, only a tiny fraction of the OM produced by primary production in the photic zone is incorporated into marine sediments. This is due to the fact that OM is thermodynamically unstable, and there is a high-energy yield in its oxidation to more stable species such as O_2, NO_3^-, SO_4^{2-} (Berner 1989). However OM in marine environments is a complex heterogeneous mixture of particles and molecules of diverse physical and chemical properties and the sources of OM in the environment spans a broad spectrum from biological sources such as vascular plants, non-vascular plants (bryophytes), algae, fungi, protozoans, bacteria, archaea and animals, to relict sources such as kerogen, coal, petroleum and combustion products (black carbon) (Benner 2004) This heterogeneity results in different components of OM accumulating and degrading at different rates (Baldock, et al. 2004), due to the principle of selective preservation, whereby non-polar low solubility compounds (e.g. lipids) and hydrolysable-resistant macromolecules (e.g. lignin, cutin) are preserved over more soluble polar compounds such as proteins and polysaccharides in the terrestrial and marine environments (Rullkotter 2006).

In soils OM is on average composed of roughly 10 – 20% carbohydrates, 10% amino acids and 5 – 15% lipids, while in sediment the figures are approximately 10 – 15% amino acids, 5 – 10% carbohydrates, 3 – 5% lignin and <5% lipids (Hedges and Oades 1997). However, importantly typically over half of OM is still molecularly uncharacterized (Hedges, et al. 2000). In addition to this large pool of uncharacterized OM there is a parallel significant unknown regarding the fate and preservation of OM

in the environment (Hedges and Keil 1995). Organic-rich sediments are generally only deposited in certain conditions: there must first be a sufficiently large supply of organic detritus, primarily from enhanced primary productivity of phytoplankton; there must be a sufficiently low-energy depositional environment for organic material to be deposited; there must not be high inputs of inorganic material to dilute organic matter concentrations; and there generally must be conditions within the sediment that favour accumulation of organic matter i.e. anoxia (Killops and Killops 2005)

The seminal model for OM degradation in sediments was first proposed by Froelich et al. (1979) and is illustrated in Figure 3. Sedimentary OM is the driving force for a complex variety of redox reactions, some of which are shown. OM here is illustrated according to the generalized Redfield ratio (Redfield 1958) of 106:16:1 C:N:P, and the standard free energies for each reaction are given in the grey boxes, whereby reactions are arranged in order of decreasing energy yield from top to bottom. These redox reactions establish a number of geochemical redox zones, which may be termed oxic, suboxic or anoxic (Froelich, et al. 1979), (also shown are sulfidic and methanic zones, as proposed by Berner, 1981). Close to the sediment-water interface (SWI) an oxic zone is established whereby dissolved O_2, which diffuses or is biologically transported into the sediment, is utilized as an electron acceptor in the degradation of OM to produce CO_3^{2-}, NO_3^- and PO_4^{3-}. Below the oxic zone solid phase Mn(IV) oxides serve as electron acceptors and subsequently NO_3^- (produced in the oxic zone) is used as an electron acceptor. This is followed by a zone whereby solid phase Fe(III) oxides and Fe(III) hydroxides are used as electron acceptors, then under anoxic conditions SO_4^{2-} reduction and CH_4 fermentation occur (Schulz 2006).

Although energetically less favourable SO_4^{2-} reduction and CH_4 production are on average quantitatively the dominant processes degrading OM due to the fact that sediments receiving significant inputs of detrital organic matter, such as those in coastal and shelf margins, can become anaerobic relatively close to the sediment/water interface. This is because of the high respiratory demand of aerobic heterotrophic bacteria and also the inability of diffusive resupply of oxygen from the water column (Albert, Martens and Alperin 1998). A fraction of the CH_4 produced during fermentation diffuses into overlying sulphate-reducing layers and is oxidized anaerobically according to the reaction in Figure 4. Figure 4. also outlines the organisms involved and supported by anaerobic oxidation of methane (AOM), and its by-products and effects.

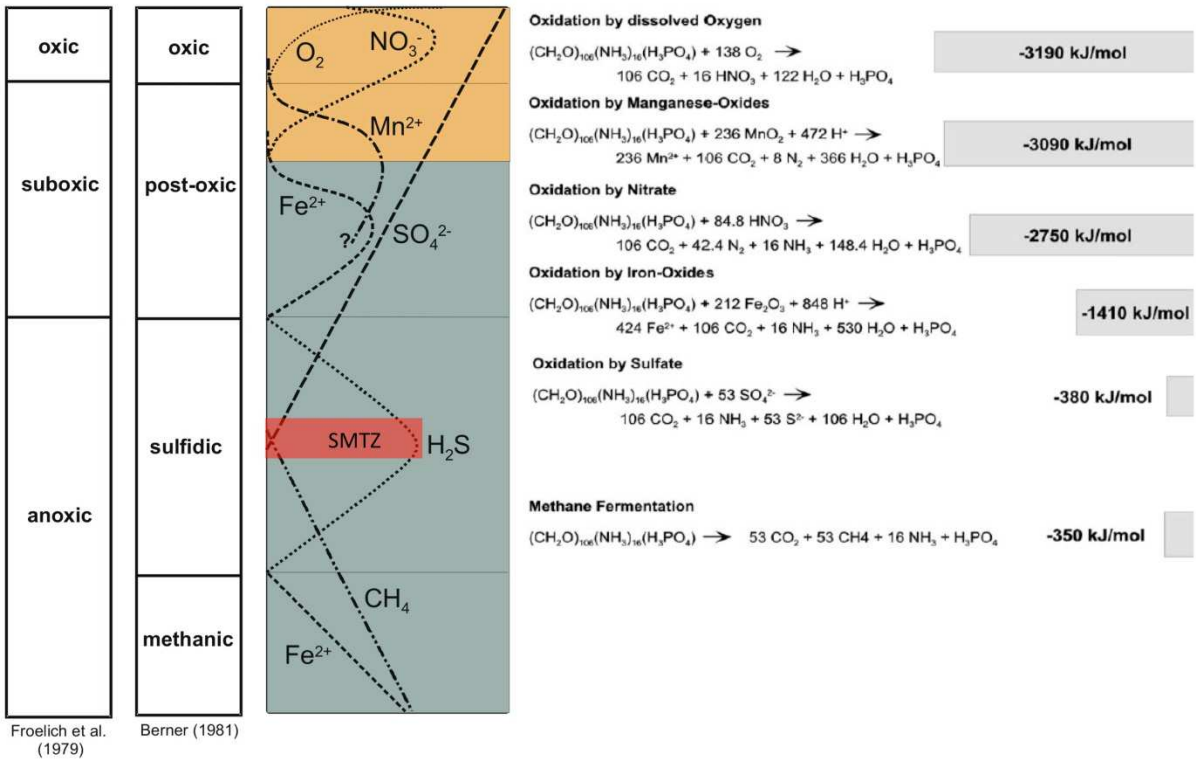

Figure 3: Geochemical zonation in marine sediments and major reactions in the early diagenesis of organic matter with different electron acceptors. SMTZ – sulphate-methane transition zone. Figure adapted from Froelich et al., 1979, Berner, 1981, and Schulz, 2006.

It is now accepted that it is microbially mediated, whereby the current leading theory is that a consortia of sulphate-reducing bacteria (SRB) and methanogenic archaea (ANME) mediate AOM (Boetius, et al. 2000). Figure 7B. shows an aggregate of these ANME (red) and SRB (green), which was obtained using fluorescent in-situ hybridization (FISH). Current knowledge regarding microbes involved in AOM shall be discussed in greater detail below in section 1.6. Key by-products include methane-derived authigenic carbonates (MDAC) and pyrite. AOM is believed to serve as an important control on the global flux of CH_4 to the atmosphere, estimated to be in the vicinity of 5-20% of net modern atmospheric CH_4 flux (20-100 $x10^{12}$ g yr^{-1}) (Valentine and Reeburgh 2000).

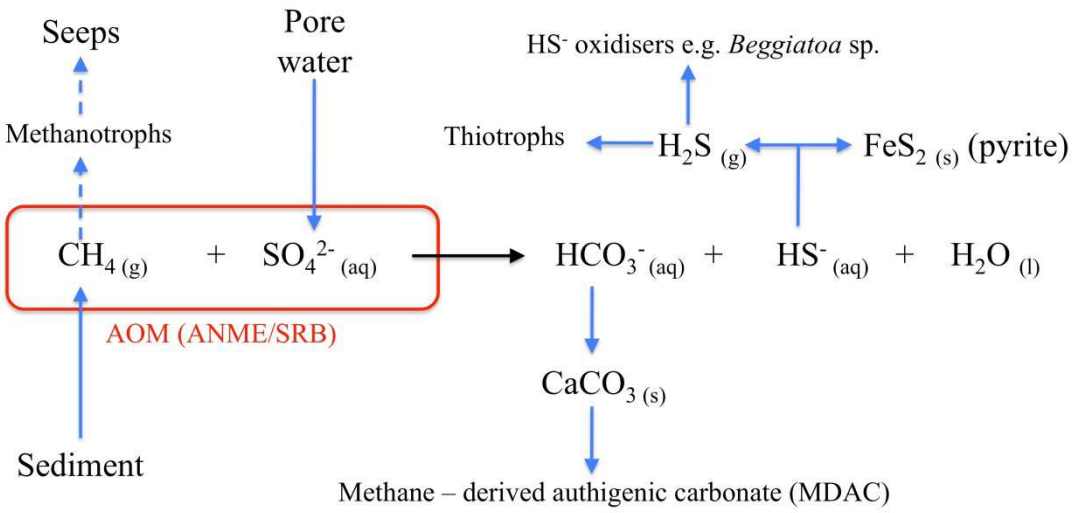

Figure 4: Anaerobic oxidation of methane (AOM): reactants (sources), microbial mediators, products, by-products and large-scale effects. ANME – anaerobic methanogens, SRB – sulphate-reducing bacteria. (Judd and Hovland, 2007)

2.4 Marine seabed fluid flow

As discussed above seabed fluid flow is of fundamental importance to the geological, chemical and biological composition of the marine environment and also the composition of the atmosphere (Judd and Hovland 2007b). These seepage fluids are predominantly gases of biogenic or thermogenic origin but can also be hydrocarbons, pore water or groundwater (Judd and Hovland 2007b). Biogenic gas is primarily CH_4, which is produced by recycling of organic matter by microbial degradation as discussed above in section 1.3. Biogenic gas is generally isotopically lighter i.e. more depleted in ^{13}C than thermogenic gas and is produced in shallow sedimentary layers (less than 1000mbsf). On the other hand thermogenic gas is primarily methane and C_2 - C_4 hydrocarbons, and is formed much deeper in the sedimentary column (generally greater than 1000mbsf) under conditions of high temperature and pressure and is generally isotopically heavier than biogenic methane. Biogenic gas generally has $\delta^{13}C$ values in the range of -60 to -80‰, while thermogenic gas has $\delta^{13}C$ values in the ranges of -20 to -60‰ (Floodgate and Judd 1992). As shown here $\delta^{13}C$ values ranges can vary considerably and during migration in the sedimentary column thermogenic gas may be subjected to microbial activity, which would give a mixed $\delta^{13}C$ signal and hinder identification of the source of gas. A more in-depth discussion of stable carbon isotope geochemistry is outlined in section 1.6.4.4. of this review. In addition seepage sources can be elucidated by a methane-to-higher-hydrocarbon ratio as shown in Equation 1.

$$C_{2+} = \left[1 - \left(\frac{C_1}{\sum C_{1-5}}\right)\right] x100 \qquad \text{(Equation 1)}$$

where C_1 is methane and $\Sigma C_{2\text{-}5}$ is the sum of ethane, propane, butane and pentane. Ratios of 0.05% or less are characteristic of biogenic gas, while for dry and wet thermogenic gas ratios are less than 5% (mostly less than 1%) and greater than 5% respectively. More recently stable hydrogen isotope analysis (δ^2D) has been used in conjunction with δ^{13}C analysis to distinguish origin of gas (Floodgate and Judd 1992). The type and size of seabed fluid flow features is normally determined by a complex interplay of sub-seabed pressure caused by gas accumulations, the lithological properties of surface and sub-bottom sedimentary layers, the local and regional hydrodynamic conditions and sedimentation rate (Croker, Kozachenko and Wheeler 2005). Seabed fluid flow features are diverse and range from hydrothermal vents, trenches, mud volcanoes, mud diapirs, pockmarks, doming, and methane-derived authigenic carbonate (MDAC) mounds and pavements (Jorgensen and Boetius 2007). In this review pockmarks, MDAC, mud volcanoes and mud diapirs will be discussed.

2.4.1 Pockmarks

Pockmarks are seabed craters, which were first discovered in the late 1960's (King and MacLean 1970) and are now known to be globally ubiquitous on the seafloor (Acosta, et al. 2001, Gay, et al. 2006, Bayon, et al. 2009). They range in size and depth from 1-200m and 0.5 – 20m respectively and are known to predominate in soft fine-grained sediments (silts/clays) (Judd and Hovland 2007a). Seeping fluids resulting in pockmark formation are generally gases such as CH_4 and other low molecular-weight hydrocarbons but can also be porewater or groundwater. The source of this fluid flux can also vary considerably, such as deep sub-seabed thermogenic, biogenic, hydrothermal, volcanic or groundwater sources. As such pockmark size and morphology varies considerably. 'Unit' pockmarks are small uniform depression (~1-10m diameter and 0.5m deep); 'normal' pockmarks are larger circular craters (10-700m diameter and 1-45m deep) with varying angles of slope; 'elongated' pockmarks have one axis much longer than the other and occurs more commonly in areas influenced by strong bottom currents; 'eyed' pockmarks have acoustically reflective material in its centre (coarse winnowed material, shell material or authigenic carbonates); 'strings' of pockmarks consist of numerous unit pockmarks showing

curvilinear patterns or chains that may be kilometers in length and thought to form along faults; and finally ‘complex’ pockmarks are clusters or amalgamations of pockmarks (Hovland, Gardner and Judd 2002). Figure 5A. shows an seismic profile collected from a boomer deployed at the Witch’s Hole Pockmark in the North Sea (Judd and Hovland 2007b). The crater-like depression can be distinguished as well as numerous acoustic signatures such as areas of enhanced reflection and acoustic turbidity, indicating shallow gas accumulations. Figure 5B. shows a multibeam echosounder bathymetry map from the Witch’s Ground Basin, North Sea (Judd and Hovland 2007b). This map highlights the extensive distribution and variety of sizes and morphologies that pockmarks can exhibit.

The leading pockmark formation mechanism theory is as follows: gas generated at depth migrates through sediment in pores or along fissures and accumulates in porous layers below silty top layers of relative impermeability; pressure increases over time in these gas reservoirs leading to seabed doming; this dome structure fails causing fractures and faults and a release of pressure; this rapid pressure induces gas flow into the water column and expulsion of surrounding sediment matrix, forming a crater; and finally settling and dispersal by currents of sediment particles (Judd and Hovland 2007b). However very few active pockmarks have been observed and pockmark formation has never been observed. Thus there remains many questions as to how pockmarks are formed, become active and what factors control their temporal activity. The importance of these features and the need for a greater understanding is because of factors such as the microbial and macrobenthic biodiversity present in these features (Jensen, et al. 1992), offshore marine and petroleum construction safety due to the possible slumps and slides; and because pockmarks may be indicators of deep-pressure build-up prior to earthquakes (Judd and Hovland 2007b);

2.4.2 Methane-derived authigenic carbonate (MDAC)

MDAC has been found in a variety of seabed environments and ranges from small nodules and concretions, to slabs and pavements, to dramatic mounds or chimney features, with relief of several tens of metres. Figure 5D. shows MDAC mound build-ups on the Crimean Shelf in the Black Sea (Reitner, et al. 2005), while Figure 5E. shows massive MDAC pavements in the Central Nile deep sea fan (Bayon, et al. 2009). MDAC formation is primarily believed to be a resulting end-product of

microbially-mediated AOM, as shown in Figure 4 and discussed in section 1.3. CH_4 is oxidized to HCO_3^-, which increases the pore water alkalinity and eventual saturation causes precipitation of solid $CaCO_3$, or MDAC. MDAC has received considerable attention from physical, chemical and biological perspectives and the reader is referred to the following literature for additional information (Croker, Kozachenko and Wheeler 2005, Bayon, et al. 2009, Jensen, et al. 1992, Reitner, et al. 2005, Aloisi, et al. 2002, Feng, et al. 2010).

2.4.3 Mud volcanoes and mud diapirs

Mud volcanoes are seafloor edifices from which seabed fluid (mud, seawater, gas, hydrocarbons) flows or erupts (Milkov 2000). On the other hand mud diapirs (also called shale diapirs) are seabed features where fluid-charged clay or mud rises through sedimentary layers due to buoyancy effects (Judd and Hovland 2007b). In constrast to mud volcanoes there may not be evidence of fluid flow and the term is generally applied to intrusive features i.e. ones that are only expressed in the subsurface. However there is considerable crossover between these terms (Judd and Hovland 2007b). Both features have been reported worldwide, often in areas of known hydrocarbon potential (Milkov 2000). These structures can be tens to hundreds of metres in diameter and their size and morphology depends on the depth and size of the gas accumulation that triggers their formation (Judd and Hovland 2007b). A sub-bottom acoustic profile showing a mud diapir associated with faults in the Gulf of Cadiz, is shown in Figure 5F. (Fernandez-Puga, et al. 2007).

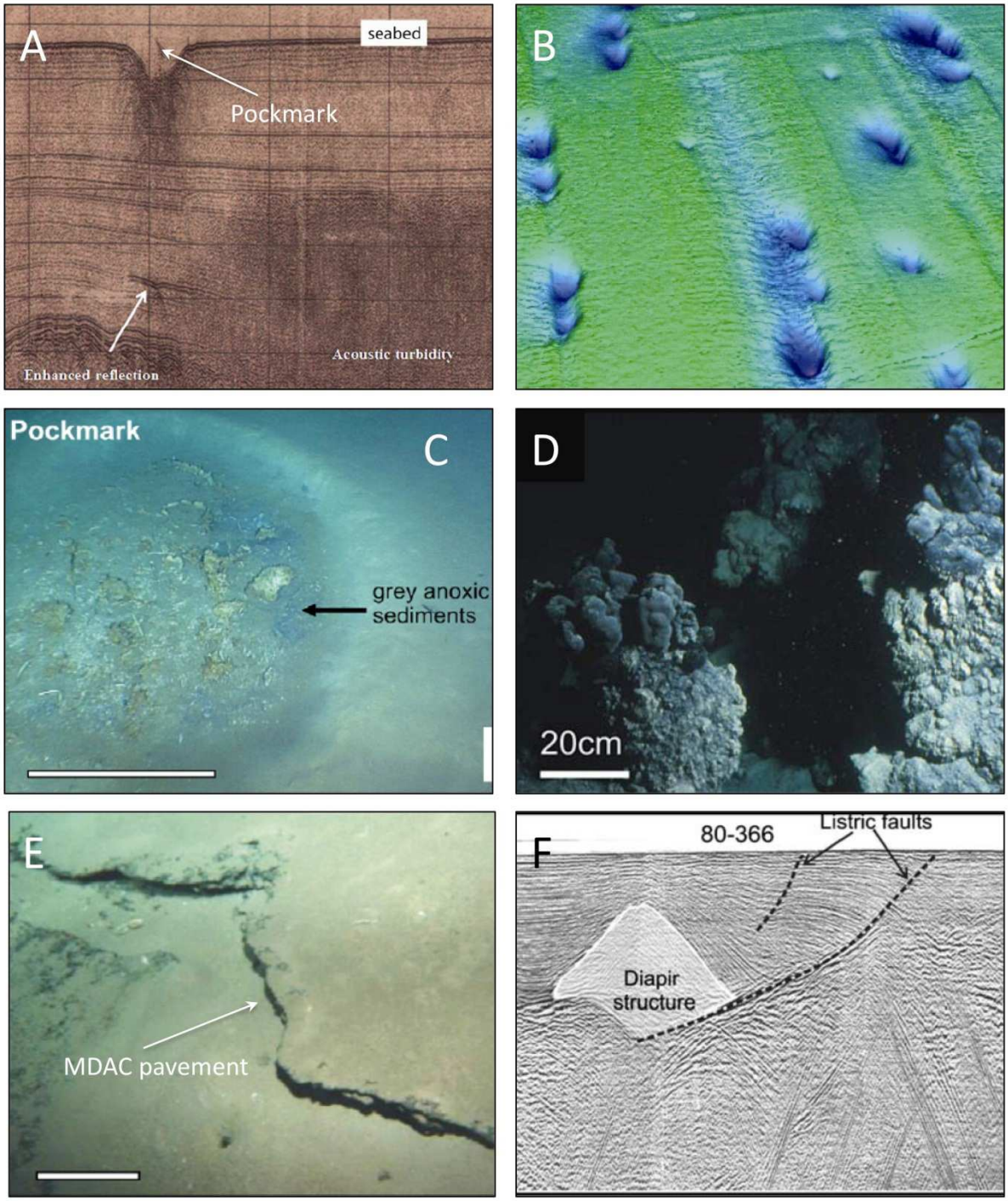

Figure 5: (A) Boomer seismic profile across the Witch's Hole pockmark, North Sea, showing various seismic signals of gas accumulations (Judd and Hovland, 2007). (B) Multibeam echosounder (MBES) bathymetric map showing numerous pockmarks, Witch Ground Basin, North Sea (Judd and Hovland, 2007). (C) Underwater image of 3m diameter unit pockmark, Central Nile deep sea fan, containing anoxic sediment, authigenic carbonates and vestimentiferan tubeworms. The scale bar represents 1m. (Bayon et al., 2009) (D) Underwater image of methane-derived authigenic carbonate (MDAC) mounds, Black Sea (Reitner et al., 2005) (E) Underwater image of massive MDAC pavement, Central Nile deep sea fan (Bayon et al., 2009). The scale bar represents 1m. (F) Seismic profile showing a mud diapir, Gulf of Cadiz, associated with Listric faults (Fernandez-Puga et al., 2007)

2.5 The marine sedimentary biosphere

Life was traditionally divided into two domains based on those that had a true nucleus (the eukarya) and those that did not (prokarya). However Woese and Fox (1977) revolutionized this concept by introducing a third domain, called the archaebacteria, now called the archaea as illustrated in Figure 6. Important representative groups of each domain are also shown. The Last universal common ancestor (LUCA), which is the unknown organism from which the three domains diverged, is also shown. Together with the bacteria, they now comprise the prokaryotes (Woese and Fox 1977). The consequences and importance of this are both far-reaching and not yet fully comprehended but two important consequences to consider are that the archaea are more closely related to the eukarya than the bacteria, and that from the LUCA, which is thought to reside very early within the Bacterial domain, all life forms evolved and diversified (Madigan et al. 2012).

When discussing microbial diversity and ecology it is necessary to categorize microbes in terms of their metabolic diversity, since all cells require an energy source and a means of obtaining this energy in order to fuel life processes. Chemoorganotrophs obtain energy from the aerobic or anaerobic oxidation of organic compounds and storage of this energy in the energy-rich bonds of adenosine triphosphate (ATP). Some of these are strict (obligate) aerobes/anaerobes while others are facultative. Chemolithotrophs on the other hand oxidize inorganic compounds such as H_2, H_2S, NH_3 and Fe^{2+}. Phototrophs in contrast to chemotrophs do not require chemicals for energy but convert light to energy by photosynthesis. Oxygenic photosynthesis produces O_2 and is characteristic of cyanobacteria and algae, while anoxygenic photosynthesis does not, and is performed by microbes such as purple and green bacteria. Furthermore microbes can be divided based on their requirement for carbon – heterotrophs, which obtain C from organic compounds, and autotrophs use CO_2 as their C source (Madigan et al. 2012).

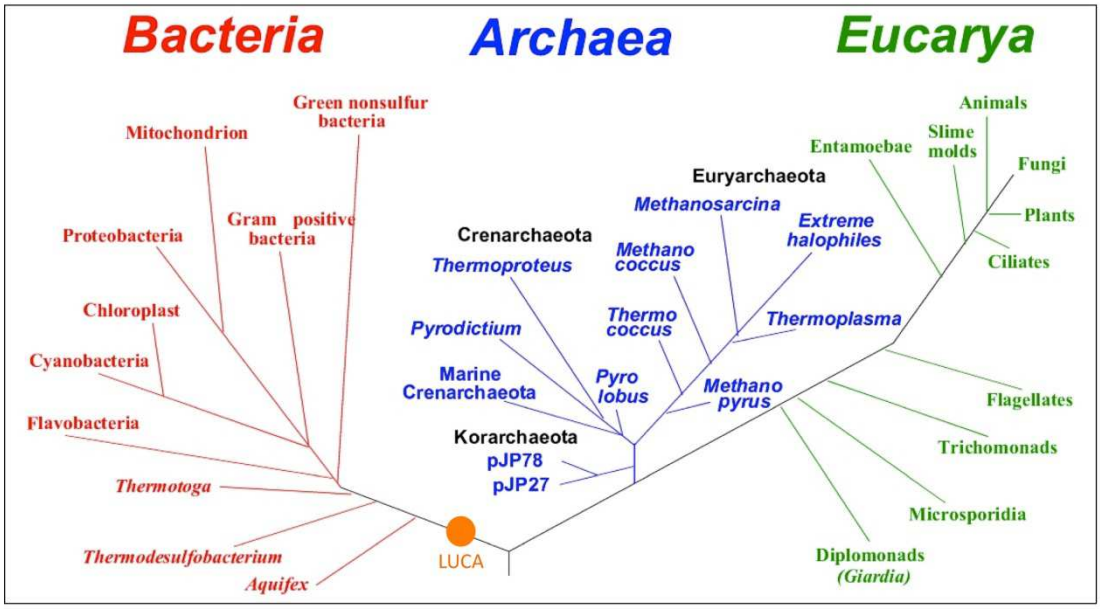

Figure 6: The phylogenetic tree of life as defined by comparative rRNA gene sequencing. The three domains of life – the Bacteria, the Archaea and the Eucarya are shown, along with a number of important representative groups. LUCA – Last universal common ancestor. (Figure adapted from Madigan et al., 2012)

Knowledge of microbial life in the seabed is still in its infancy and only since the 1950's has significant breakthroughs occurred, including: the discovery of millions of viable bacteria per gram of sediment at water depths of over 10,000m, the discovery of core material of high microbial diversity from subsurface sediments and the oceans crust during the Deep Sea Drilling Project in 1968; to the discovery by the ROV *ALVIN* of hydrothermal vents or 'black smokers' of rich biodiversity at the Pacific mid-oceanic ridge (Jorgensen and Boetius 2007). The marine subsurface is one of the most extensive microbial habitats on earth, whereby marine sediments cover more than two-thirds of the Earths's surface and microbial cells and activity are widespread in these sediments (Teske and Sorensen 2008). In sites of particular nutrient and energy abundance microbial life can thrive, for example at huge bacterial mats (Figure 7A.). In tandem with the decreasing abundance of light and availability of labile OM microbial abundance decreases with water depth (Madigan et al. 2012) as shown for bacteria in Figure 7C. Compared with the water column, the ocean seafloor provides a vast area of solid surfaces and heterogenous pore spaces, a high concentration of detrital organic matter per unit volume to support microbes. In addition transport processes, such as mixing and advection, which may limit microbial growth in the water column, are also normally limited to a few centimetres

per year. Accordingly seafloor sediments contain 10 – 10,000 fold more cells per unit volume than productive ocean-surface waters (Jorgensen 2006). This literature review shall focus on what is known about the prokaryotic domains of the bacteria and archaea inhabiting the ocean's seafloors.

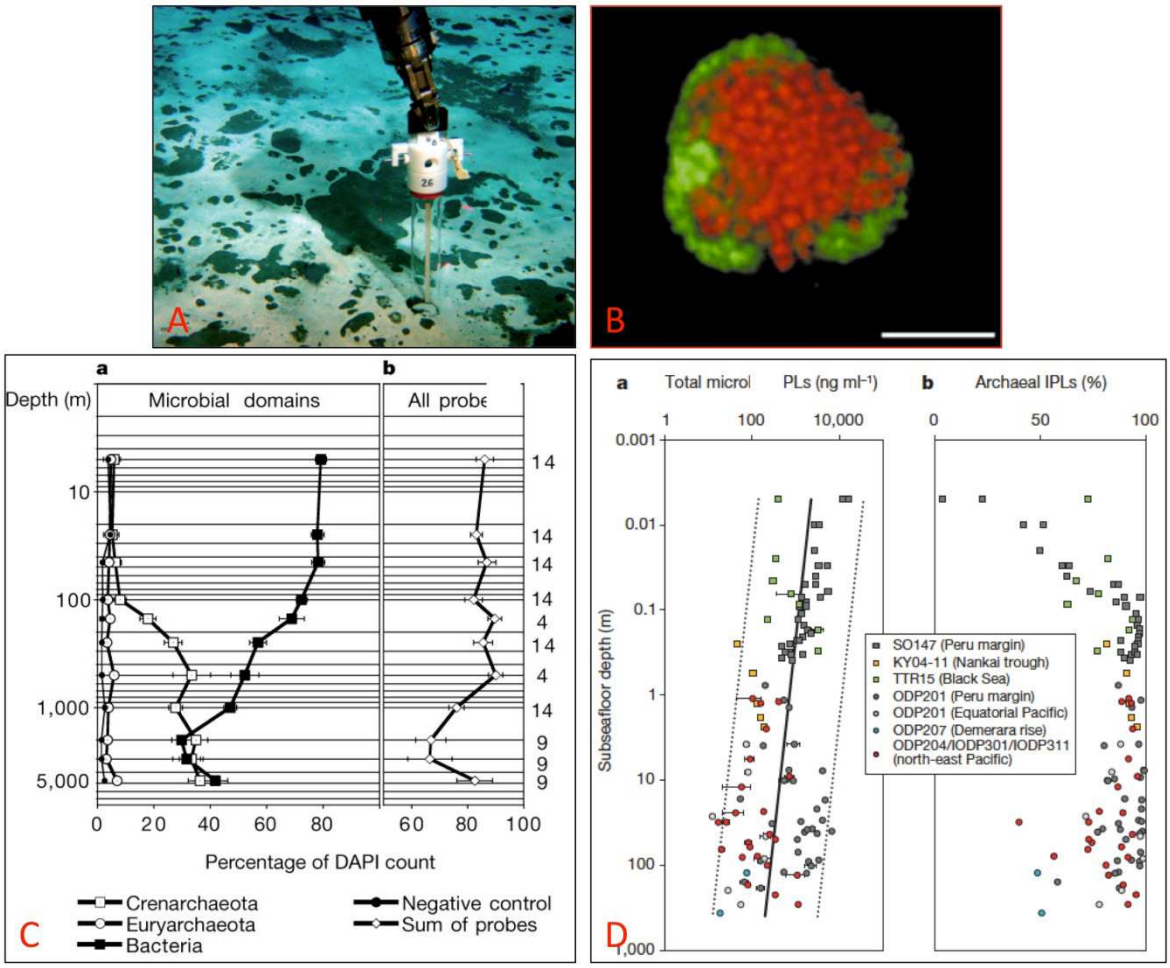

Figure 7: (A) Remotely operated vehicle sampling a deep sea bacterial mat, Haakon Mosby Mud Volcano (IFREMER, France). (B) Fluorescent in-situ hybridization (FISH) identification of an archaea (red)/sulphate-reducing bacteria (green) aggregate apparently mediating anaerobic oxidation of methane (AOM). (Boetius et al., 2000) (C) [a] Mean annual water depth profiles (log scale) of crenarchaeota, euryarchaeota and bacteria in the North Pacific Ocean. Numbers on x-axis represent percentage of total abundance, which was measured using the DAPI nucleic acid stain. [b] Corresponding depth profile of total bacteria, crenarchaeota and euryarchaeota. (Karner et al., 2001) (D) [a] Subseafloor depth (log scale) profiles from a number of locations of total intact polar lipids (IPL's) and [b] relative contribution of archaeal IPL's to total IPL's (Lipp et al., 2008)

2.5.1 Seabed prokaryotic abundance and diversity

Bacteria appear to comprise a large fraction of the total microbial community in the photic zone of the oceans, as illustrated in the North Pacific Ocean in Figure 7C. However bacterial dominance has been shown to decrease below the photic zone, whereby the archaeal abundance, specifically the group crenarchaeota, increases with depth (Karner, DeLong and Karl 2001). In the seabed the archaea, in terms of cell

biomass (based on intact polar lipids, see section 1.6.4 for more information), seem to comprise a small proportion of the total microbial community of the oxic seafloor, while bacteria dominate (Figure 7D). However in the subseafloor, archaea have been shown to increase in abundance and may even dominate (see section 1.6.4 for more information) (Lipp, et al. 2008).

The bacteria domain hosts an enormous variety of prokaryotes, with a diverse range of morphologies and physiologies. Currently the largest phylum is the Proteobacteria. The gram-positive phylum of bacteria includes *Bacillus, Clostridium, Streptomyces, Lactobacillus and Streptococcus*. The Cyanobacteria are phylogenetic relatives of the gram-positive bacteria and are oxygenic phototrophs. Two other major phyla are the green sulfur bacteria and the green nonsulfur bacteria. Species in these phyla are autotrophic. Other major bacterial phyla include the *Chlamydiae*, the *Deinococcus-Thermus*, the *Flavobacteria*, the *Thermatoga*, the *Thermodesulfobacterium* and the *Aquifex* groups. The proteobacteria appear to dominate the marine sedimentary environment in many cases. In deep gas hydrate-bearing sediments in the Cascadia margin, proteobacteria comprised 96% of all bacterial clones (Marchsei, 2001). Most marine bacterial groups described by culture-independent methods have not been cultured in the lab. Among those cultured the most common are Alphaproteobacteria within the Roseobacter lineage. They occur in samples ranging from plankton, sediments, sea ice to animal surfaces and typically comprise 20% of communities in coastal waters, 15% in mixed layer ocean communities and less than 1% in waters deeper than a few hundred metres (Fuhrman and Hagstrom 2008). In many cases the Gammaproteobacteria have been cultured and include members of the *Vibro, Alteromonas, Pseudoalteromonas, Marinomonas, Shewanella, Glacieola, Oceanospirillum and Colwellia* sp. These cultured organism have shown a tendency for rapid potential growth rates, display a large versatility for inorganic electron acceptors and are seemingly well suited to feast-and-famine lifestyles (Fuhrman and Hagstrom 2008). The Betaproteobacteria are a large group (perhaps 75 genera) of heterogenous and primarily uncultured bacteria, which appear to have diverse metabolic capabilities (Madigan et al. 2012).

While marine subsurface archaea are now thought to be the most dominant microbial domain of the deep marine subsurface (Lipp, et al. 2008, Biddle, et al. 2006), they consist almost exclusively of uncultured, distinct phylogenetic lineages that have only been discovered in recent years (Vetriani, et al. 1999). The diverse

range of archaeal metabolisms and extremophile physiologies have evolved as adaptations to energy limitation in extreme environments and their importance is highlighted by the fact that according to current knowledge, the production and consumption of methane in marine sediments, which is one of the most widespread and important biogeochemical processes in sediments, is mediated by certain archaea (Teske and Sorensen 2008).

Based on molecular approaches marine subsurface archaea have been divided into a number of lineages. The Marine Benthic Group B (MBG-B) was proposed by Vetriani et al. (1999) and it represents one of the most dominant archaeal lineages in 16s rRNA archaeal clone libraries. This group is synonymous with another group, called the Deep-Sea Archaeal Group (DAG), which was proposed by Inagaki et al. (2003). DSAG/MBG-B archaea have been detected and shown to be metabolically active in a wide variety of anoxic marine environments including methane-consuming Black Sea microbial mats and carbonate reefs (Knittel, et al. 2005), surficial methane seeps in the Gulf of Mexico (Llyod, Lapham and Teske 2006), deep-sea sediments from the Okhotsk Sea (Inagaki, et al. 2003), hydrate-bearing sediments of the Pacific Margin and in the Nankai Trough (Inagaki, et al. 2006), organic-poor subsurface sediments from the Equatorial Pacific (Sorensen, Lauer and Teske 2004) and in diverse hydrothermal vent sites (Takai and Horikoshi 1999). The Ancient Archaeal Group (AAG) and the Marine Hydrothermal Vent Group (MHVG) are two recently described groups, which currently have only been detected in a few studies. They appear to share the vent and subsurface habitat with the DSAG/MBG-B group. These groups were originally detected in hydrothermal vent sites near Japan (Takai and Horikoshi 1999) but have since been described in cold, organic-rich Peru Margin subsurface sediments at ODP site 1227 (Sorensen and Lauer 2006).

The Miscellaneous Crenarchaeotic Group (MCG) is another group, which are one of the most predominant groups in archaeal 16S rRNA clone libraries from marine deep subsurface sediments, and is known to be metabolically active. In contrast to the DSAG/MBG-B group, the MCG archaea have a more diverse habitat range that includes terrestrial and marine, hot and cold, surface and subsurface environments (Teske and Sorensen 2008). Due to the rapidly increasing number of MCG clones from different environments this group has been sub-divided into numerous subgroups, which will not be discussed here (see Teske et al., 2008 and references therein). The Marine Group I (MG-I) archaea account for a major fraction

of all prokaryotic picoplankton in seawater (Karner, DeLong and Karl 2001, DeLong 1992), but are also known to exist in the subsurface at organic-poor open ocean sites in the Equatorial Pacific (Teske 2006) and in the Peru Margin (Sorensen, Lauer and Teske 2004). Some members of this group have been cultured and indicate that at least some of this group are aerobic, chemolithoautotrophic, nitrifying archaea that oxidize ammonia to nitrite (Teske and Sorensen 2008). The South African Goldmine Euryarchaeotal Group (SAGMEG) was originally described in the deep terrestrial subsurface in South African Gold mines (Takai, et al. 2001), but were subsequently found in deep marine hydrate-bearing sediments (Reed, et al. 2002), in marine subsurface sediments in the Sea of Okhotsk (Inagaki, et al. 2003), and in marine sediments on the Peru Margin (Inagaki, et al. 2006). Other groups including the Marine Benthic Groups A and D (MBG-A and MBG-D) are crenarchaeotal groups, the Terrestrial Miscellaneous Euryarchaeotal Group (TMEG) and the Miscellaneous Eurarcharotic Group (MEG) (previously known as Deep-Sea Hydrothermal Vent Euryarchaeotal Group 6) (Teske and Sorensen 2008).

2.6 Methodology

1.6.1 Seismic profiling

Seismic profiling of the seabed is achieved by reflecting an acoustic pulse from hull-mounted or towed instruments, which is received and processed to produce 2D profiles of time (with geographical coordinates) against two-way travel time, according to Equation 2.

$$D = \frac{vt}{2} \qquad \text{(Equation 2)}$$

where D is the water depth (m), v is the pulse velocity in water (ms^{-1}), and t is the pulse travel time (s). Laterally continuous reflections of a sub-bottom profile represent zones of contrasting acoustic impedance, or sedimentary and/or rock interfaces. Penetration and resolution are two of the most important parameters for seismic investigations of the seafloor and sub-seabed (Judd and Hovland 1992). Low frequency signals achieve greater penetration as they are not attenuated as much as high frequency signals, while resolution of adjacent features is best determined by the time duration and frequency range of the pulses, and is best achieved by using high frequency pulses. High frequency instruments such as pingers and boomers can

resolve sediment layers of less than 1m thick but generally can only penetrate much less than 50mbsf. Figures 5A and 5B show examples of boomer profiles of the sub-seabed after processing. Low frequency instruments such as airguns can penetrate through several layers of sediment and/or rock, but have limited resolution. Echo sounders and side scan sonar instruments generally operate on much greater frequencies and have very limited resolution but can provide high resolution seafloor topography (Judd and Hovland 1992). Figure 5B shows an example of a processed multibeam echosounder bathymetry map.

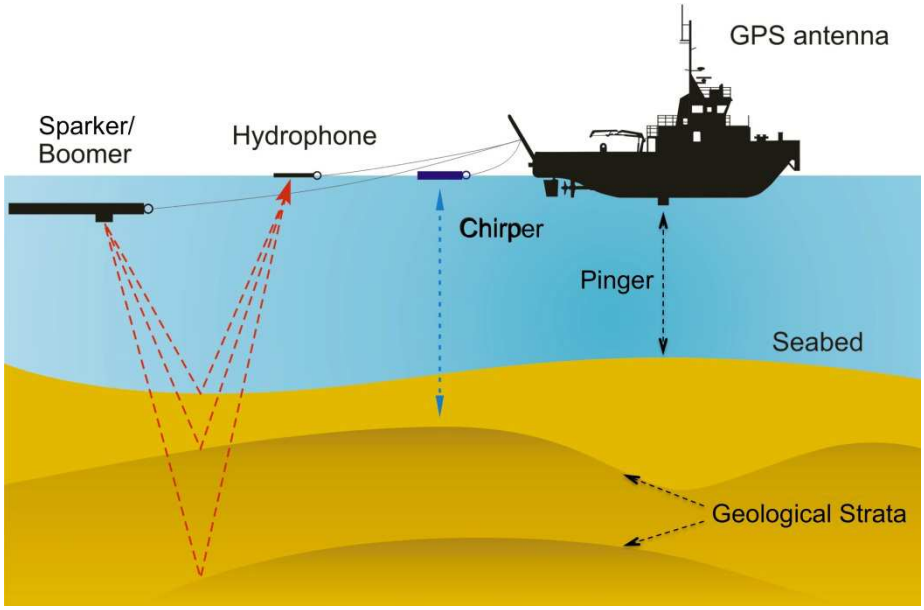

Figure 8: Schematic diagram of seabed and sub-seabed acoustic profiling at sea. (Figure modified from Wessex Archaeology, 2010 [http://ets.wessexarch.co.uk/recs/how-we-study-the-seafloor/geophysical-survey/]).

Shallow gas flow and accumulations have a significant effect on seismic sound velocity, reducing it by as much as one-third the speed in gas-free sediments. Thus there are a variety of signatures in acoustic sub-bottom profiling which indicate the presence of gas and include: acoustic turbidity, which appears as regions of chaotic reflection and absorption and can be observed in sediments with as little as 1% gas; acoustic blanking, which appears as regions of weak/absent reflection in sub-bottom profiles and is believed to be caused by overlying gas-charged sediments and/or disruption of sediment layers by migrating pore fluids; and gas chimneys or columnar disturbances, which appear as vertically extended disturbed sub-bottom reflectors believed to be formed by vertical migration of gas or fluid (Croker, Kozachenko and Wheeler 2005, Judd and Hovland 1992). Gas fronts are common occurrences whereby gas-charged sediments form sharp boundaries with surrounding

sediment. In addition to video camera, geochemical and biological methods gas escape to the surface and the associated features i.e. pockmarks, mud volcanoes, mud diapirs can be identified by sidescan sonar and single and multi-beam echosounder (Yuan and Bennell 1992).

2.6.2 Sampling

An in-depth discussion of the seabed sampling techniques used in marine research is beyond the scope of this literature review. A very brief introduction to the main methods employed for coring and grab sampling sediments is given here. Images of common sediment sampling tools used are shown in Figure 7. A box corer (Figure 7A.) is a sampling tool used primarily for sampling soft surface sediments with minimal disturbance. This is an important sampling tool for quantitative investigations of benthos micro- and macrofauna, for geochemical studies of the sediment/water interface for example. Sampling surface area ranges between 200cm^2 and 2500cm^2 and penetration depths between 20 and 50cm depending on the instrument size. Grab samplers are important sampling tools. A Van Veen grab (Figure 7B.) consists of two semi-circular buckets with a long arm attached to each, and is designed primarily for macrofaunal benthos. A day grab (Figure 7C.) consists of two semi-circular buckets attached within a pyramidal frame with an 80-90cm square base, and is designed to sample a wide range of sediments from muds to mixed gravel. A shipek grab (Figure 7D.) consists of two concentric half cylinders, whereby the outer cylinder samples the sediment and is designed to collect a wide range of sediment types from fine-grained soft sediments to gravels. Sediment cores are of particular importance for investigating subsurface and deep sedimentary layers and also allow paleoclimatic studies. A gravity core is a type of coring instrument designed to collect a 1-2m (and greater) core for investigation of the subsurface sedimentary layers. The steel barrel containing the plastic core liner penetrates the seafloor by virtue of its own weight (additional weight can be added to improve recovery). It is best suited to fine grained sediments and not so for hard substrates. A vibrocore (Figure 7F.) is a type of coring tool designed for use in coarse grained or highly compacted sediments, whereby the steel core barrel is driven into the sediment by a vibrating motor. Typical core barrels are 3m and 6m. In contrast to the gravity corer, the use of the vibrocore is restricted to calm conditions.

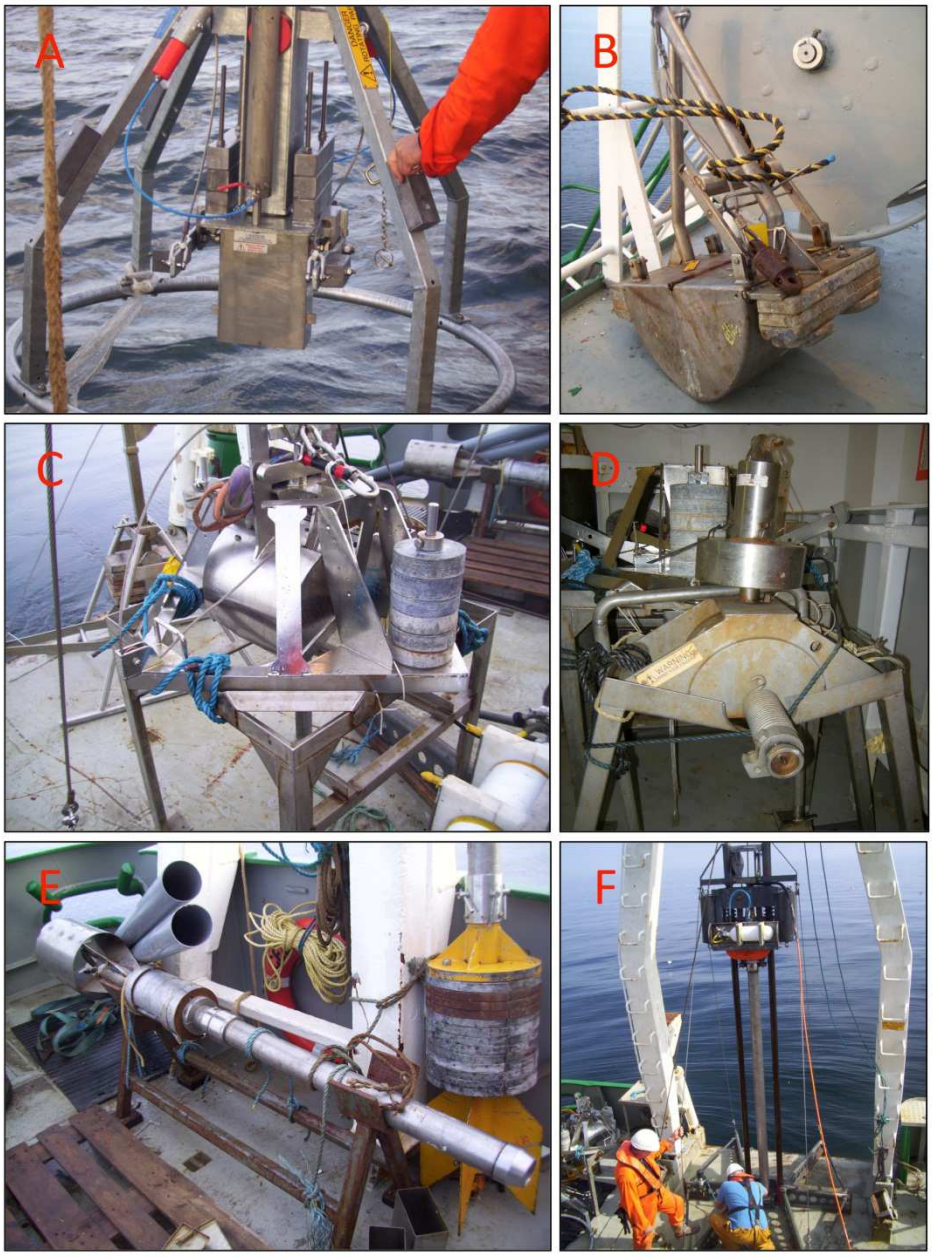

Figure 9: Marine Institute seabed sampling equipment: (A) Reineck box corer, (B) Van Veen grab, (C) Day grab, (D) Shipek grab, (E) Gravity corer (1 metre), (F) GeoResources 3000 vibrocorer (3 metre) (Photographs – Shane O'Reilly)

2.6.3 Pore water analysis

Pore water analysis is extremely important because pore waters are very sensitive indicators of early and developing diagenetic changes in the solid sedimentary phase, and analysis or pore waters is methodologically far easier to perform and interpretation of results less ambiguous (Berner 1980). The following sections shall outline and discuss the general approaches for sampling, preserving and analyzing important pore water analytes. Interstitial CH_4 analysis will also be discussed in this section. Interpretation of interstitial water profiles can be complex and is a discipline

in itself, which may employ advanced mathematical expressions and modeling (Schulz 2006) and shall not be discussed here.

2.6.3.1 Sampling and preservation

The traditional method for sampling of pore waters from sediment cores is by cutting a short whole round section (typically 5-15cm) of core and applying pressure using a hydraulic press to squeeze interstitial porewater, followed by filtration (Schulz 2006). This a labour intensive process and limits sampling resolution, thus hindering the amount of information that can be achieved from the sedimentary record (Dickens et al. 2007). Rhizon samplers (Rhizosphere Research Products, NL-6706 Wageningen) consist of a hydrophilic porous polymer tube (5 or 10cm in length), with a typical pore diameter of 0.1μm, extended with a polyvinyl chloride polymer tube. A supporting wire is connected to one end of the porous polymer. Advantages compared with other pore water sampling methods include: the pore size ensures extraction of microbial- and colloidal-free, ready-to-analyze solution (Knight, et al. 1998), low mechanical disturbance of sediment due to small diameter (2.4mm), low dead volume (0.5mL), minimized sorption processes on the inert polymer, *in-situ* analysis is possible, and they are reusable once confirmed intact and cleaned with acid/base and water (Seeberg-Everfeldt, et al. 2005).

Preservation of pore water samples is important and will depend on the analyte of interest. For example HS^- is volatile and therefore samples should be obtained with minimal aeration, with the addition of 0.6ml 50mM zinc acetate (per 1.5ml sample) to precipitate the sulphide as zinc sulphide and should be stored in the dark at 4^0C for a maximum of 4 weeks. PO_4^{3-} on the other hand requires different preservation measures. Analysis should ideally commence within 2hrs to prevent microbial metabolism but preservation for up to 4 weeks is possible by acidification of the sample (i.e. 1ml 4M H_2SO_4/ 100ml sample) or addition of a poison such as chloroform (1-3 drops/ml) or sodium merthiolate. Samples should be stored in glass bottles/vials at 4^0C (Schulz 2006, Gieskes, Gamo and Brumsack 1991). Methane can be sampled in a number of manners but the most common is by sampling a sediment plug from a retrieved core and sealing in a gas tight container. Significant degassing occurs during sampling due to pressure differences from in-situ conditions and limits comparisons between studies and drawing conclusions regarding actual seabed CH_4 concentrations. However the overall profiles and comparison between sites within a

study yield valuable information about geochemical processes and possible seepage. Analysis should ideally be carried out immediately but sealing the sediment plug in an inert atmosphere with a suitable inhibitor of microbial activity (e.g. Hg-containing compounds) permits storage and analysis on land (Schulz 2006)

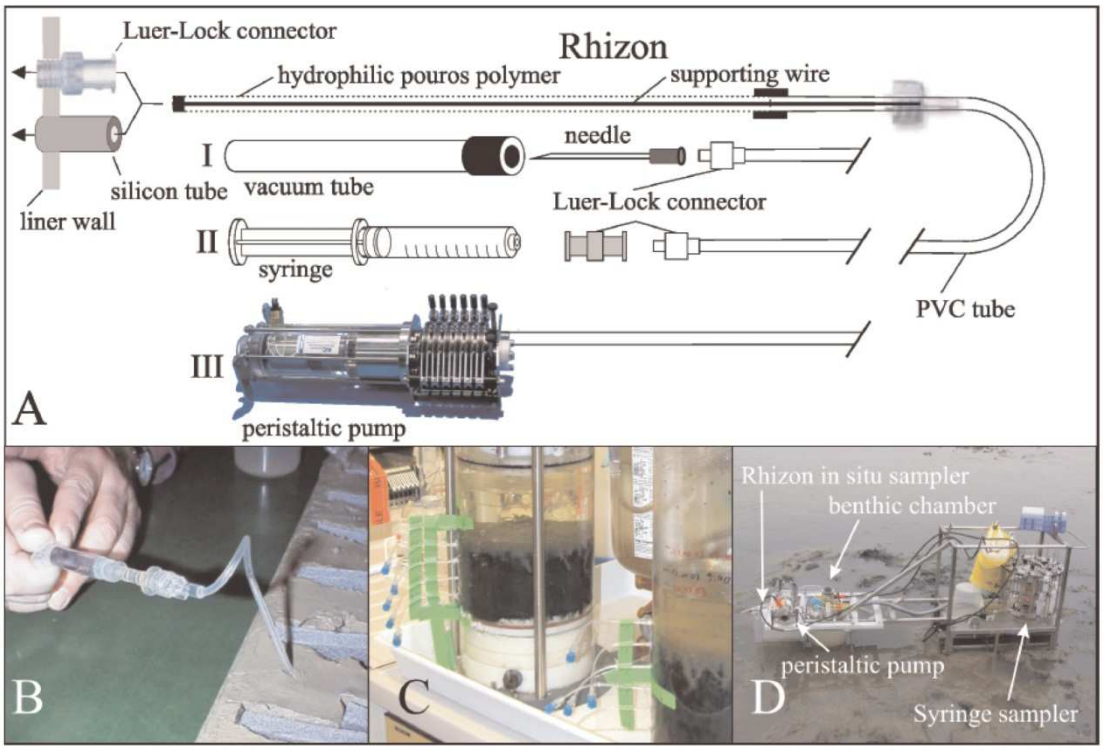

Figure 10: (A) Schematic diagram of a Rhizon and devices used for extraction (vacuum tubes, syringes and peristaltic pumps, I-III). (B) Pore water sampling from a split sediment core, (C) use of Rhizons for pore extraction through pre-drilled holes in a liner or for microcosm experiments, and (D) use of Rhizons for *in-situ* studies using a benthic chamber. (Figure from Seeberg-Elverfeldt et al., 2005)

2.6.3.2 Analysis

An in-depth account of the analytical techniques employed in pore water analysis is beyond the scope of this literature review but a brief account of some of the most important analytes shall be discussed here. The standard method for analysis of SO_4^{2-} is by ion chromatography (IC) (DIONEX®) using a mixture of $Na_2CO_3/NaHCO_3$ as an eluant. An alternative semi-quantitative method is the $BaCl_2$ turbidimetric technique (after stabilization with glycerol) (Gieskes, Gamo and Brumsack 1991). Chloride is normally measured in tandem with SO_4^{2-} by IC. The standard procedure for pore water analysis of HS^- is by the methylene blue method. This involves the compound dimethyl-p-phenylene-diamine forming an intermediate with hydrogen sulfide that transforms to leucomethylene blue. Leucomethylene blue is oxidized to methylene blue by ferric iron. The absorbance of the methylene blue is determined

spectrophotometrically at 664nm. A linear relationship between the absorbance and concentration (i.e. Beer-Lambert Law holds) can be assumed for HS^- concentrations from 0- 1.5mg/L and the absolute upper limit of the method is 20mg L^{-1} (Grasshoff, Kremling and Ehrhardt 1999)

The standard method for analysis of PO_4^{3-} is based on reaction with an acidified molybdate reagent to yield a phosphomolybdate complex, which is then reduced to a blue-coloured compound that can be measured spectrophotometrically at 820nm. Ascorbic acid is used as the reducing agent (Gieskes, Gamo and Brumsack 1991). Reduced iron, Fe^{2+} in weak acid solution (pH3.5 - 5.8) Fe^{2+} forms a violet color complex with Ferrospectral (Merck # 111613) reagent, which can be measured spectrophotometrically at 565nm. Ascorbic acid is the chosen reducing agent. The limit of detection of Fe for this method is approx. 1µg L^{-1} and Lambert-Beer's Law is valid to about 1.2mg L^{-1} Fe (Grasshoff, Kremling and Ehrhardt 1999). The standard for interstitial CH_4 analysis is using gas chromatography with flame ionization detection, and calibration using appropriate gas standards. Specific columns, such as J&W ® HP-PLOTQ (Bonded polystyrene-divinylbenzene stationary phase), are required to analyse CH_4 and $C_2 – C_4$ hydrocarbons(Schulz 2006). Other analytes of interest may be include NH_4^+, NO_3^-, Mn^{2+}, Si^{4+}, alkalinity, Ca^{2+}, Mg^{2+} and the reader is referred to Gieskes et al. (1991) and Grasshoff et al. (1999) for discussion of the analysis of these analytes and also more in-depth accounts of pore water analysis methods discussed above.

2.6.4 Lipid biomarker analysis

The study of specific organic compounds, often termed 'biomarkers', has become highly popular for past climatic and environmental conditions and past biological assemblages (Eglington, et al. 1962, Pancost and Boot 2004). Biomarkers are molecular fossils that originated from once living organisms and they have the basic characteristics of possessing repeating structural subunits, with each parent biomarker being common in certain organisms and with its identifying structure being chemically recalcitrant (Peters, Walters and Moldowan 2005). Relative to soils, marine sediments are much more closed, constant and persistent systems (Hedges and Oades 1997) and thus may be used for dating and reconstructing past environmental conditions over a significant portion of geological history (Hedges and Oades 1997, Pancost and Boot 2004, Rothwell and Rack 2006, Eglington and Eglington 2008).

Lipids possess many of the characteristics essential for biomarkers in that they can be directly extracted and analysed from environmental samples, are highly source specific and chemically recalcitrant (Hedges, Keil and Benner 1997). The most commonly used definition for lipids is that they are a range of compounds that are soluble in organic solvents (Christie 1982). This includes a diverse range of compounds such as fatty acids, steroids, acylglycerols, phospholipids, terpenes, carotenoids and fat-soluble vitamins. Lipids can be divided into two broad classes; simple or complex, or more commonly in chemistry as neutral or polar. Simple lipids can be hydrolyzed to give one or two hydrolysis products while complex lipids can be hydrolyzed into three or more (Christie 1982). The focus of this review will be on lipids that are used as biomarkers in organic geochemistry and microbiology, in particular in the marine environment. Examples of typical biomarkers, and their structures, used in this field are given in Figure 11.

The most common plant and animal fatty acids are those ranging from approximately 14-24 carbons, with predominantly even number distribution and with a terminal carboxyl group. They may be saturated, unsaturated or polyunsaturated (generally up to 6 double bonds) and usually *cis*-configuration and have a wide range of sources. Plant fatty acids are more complex than animal fatty acids and can contain a variety of functional groups (e.g. acetylenic bonds, epoxy-, hydroxy-, keto- groups and cyclopropene rings). Bacterial fatty acids are usually saturated or monounsaturated (Christie 1982) and are considered the major source of *iso*-, *anteiso*-, cyclopropyl and mid-chain branched fatty acids in marine ecosystems (Volkman 2006). C_{18}-C_{22} polyunsaturated fatty acids (PUFA) are present in almost all marine organisms but their primary source if from microalgae. For example diatoms and eustigmatophytes are rich in 20:5(*n*-3) (eicosapentaenoic acid, EPA), moderate levels of 20:4(*n*-6) (arachidonic acid, AA) and negligible 22:6(*n*-3) (docosahaenoic acid, DHA), while dinoflagellates have high levels of DHA and moderate to high amounts of EPA and their precursors 18:5(*n*-3) and 18:4(*n*-3) (Volkman 2006).

Long chain *n*-alkanes with a strong odd carbon number predominance are established biomarkers for terrestrial higher plants, while *n*-C_{15}, *n*-C_{17} and *n*-C_{19} are indicative of algal organic matter (Volkman 2006). Wax esters usually consist of straight-chain saturated or monounsaturated compounds up to C_{30} fatty acids esterified to long chain primary alcohols, but branched and hydroxy fatty acids and monounsaturated, branched, secondary alcohols and dohydroxy alcohols have also

been found. Wax esters are found in animals and insect secretions, as protective coatings on plant leaves and fruits and also in lipid membranes of algae, fungi and bacteria (Christie 1982). Acylglycerols are simple lipids consisting of glycerol ester-linked to one, two or three fatty acids. Triacylglycerols are by far the most abundant single lipid class, while di- and monoacylglycerols are usually present in trace amounts in fresh animal and plant tissue. However diacylglycerols are important biosynthetic precursors of triacylglycerols and comple lipids (Christie 1982). Sterols and their derivatives are ubiquitous in marine environments and sources are diverse and include microalgae, plants and animals. Microalgae are the primary source of sterols in the marine water column and often in marine sediments (Christie 1982).

Lipids are also of considerable use in assessing microbial diversity and community structure, by analyzing intact membrane polar lipids (White, et al. 1979). Phospholipids are key components of all biological membranes, and are composed of glycerol bonded to at least one O-alkyl, O-acyl or O-alkyl-1'-enyl and one polar head group. The most common include phosphatidylcholine, phosphatidyletanolamine, phosphatidyl serine (which all contain one nitrogenous base) and phosphatidyl inositol. (Christie 1982) One of the most important and developed use of lipids as biomarkers is phospholipid fatty acid analysis (PLFA), whereby profiles of PLFA fatty acid methyl esters (FAMEs) have taxanomic utility and are indicative of major microbial input, community composition and changes (White, et al. 1979, White 1983, White and Ringelberg 1998). They can be used as a measure of viable biomass since phosphate groups are rapidly hydrolyzed (minutes to hours) upon cell death (White, et al. 1979). The reader is referred to Killops et al. (2005), Peters et al. (2005) and Volkman et al. (2006) for in-depth discussion of general lipid biomarkers in marine environments (in particular in sediments, petroleum and kerogen), to Christie et al. (1982) for further information on lipids and lipid analysis, and to White et al. (1998), Zelles et al. (1999) and Elvert et al. (2003) for more in-depth discussion of PLFA analysis.

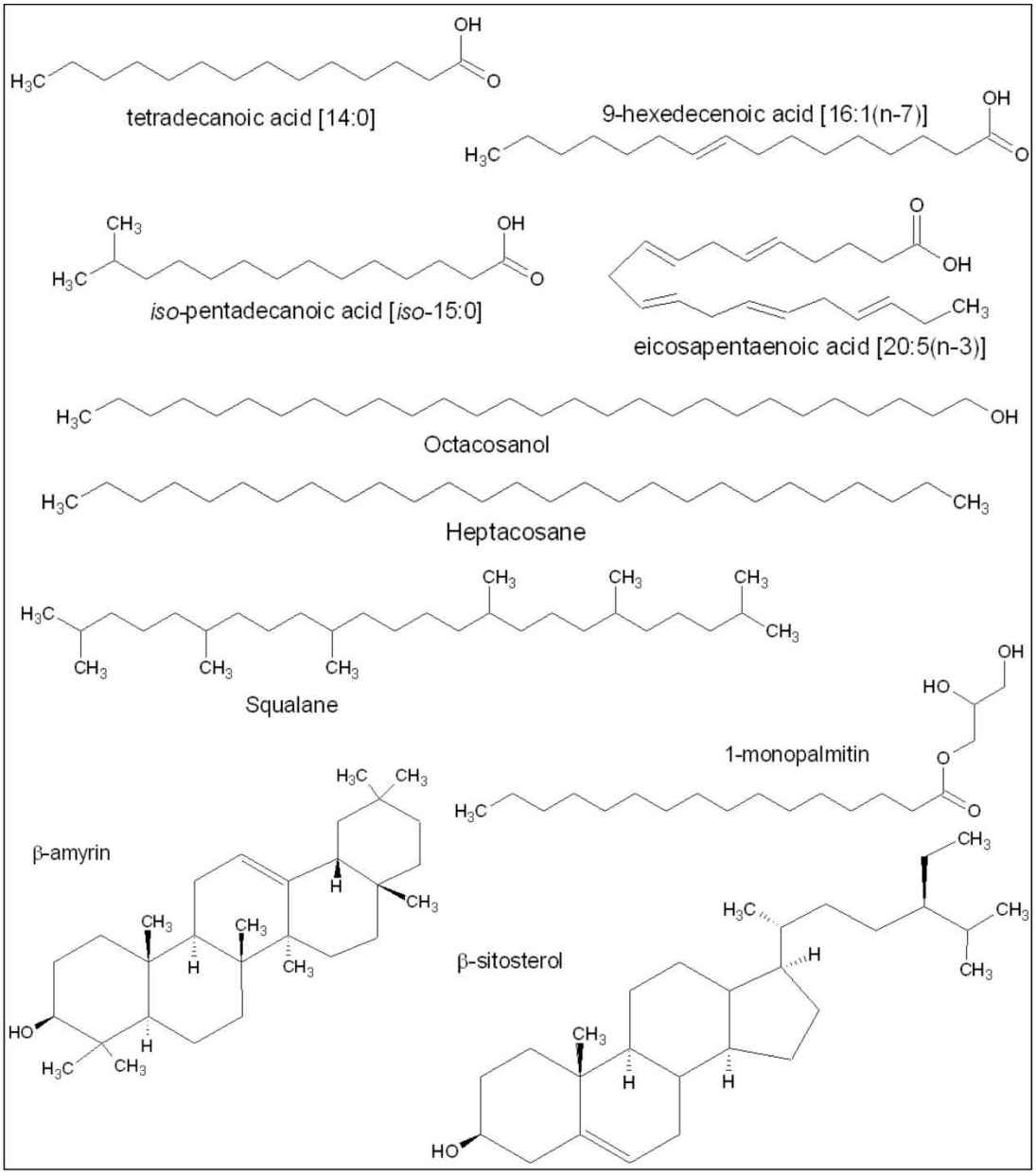

Figure 11: Examples of lipids encountered in environmental samples

2.6.4.1 Extraction from solid environmental samples

Extraction is the transfer, or partitioning, of a solute (*S*) from one phase (1) to another (2). This phenomenon is described by the partition coefficient, shown in Equation 3.

$$K_D = \frac{A_{S_2}}{A_{S_1}} \approx \frac{[S]_2}{[S]_1} = \frac{(1-q)m/V_2}{qm/V_1} \qquad \text{(Equation 3)}$$

where K_D is the partition coefficient, A is the activity of the solute, *S*, in each phase, which when not known is substituted by the concentration of the solute in the relevant phase. Thus the higher the value for K_D the greater the amount of S that remains in phase 1. For two liquid phases K_D can also be expressed in terms of the volume of

each solvent phase, V_1 and V_2, m is the total moles of S, and q is the fraction of S remaining in phase 1 at equilibrium (Harris 2007). Equation 3 can be rearranged in terms of q to express the remaining solute in phase 1 after n number of extractions i.e. the extraction efficiency (Equation 4).

$$q^n = \left(\frac{V_1}{(V_1 + KV_2)} \right)^n \qquad \text{(Equation 4)}$$

A range of extraction techniques exists for the extraction of organic compounds from solids such as soil or sediment and in recent years a number of automated options have been reported and are common (Dean 2003). The two primary features, which affect lipid solubility in organic solvents, are the presence of non-polar moieties such as hydrocarbon chains and polar moieties such as phosphate or sugar residues (Christie 1982). Simple lipids such as steryl esters or triacylglycerols are also called neutral lipids because they do not contain sufficiently polar functional groups and are thus highly soluble in hydrocarbon solvents such as hexane, readily soluble in more polar solvents such as chloroform or diethyl ether and only relatively insoluble in polar solvents such methanol. Chain length however significantly affects solubility, with shorter hydrocarbon chains displaying an increased solubility in more polar solvents and vice versa (Christie 1982). The most widely used solvent mixture for lipid extraction is 2:1 (v/v) chloroform:methanol, which generally offers high lipid yield of varying polarities, but which will vary depending on the sample type i.e. animal tissue, water, soil, sediment etc. (Christie 1982).

The simplest approach is shake-flask extraction whereby various methods of agitation of the sample in a solvent mix include manual shaking in a separating funnel or agitation in an appropriate container (PTFE or glass) on a horizontal shaker. Fresh solvent is sequentially added a number of times after removal of the extract by centrifugation of filtration. Ultrasonic-assisted extraction is similar to the above but includes sonication via a probe or sonication bath. Soxhlet is commonly regarded as the benchmark technique upon which other techniques are compared. The basic setup consists of a solvent reservoir, an extraction body, a heating mantle and a reflux condenser connected to a water supply. Typically 10g of solid is placed in a porous cellulose thimble, this is placed in the inner Soxhlet tube and having connected the

apparatus to the round-bottomed flask containing the extraction solvent mix and the reflux condenser, the sample is extracted with continual recycling of the solvent for 6-24 hours (Dean 2003). The most widely used method for extraction of microbial lipid i.e. phospholipids is the modified Bligh-Dyer method (Bligh and Dyer 1959), which has been subsequently modified further (White and Ringelberg 1998). In this approach the sample is extracted briefly by sonication and subsequently on a hozizontal shaking (2-18 hours) in a monophasic solvent mixture of methanol: chloroform: phosphate buffer (2:1:0.8 v/v). The phase is then split by addition of chloroform and phosphate buffer to achieve a final solvent volume ratio of 1:1:0.9 (v/v) to split the phases. The lipids including polar lipids are partitioned into the lower chloroform phase and removed.

A more recent method that is becoming common for extraction of lipids is accelerated solvent extraction (ASE) (also called pressurized fluid extraction). This technique utilizes the increased solvent extraction capabilities at higher temperatures and pressures, which includes; increased analyte solubility, increased solvent diffusion rates, lower solvent viscosity, improved mass transfer, and a disruption of solute-matrix interactions, and thus increases potential yield, reduces solvent use and long term cost (Dean 2003). The most widely available ASE systems are those offered by DIONEX ® and consist of a solvent supply, a gas supply (usually N_2), an extraction cell and collection vial carousel, sample oven and purge system. They generally operate from 4-200^{0}C and 6.9-20.7 MPa. Other techniques that are not commonly used for lipid extraction from environmental samples include supercritical fluid extraction (SFE) and microwave-assisted extraction (MAE) (Dean 2003).

2.6.4.2 Fractionation of total lipid extracts

Total lipid extracts (TLE) are highly complex mixtures of individual lipid classes and it is generally desired to obtain these classes in as pure a state as possible (Christie 1982). Lipid isolation has generally been carried out by preparative thin-layer chromatography (TLC), adsorbent column chromatography or by high performance liquid chromatography (HPLC). However TLC and column chromatography are time consuming, the TLC process causes oxidation of polyunsaturated bonds in many cases and is sensitive to sample load. Column chromatography requires high solvent volumes, isolation of pure lipid classes in complex mixtures can be difficult by both HPLC and column chromatography, and HPLC equipment can be expensive

(Kaluzny, et al. 1985, Kim and Salem 1990, Ruiz-Gutiérrez and Pérez-Camino 2000). The most popular approach is by liquid-solid chromatography, in particular silicic acid column chromatography or more recently solid phase extraction. These methods generally rely on the principle that lipids are bound to the adsorbent by polar (H-bonding, dipole-dipole), ionic exchange (negative/positively charged interactions between analyte and adsorbent) and/or Van der Waal's forces (C-H links between analyte and adsorbent), followed by subsequent isolation of lipid classes of increasing polarity by a solvent regime of successively increasing polarity.

Kaluzny et al. (1985) developed a method for rapid high purity, high yield (>95% recovery) isolation of lipid classes from complex animal tissue mixtures by solid phase extraction using aminopropyl bonded (-Si-$(CH_2)_3$-NH_2) phase columns and a vacuum manifold. This method (similar to standard SPE approaches in practical terms) involved washing of the column (500mg), conditioning of aminopropyl functional groups using hexane, addition of the lipid mix dissolved in $CHCl_3$ and subsequent sequential elution and collection of lipid classes using solvents of increasing polarity. The method allowed elution of neutral lipids using 2:1 chloroform:isopropanol, free fatty acids by 2% acetic acid in diethyl ether and final elution of phospholids using methanol. Neutral lipids were then subsequently fractionated as follows: cholesteryl esters elution with hexane; triacylglycerol elution with 1% diethyl ether, 10% dichlormethane in hexane elution; sterol elution with 5% ethyl acetate in hexane; diacylglycerol elution with 15% ethyl acetate in hexane; and final elution of monoacylglycerols with 2:1 (v/v) chloroform:methanol (Kaluzny, et al. 1985).

This method has been extensively used and modified for specific requirements (Kim and Salem 1990, Ruiz-Gutiérrez and Pérez-Camino 2000, Bernhardt, et al. 1996, Rizov and Doulis 2001, Giacometti, Milosevic and Milin 2002). Of note is the optimization of the above methods for separation of microbial lipids mixtures (Pinkart, Devereux and Chapman 1998). Yield and purity of microbial phospolipids was increased by elution of neutral lipids with neat chloroform, which reduced co-elution of phospholipids, and by elution of phospholipids with 6:1 (v/v) methanol:chloroform followed by 0.05M sodium acetate in 6:1 (v/v) methanol:chloroform, with the latter increasing yields of acidic phospholipids (e.g. phosphatidylcholine and phosphatidylethanolamine).

2.6.4.3 Gas chromatography-mass spectrometry (GC-MS)

Modern gas chromatography (GC) involves the vaporization and transport of volatile or semi-volatile analytes in a gaseous mobile phase (usually with He as the carrier gas) through a capillary column containing a stationary phase of a bonded non-volatile liquid (or solid), whereby analytes are separated based on relative affinities for stationary phase functional groups. A GC broadly consists of an injector, the carrier gas, a column, an oven and a detector. A wide variety of columns and stationary phases types are available but the most commonly used columns are long (15-100m), narrow i.d. (0.1 – 0.5mm) open tubular capillary columns. When compared to other column types (e.g. packed columns) they afford higher resolution, reduced analysis time, greater sensitivity but lower sample capacity. These typically consist of fused silica (SiO_2) coated with polyimide, to which a 0.1 - 5μm non-volatile liquid (or less commonly, solid) stationary phase is bonded to the inner column wall (Harris 2007). Capillary GC stationary phases are categorized based on their polarity, and common non-polar phases include (phenyl)-dimethylpolysiloxane, intermediate phases include (cyanopropylphenyl)-dimethylpolysiloxane, and polar phases include poly(ethylene glycol) (commonly called carbowax). There are a number of important parameters to consider when attempting to optimise chromatographic separation and these are summarized in Table 1.

The first use of gas-chromatography mass spectroscopy (GC-MS) as a hyphenated technique was in 1957, only four years after the first description of GC. Initially packed GC columns were used, which required eluant split systems or concentrators, but today open capillary tubes are used and can be directly passed to the mass spectrometer. Mass spectrometry is a technique for studying the masses of atoms or molecules or fragments of molecules, whereby gaseous analytes are ionized and ions produced are accelerated by an electric field and separated according to their mass-to-charge (m/z) ratio (Harris 2007).

Table 1: Important equations for optimization of chromatographic separation

Name	Equation	Parameters
Adjusted retention time	$t'_r = t_r - t_m$	t_r= retention time of solute t_m = retention time of unretained solute
Retention volume	$V_r = (t_r)(u_v)$	t_r= retention time of solute u_v = volume flow rate
Capacity factor	$k' = t_s / t_m$	t_s= time solute spends in stationary phase t_m = time solute spends in mobile phase
Relative retention	$\alpha = \frac{t'_{r2}}{t'_{r1}} = \frac{k'_2}{k'_1} = \frac{K_2}{K_1}$	Subscript 1 and 2 refer to two solutes. t_r= retention time of solute k' = capacity factor K = partition coefficient
Separation factor	$\gamma = t_{r2} / t_{r1}$	t_r= retention time of solute ($\gamma > 1$)
Number of plates	$N = \frac{16 t_r^2}{w^2} = \frac{5.55 t_r^2}{w_{1/2}^2}$	t_r= retention time of solute w= width at base $w_{1/2}$= width at half height
Plate height	$H = \frac{\sigma^2}{x} = \frac{L}{N}$	σ= standard deviation of band x= distance travelled by centre of band L= length of column N = number of plates
Resolution	$R = \frac{\Delta t_r}{w_{av}} = \frac{\Delta V_r}{w_{av}} = \frac{\sqrt{N}}{4}(\gamma - 1)$	Δtr = difference in retention times ΔVr = difference in retention volumes w_{av} = average baseline width (time or volume units) N = number of plates

Ionization techniques in GC-MS are diverse but the most important and most common is electron-impact ionization. This is a harsh ionization method, whereby highly fragmented species are produced after being bombarded by electrons (70 eV) emitted from a tungsten filament. A schematic outline of the components of a typical electron impact ionization mass spectrometer is shown in Figure 12A. The analytes eluting from the GC column pass into a transfer line to the ionization chamber where they are bombarded by electrons from the tungsten filament. Ionized species are then separated by a quadrupole, which consists of four metal rods with specific currents, and allows passage of a specific size of molecules across a predefined mass scan range (often 50 – 650 m/z). The ionized parent molecule, having lost one electron, is termed the molecular ion ($M^{+\cdot}$). The molecular ion usually undergoes further characteristic fragmentation and may be of very low abundance, or even absent, on a mass spectrum. Multiple fragment ions yield high structural information but if the molecular ion is required, and is too low or absent, then softer ionization methods such as chemical ionization can be used (Harris 2007).

Figure 7B. shows a typical total ion chromatogram of FAME's from a lipid extract. Specific mass fragmentation patterns for each lipid type allow identification. Saturated FAMEs show base peaks at m/z 74 and important ions at m/z 87, 143, M^+, M^+-29, M^+-31 and M^+-43 as shown in Figure 7B. (inset). Weak ions due to α-cleavage at branching points are observed on the spectra of *iso* and *anteiso*-branched

FAMEs. MUFA display reduced m/z 74 and 87 ions and enhanced m/z 55 ion, and the M^+ and M^+-33 are also distinguishable. *cis* and *trans* geometries can be identified based on relative retention times, whereby *cis* isomers elute first on non-polar columns.

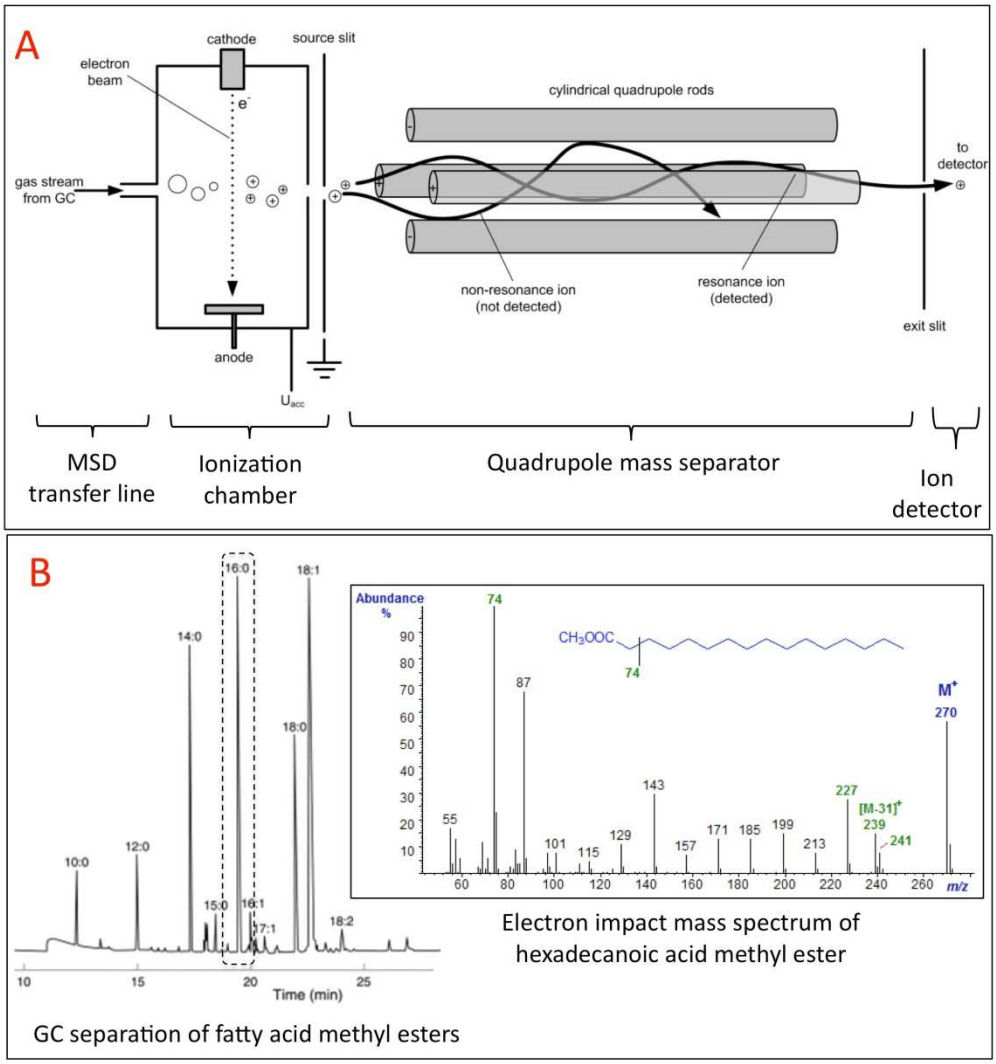

Figure 12: (A) Schematic diagram of a typical electron impact (EI) ionization quadrupole mass spectrometer. (B) Total ion chromatogram (TIC) of fatty acid methyl esters. Inset shows resulting EI mass spectrum for hexadecanoic acid methyl ester (broken box on TIC)

The position of double bonds on the chain are routinely identified by creating dimethyl disulphide adducts (DMDS), whereby two SCH_3 groups are added across the double and show distinct mass spectral ions. PUFA show base peaks at m/z 79 but are more complex to identify based on mass spectra due to a successive decrease in M^+ with increasing number of double bonds. However PUFA generally can be readily identified based on relative retention times, whereby PUFA of the same chain length elute in pairs if they differ by one double bond and the position of the last double

bond differs by 3 carbons (e.g. 20:4(*n*-6) and 20:5(*n*-3)) (Volkman 2006). *n*-alkanes give characteristic mass spectra showing a series of C_nH_{2n+1} ions that decrease in abundance, with base peaks usually at m/z 57, 71 or 85. Another example of diagnostic fragmentation patterns are sterols, which are usually analysed as their trimethylsilyl-ether derivatives. Sterols with Δ^5 unsaturation show base peaks at m/z 129 and fragmentation peaks at M^+-90 and M^+-129, while sterols with $\Delta^{5,22}$ unsaturation shows base peaks at m/z 255 and fully saturated sterols show base peaks at m/z 215 (Volkman 2006)

2.6.4.4 Gas chromatography-isotope ratio mass spectrometry (GC-IRMS)

The isotope-ratio mass spectrometer (IRMS) was first described in the first half of the 20th century (Nier 1939, Murphey and Nier 1941, Wickman 1952) but has only been used as a detector for gas chromatography since the late 1970's (Sano, et al. 1976, Matthews and Hayes 1978). All elements in organic molecules, apart from F, possess two stable isotopes and IRMS is concerned with the light stable isotopes i.e. ^{13}C, ^{2}H, ^{15}N, ^{18}O, ^{34}S, and ^{37}Cl. The relative abundances of these isotopes vary in natural materials due to differences in rates of physical and chemical processes (Sessions 2006). Gas chromatography isotope-ratio mass spectrometry (GC-IRMS) (also referred to as isotope-ratio-monitoring GCMS, continuous-flow IRMS, compound-specific isotope analysis and even carrier-gas IRMS) was first developed for C, followed by N, H and O, and as of yet is not possible for S and Cl. Carbon IRMS is the most popular and developed technique and shall be the focus of this review. A schematic outline of a typical GC-IRMS system is shown in Figure 13. It consists essentially of a coupled system whereby eluted analytes from the GC column flow to a combustion interface (operated at 600 – 850^{0}C) and are combusted to CO_2 over solid CuO. This formed CO_2 then travels through a Nafion membrane assembly to remove H_2O to the MS, whereby by fine-tuned analysis of $^{12}CO_2$, $^{13}CO_2$ and $^{14}CO_2$ (m/z 44, 45 and 46 respectively) is performed using a magnetic sector and Faraday cup setup, as shown in Figure 13. As well as a host of other applications GC-IRMS has become a fundamental tool for studying the source, transport and degradation of OM in the marine setting (Volkman 2006) and also for elucidating marine microbial processes and ecology (Madigan et al. 2012).

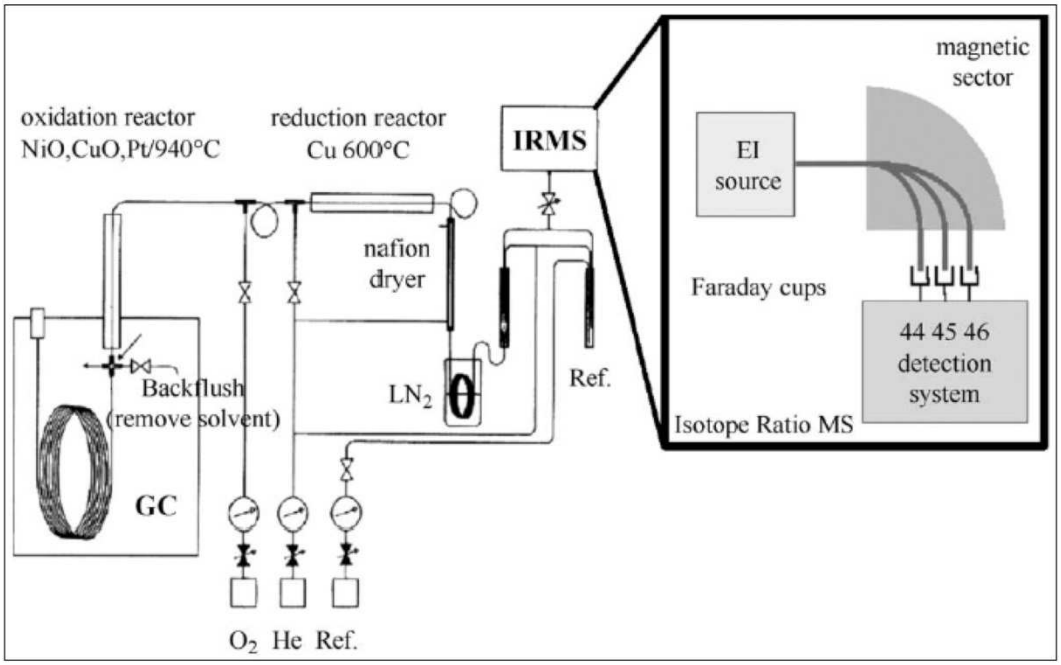

Figure 13**:** Schematic diagram outlining the setup of a typical isotope ratio mass spectrometer coupled to a gas chromatograph to measure $^{13}C/^{12}C$ isotope ratios. (Figure from Meier-Augenstein, 2002).

Natural C is composed of 98.9% ^{12}C and 1.1% ^{13}C, but due to slight differences in energy yield between ^{12}C and ^{13}C, and the corresponding preferential reaction (both abiotic and metabolic) of one isotope species over another, there are slight variations in ^{13}C abundance in environmental C pools (including organisms) (Killops and Killops 2005). Relative abundances of stable isotopes are commonly expressed as 'delta' notation according to Equation 5.

$$\delta^{13}C_{sample} = \left(\frac{R_{sample} - R_{standard}}{R_{standard}} \right) x1000 \text{ ‰} \qquad \text{(Equation 5)}$$

where R is the absolute $^{13}C/^{12}C$ ratio of a sample or standard, and is expressed in units of per mil (i.e. parts per thousand). Positive $\delta^{13}C$ values correspond to enrichment in ^{13}C while negative $\delta^{13}C$ values correspond to depletion. Common standard reference materials for $^{13}C/^{12}C$ are PeeDee Belemnite (PDB), with R= $1.123x10^{-2}$ and Solenhofen limestone (NBS-20) whereby R= $1.1218x10^{-2}$. Stable isotope analysis involves the conversion of analytes to simple molecules by combustion (C and N) or pyrolysis (H and O), which are then analysed and continuously compared to a reference standard by specialized mass spectrometers that maximize for ion beam current and stability (Sessions 2006). Reports has been published detailing the

combustion interface (Merritt, et al. 1995) factors controlling mass spectroscopic precision and accuracy (Merritt and Hayes 1994), methods for isotope calibration (Merritt, Brand and Hayes 1994), fractionation processes in derivatized analytes (Rieley 1994) and data acquisition and processing (Ricci, et al. 1994). For many environmental applications, where complex total ion chromatograms are common, the most important parameter limiting isotopic analysis is separation of chromatographic peaks (Sessions 2006). A detailed account of these is beyond the scope of this review and the reader is referred to these reviews for more in-depth analysis.

2.6.5 Molecular microbial ecology

The vast majority of microbes, well over 99% of all species, have not being cultured under laboratory conditions (Madigan et al. 2012). While culture-dependent approaches were and are important in the study of microbes in the environment, there has been an explosion in research and understanding of microbes and microbial ecology using culture-independent methods in recent years (Burlage 1998). These techniques include: in-situ staining methods, such as with 4,6'-diamidino-2-phenylindole (DAPI), green fluorescent protein (GFP); in-situ hybridization such as with fluorescent in-situ hybridization (FISH); and also molecular methods such as denaturing gradient gel electrophoresis (DGGE) and molecular cloning. It is the latter that shall be discussed further here.

2.6.5.1 DNA extraction and purification

The standard method for separation, identification and purification of DNA is by agarose gel eletrophoresis, which involves separation of DNA primarily based on molecular size (chain length i.e. number of base-pairs) by migration towards the anode in a solid matrix of defined pore size (determined by concentration of agarose) and comparison with commercially available DNA size markers in adjacent lanes. Addition of ethidium bromide, which intercalates with DNA, and subsequent UV transillumination visualization of fluorescent DNA is the standard approach. Gel bands can also be excised and purified by a variety of approaches (Holmes and Peck 1998).

2.6.5.2 Polymerase chain reaction

The polymerase chain reaction allows large-scale amplification of as little as 1 copy of a specific target DNA or RNA sequence. This specificity is achieved by synthesizing and flanking a target sequence with DNA primers, which consist of two oligonucleotides (forward and reverse primers) strands specific for 20-30 base-pairs on either side of the target DNA sequence (Holmes and Peck 1998). The basic principle, as described in Figure 14. involves: denaturation by heating of dsDNA; primer annealing; primer extension and DNA replication between the primers; followed by another full cycle starting with denaturation of dsDNA. This cycle repeats a number of times with exponential increase in the target DNA sequence, for example after 22 cycles about 10^6 fold amplification is achieved (Primrose, Twyman and Old 2001).

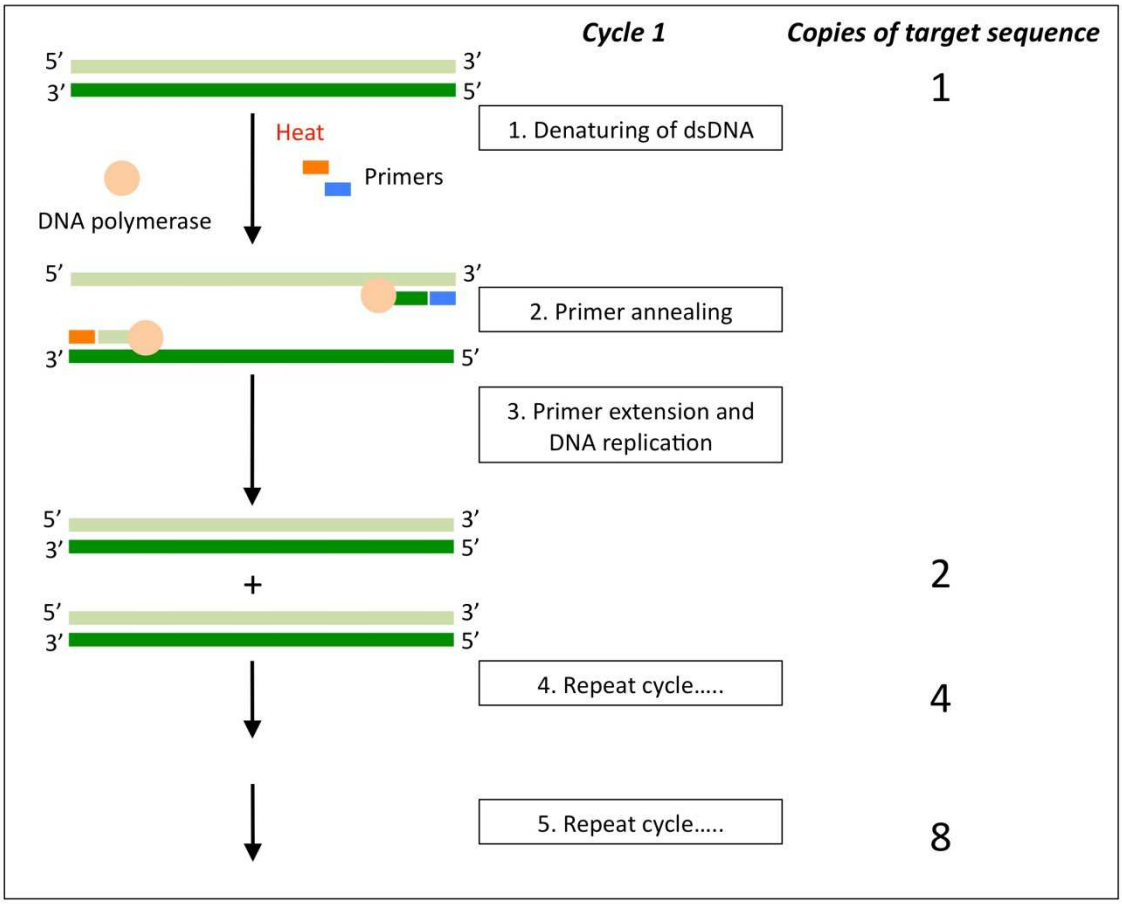

Figure 14: The polymerase chain reaction allowing exponential amplification of a target DNA sequence. Target DNA is heated to separate strands, and upon addition of DNA polymerase and specific forward and reverse primers, primer annealing and extension occurs. One cycle yields two copies of the target sequence and upon repeating the cycle results in exponential amplification of the terget sequence. (figure adapted from Madigan et al., 2012)

The most common polymerase used in PCR is Taq polymerase, which is a thermostable enzyme isolated from the hyperthermophile *Thermus aquaticus*. It has an optimal activity at 70-80^{0}C and is active up to 90^{0}C. This is critical because *Taq* does not need to be replenished after each cycle and it allows automation using highly accurate thermocyclers (Primrose, Twyman and Old 2001). While PCR is an extremely powerful and revolutionary technique, a major limitation in its utility in microbial ecology is that only phylotypes containing matching or closely matching priming sites may be detected. As the number of mismatches increases, amplification efficiency will decrease and hence species with high mismatches will be under-represented or excluded from a metagenomic study (Teske and Sorensen 2008).

2.6.5.3 Denaturing gradient gel electrophoresis (DGGE)

Denaturing gradient gel electrophoresis (DGGE) (Fischer and Lerman 1979, Fischer and Lerman 1983) is a powerful molecular ecological tool that allows the separation of DNA fragments of the same size but with different sequences. Separation is achieved by applying dsDNA to a polyacrylamide gel containing a linearly increasing denaturant concentration and separation of DNA based on the decreased electrophoretic mobility of partially melted double-strands. DNA denaturants used are usually urea and formamide. A related technique called temperature gradient gel electrophoresis (TGGE) involves separation based on temperature gradients. The mechanism for how separation based on sequence variation is achieved is as follows; when the melting domain (stretches of base-pairs with identical melting points) of a DNA fragment with lowest melting temperature reaches its melting temperature at a particular position on a DGGE gel it will transition from a helical to a melted structure and effectively halt migration (Fischer and Lerman 1983). Attachment of a GC-rich sequence (30-50bp) to a DNA fragment allows almost 100% of sequence variants to be detected, since the GC-rich region is a high melting domain and prevents complete dissociation of dsDNA (Myers, et al. 1985, Sheffield, et al. 1989). This is achieved by using specifically designed primers in a nested PCR amplification approach. Melting behaviour and optimal denaturing gradients can be determined using perpendicular gradient gels, while optimal times can be assessed using parallel gels (Muyzer and Smalla 1998).

DGGE is thus a powerful tool for studying microbial community complexity, change and enrichment cultures, among many other applications. DGGE was first

utilized in microbial community profiling by Muyzer et al. (1993) when applied to a microbial mat and bacterial biofilms and since then has become an indispensable tool in microbial ecology (Madigan et al. 2012). One of the primary limitations of DGGE is the limitation of separation to 500bp or less, which restricts the amount of sequence information for phylogenetic analysis and probe design (Muyzer and Smalla 1998). Another limitation is that it is not always possible to separate DNA fragments with certain sequence variations (e.g. (Vallaeys, et al. 1997)) and at best, bacterial populations representing only approx.. 1% of the total community can be detected using PCR-DGGE (Muyzer, de Waal and Uitterlinden 1993). It can also be difficult to retrieve clean and representative sequences from DGGE bands due to co-migration, and finally over estimation of microbial community diversity can be a pitfall due to sequence microhetergeneity (Nübel, et al. 178) and/or double bands caused by degenerative primers in PCR reactions (Kowalchuck, et al. 1997).

2.6.5.4 Molecular cloning

In molecular cloning a fragment of DNA is isolated and replicated after being transferred into a plasmid vector in a host bacterium. The steps involved in molecular cloning are outlined in Figure 15. The major steps are: the isolation of the foreign DNA including the fragment of interest; restriction enzyme cutting of the DNA fragment and vector; ligation of resulting DNA and vector; transformation of ligated plasmid vector into competent cells; plating and culturing of the clone library; culturing of recombinant clones and plasmid extraction; and finally downstream processing, which may include restriction analysis or sequencing. (Madigan et al. 2012). Restriction endonucleases are enzymes utilized for cleaving specific base sequences in dsDNA and breaking phosphodiester bonds between two nucleotides. Over 350 of these have been isolated and fall into groups of four, five or six base recognition sequences. Common examples include *Eco* R1, *Bam* H1 and *Hind III*. DNA ligases are enzymes that catalyze synthesis of phosphodiester bonds between 3’ hydroxyl groups and 5’ phosphoryl groups of two nucleotides and are often applied to covalently bond two strands of sticky-ended DNA fragments (Holmes and Peck 1998).

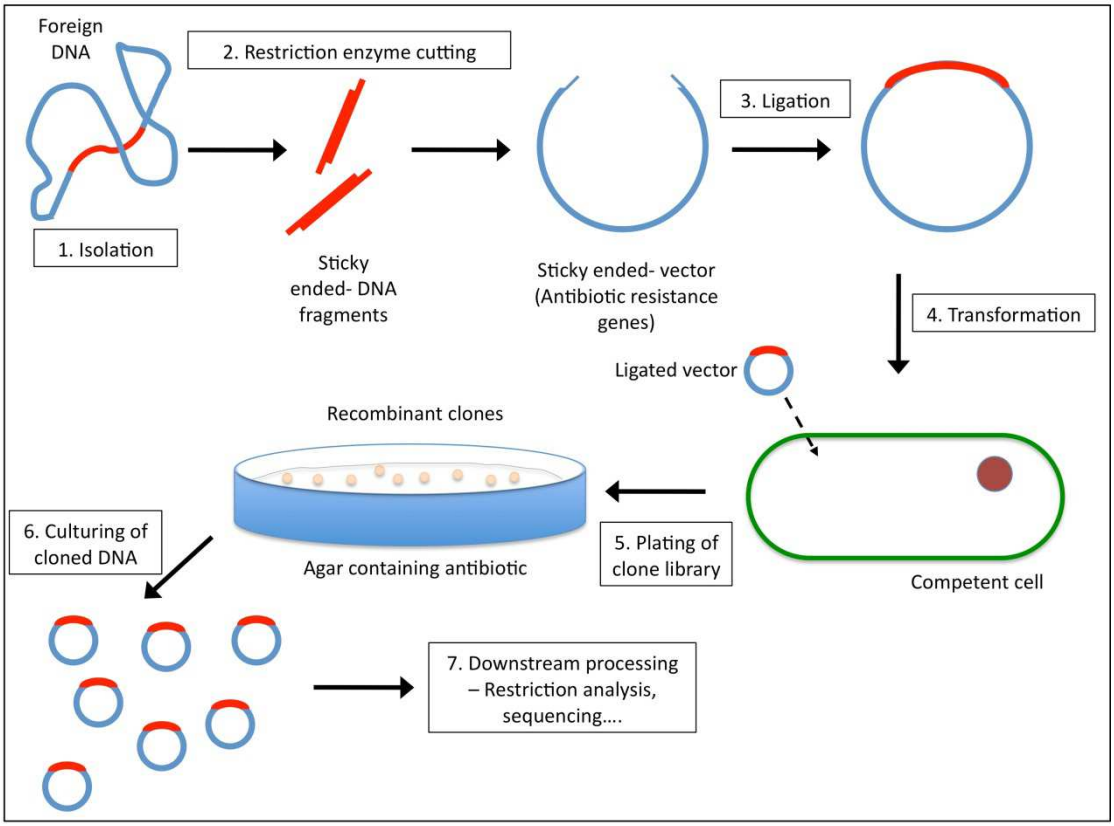

Figure 15: Outline of the major steps in molecular cloning: 1. Isolation of DNA ; 2. Restriction enzyme cutting of DNA fragment and vector; 3. Ligation of vector with DNA fragment; 4. Transformation of ligated vector into competent cell; 5. Plating of clone library to grow recombinant clones; 6. Selection, and culturing of recombinant colonies, and plasmid extraction; 7. Downstream processing of plasmid DNA, such as restriction analysis or sequencing.

2.6.5.5 Phylogenetic tree construction and analysis

In basic terms phylogenetic trees attempt to show how species are related based on similarities in a homologous (of common ancestry) gene or protein sequence, whereby the more similar the sequences, the more closely the organisms are related ref/s. The most widely used and successful gene for prokaryotes is the gene coding 16S ribosomal RNA (rRNA) subunit (Woese and Fox 1977, Vetriani, et al. 1999, Teske 2006). They are particularly suited to phylogenetic analysis because they are universally distributed, functionally constant, sufficiently conserved, and of adequate length to provide evolutionary relationships (Madigan et al. 2012). DNA sequences for comparison must be subjected to sequence alignment in order to identify mismatches, gaps and/or deletions and thereby provide information on relative sequence differences and evolutionary relationship. The aligned sequences are then used to construct a phylogenetic tree (or cladogram), which consists of a series of nodes and branches, with each node corresponding to a point in evolution where the two downstream sequences diverged and each branch describes the order of descent

and its length describes the number of changes along that branch. An in-depth account of steps and measures taken in phylogenetic analysis is beyond the scope of this review.

2.7 Project Description

The aim of this project is to investigate seabed fluid flow features in Irish waters by combining geochemical, geomicrobiological and geophysical methods in a multidisciplinary approach, in order to characterize processes involved in the formation, regulation and activity of these features. These include pockmarks of diverse sizes and settings in the Malin Sea, Irish Sea and Dunmanus Bay, and also mud diapirs and authigenic carbonate mounds in the Irish Sea. Many of these features have only been recently identified and are still poorly understood or un-studied, which as also the case globally. Their importance from a purely scientific perspective has been outlined but the potential commercial and economic values, in particular in terms of energy resources and novel biotechnological applications, is also evident. This project will involve the use of state-of-the-art techniques in each field such as lipid biomarker analysis and stable carbon isotope monitoring, advanced nuclear magnetic resonance (NMR), DGGE and phylogenetic analysis of clone libraries. This is a collaborative project involving Dublin City University (geochemistry), Queen's University Belfast (molecular microbial ecology), University of Toronto, Scarborough (advanced NMR), Geological Survey of Ireland (geology/geophysics). The research expeditions have been funded by the Irish Marine Institute via the Integrated Mapping for the Sustainable Development of Ireland's Marine Resource (INFOMAR) program and the PhD project is funded by the Irish Research Council for Science, Engineering and Technology (IRCSET).

References

Acosta, J., Munoz, A., Herranz, P., Palomo, C., Ballesteros, M., Vaquero, M. and Uchupi, E. 2001. Pockmarks in the Ibiza Channel and western end of the Balearic Promontory (western Mediterranean) revelaed by multi-beam mapping. *Geo-Marine Letters,* 21pp.123-130.

Albert, D.B., Martens, C.S. and Alperin, M.J. 1998. Biogeochemical processes controlling methane in gassy sediments - Part 2: groundwater flow control of acoustic turbidity in Eckenforde Bay sediments. *Continental Shelf Research,* 18pp.1771-1793.

Aloisi, G., Bouloubassi, I., Heijs, S.K., Pancost, R.D., Pierre, C., Sinninghe Damsté, J.S., Gottschal, J.C., Forney, L.J. and Rouchy, J. 2002. CH4-consuming microorganisms and the formation of carbonate crusts at cold seeps. *Earth and Planetary Science Letters,* 203(1), pp.195-203.

Baldock, J.A., Masiello, C.A., Gelinas, Y. and Hedges, J.I. 2004. Cycling and composition of organic matter in terrestrial and marine ecosystems. *Marine Chemistry,* 92pp.39-64.

Bayon, G., Loncke, L., Dupre, S., Caprais, J.-., Ducassou, E., Duperron, S., Etoubleau, J., Foucher, J.P., Fouquet, Y., Gontharet, S., Henderson, G.M., Huguen, C., Klaucke, I., Mascle, J., Migeon, S., Olu-Le Roy, K., Ondréas, H., Pierre, C., Sibuet, M., Stadnitskaia, A. and Woodside, J. 2009. Multi-disciplinary investigation of fluid seepage on an unstable margin: The case for the Central Nile deep sea fan. *Marine Geology,* 261pp.92-104.

Benner, R. 2004. What happens to terrestrial organic matter in the ocean. *Marine Chemistry,* 92pp.307-310.

Berner, R.A. 1989. Biogeochemical cycles of carbon and sulphur and their effect on atmospheric oxygen over Phanerozoic time. *Paleogeography, Paleoclimatology,* 73pp.97-122.

Berner, R.A. 1980. *Early diagenesis: A theoretical approach.* 1st ed. Princeton, New Jersey: Princeton University Press.

Bernhardt, T.G., Cannistraro, P.A., Bird, D.A., Doyle, K.M. and Laposata, M. 1996. Purification of fatty acid ethyl esters by solid-phase extraction and high-performance liquid chromatography. *Journal of Chromatography B: Biomedical Applications,* 675(2), pp.189-196.

Biddle, J.F., Lipp, J.S., Lever, M.A., Llyod, K.G., Sorensen, K.B. and Anderson, R. 2006. Heterotrophic archaea dominate sedimentary subsurface ecosystems off Peru. *Proceedings of the National Academy of Sciences of the USA,* 103pp.3846-3851.

Bligh, E.G. and Dyer, W.J. 1959. A rapid method of total lipid extraction and purification. *Canadian Journal of Biochemistry and Physiology,* 37(911), pp.917.

Boetius, A., Ravenschlag, K., Schubert, C.J., Rickert, D., Widdel, F., Gieseke, A., Amann, R., Jorgensen, B.B., Witte, U. and Pfannkuche, O. 2000. A marine microbial consortium mediating anaerobic oxidation of methane. *Nature,* 407pp.623-626.

Burlage, R.S. 1998. Molecular techniques *IN:* Burlage, R.S., Atlas, D., Stahl, D., Geesey, G. and Sayler, G. (eds.) *Techniques in microbial ecology.* 1st ed. New York Oxford University Press, pp.289-336.

Christie, W.W. 1982. *Lipid analysis.* 2nd ed. Oxford Press: Pergamon.

Croker, P.F., Kozachenko, M. and Wheeler, A.J. 2005. *Gas-related structures in the Western Irish Sea (IRL-SEA6).* Dublin: Petroleum Affairs Division.

Dean, J.R. 2003. *Methods for environmental trace analysis.* 1st ed. Chichester, West Sussex: Wiley.

DeLong, E.F. 1992. Archaea in coastal marine environments. *Proceedings of the National Academy of Sciences of the USA,* 89pp.5685-5689.

Denman, K.L., Brasseur, G., Chidthaisong, A., Ciais, P., Cox, P.M., Dickinson, R.E., Hauglustaine, D., Heinze, C., Holland, E., Jacob, D., Lohmann, U., Ramachandran, S., da Silva Dias, P.L. and Wofsy, S.C. 2007. Couplings between changes in the climate system and biogeochemistry *IN:* Solomon, S., Qin, D., Manning, M., Chen, Z., Marquis, M., Averyt, K.B., Tignor, M. and Miller, H.L. (eds.) *Climate Change 2007: The physical science basis. COntribution of Working Group I to the Fourth Assessment Report of the Intergovernmental Panel on Climate Change.* Cambridge, United Kingdom and USA Cambridge University Press, pp.499-589.

Dickens, G.R., Koelling, M., Smith, D.C., Schnieders, L. and and the IODP Expedition 302 Scientists 2007. *Rhizon sampling of porewaters on scientific drilling expeditions: An examples from the IODP expedition 302, Arctic Coring Expedition (ACEX).* doi:10.2204/iodp.sd.4.08.2007. Proc. IODP Scientific Drilling.

Eglinton, G., Gonzalez, A.G., Hamilton, R.J., Raphael, R.A., 1962. Hydrocarbon constituents of the wax coatings of plant leaves: a taxonomic survey. *Phytochemistry* 1pp.89– 102.

Eglington, T.I. and Eglington, G. 2008. Molecular proxies for paleoclimatology. *Earth and Planetary Science Letters,* 275pp.1-16.

Feng, D., Chen, D., Peckmann, J. and Bohrmann, G. 2010. Authigenic carbonate crusts from methane seeps of the northern Congo fan: microbial formation mechanism. *Marine and Petroleum Geology,* 27pp.748-756.

Fernandez-Puga, M.C., Vazquez, J.T., Somoza, L., Diaz del Rio, V., Medialdea, T., Mata, M.P. and Leon, R. 2007. Gas-related morphologies and diapirism on the Gulf of Cadiz. *Geo-Marine Letters,* 27pp.213-221.

Fischer, S.G. and Lerman, L.S. 1983. DNA fragments differing by single base-pair substitutions are separated in denaturing gradient gels: correspondence with melting theory. *Proceeding of the National Academy of Sciences of the USA,* 80pp.1579-1583.

Fischer, S.G. and Lerman, L.S. 1979. Length-independent separation of DNA restriction fragments in two-dimensional gel electrophoresis. *Cell,* 16pp.191-200.

Floodgate, G.D. and Judd, A.G. 1992. The origins of shallow gas. *Continental Shelf Research,* (12), pp.1145-1156.

Fluckiger, J., Monnin, E., Stauffer, B., Schwander, J., Stocker, T.F., Chappellaz, J., Raynaud, D. and Barnola, J.-. 2002. High resolution Holocene N_2O ice core record and its relationship with CH_4 and CO_2. *Global Biogeochemical Cycles,* 16pp.1-8.

Froelich, P.N., Klinkhammer, G.P., Bender, M.L., Luedtke, N.A., Heath, G.R., Cullen, D., Dauphin, P. and Hammond, D. 1979. Early oxidation of organic matter in pelagic sediments of eastern equatorial Atlantic: suboxic diagenesis. *Geochimica Et Cosmochimica Acta*, 43pp.1075-1090.
Fuhrman, J.A. and Hagstrom, A. 2008. Bacterial and archaeal community structure and its patterns *IN:* Kirchman, D.L. (ed.) *Microbial ecology of the oceans.* 2nd ed. New Jersey, USA Wil, pp.45-90.
Futterer, D.K. 2006. The solid phase of marine sediments *IN:* Schulz, H.D. and Zabel, M. (eds.) *Marine Geochemistry.* 2nd ed. Berlin Springer, pp.1.
Gay, A., Lopez, M., Cochonat, P., Séranne, M., Levaché, D. and Sermondadaz, G. 2006. Isolated seafloor pockmarks linked to BSRs, fluid chimneys, polygonal faults and stacked Oligocene–Miocene turbiditic palaeochannels in the Lower Congo Basin. *Marine Geology*, 226(1-2), pp.25-40.
Giacometti, J., Milosevic, A. and Milin, C. 2002. Gas chromatographic determination of fatty acids contained in different lipid classes after their separation by solid-phase extraction. *Journal of Chromatography A*, 976pp.47-54.
Gieskes, J.M., Gamo, T. and Brumsack, H. 1991. *Chemical methods for interstitial analysis aboard JOIDES Resolution: Technical note 15.* Texas: Ocean Drilling Program.
Grasshoff, K., Kremling, K. and Ehrhardt, M. 1999. *Methods of seawater analysis.* 3rd ed. Weinham, Germany: Wiley-VCH.
Harris, D.C. 2007. *Quantitative Chemical Analysis.* 7th ed. New York: W.H. Freeman and Company.
Hedges, J.I., Eglinton, G., Hatcher, P.G., Kirchman, D.L., Arnosti, C., Derenne, S., Evershed, R.P., Kogel-Knabner, I., de Leeuw, J.W., Littke, R., Michaelis, W. and Rullkotter, J. 2000. The molecularly uncharacterised component of nonliving organic matter in natural environments. *Organic Geochemistry*, 31pp.945-958.
Hedges, J.I. and Keil, R.G. 1995. Sedimentary organic matter preservation: an assessment and speculative synthesis. *Marine Chemistry*, 49pp.81-115.
Hedges, J.I., Keil, R.G. and Benner, R. 1997. What happens to terrestrial organic matter in the ocean. *Organic Geochemistry*, 27pp.195-212.
Hedges, J.I. and Oades, J.M. 1997. Comparative Organic Geochemistries of soils and marine sediments. *Organic Geochemistry*, 27pp.319-361.
Holmes, D.J. and Peck, H. 1998. Nucleic acids *IN:* Anonymous*Analytical Biochemistry.* 3rd ed. Harlow, England Prentice Hall, pp.443-473.
Hovland, M., Gardner, J.V. and Judd, A.G. 2002. The significance of pockmarks to understanding fluid flow processes and geohazards. *Geofluids*, 2pp.127-136.
Inagaki, F., Nunoura, T., Nakagawa, S., Teske, A., Lever, M.A., Lauer, A., Suzuki, M., Takai, K., Delwiche, M., Colwell, F.S., Nealson, K.H., Horikoshi, K., D'Hondt, S. and Jorgensen, B.B. 2006. Biogeographical distributions and diversity of microbes in methane hydrate-bearing deep marine sediments on the Pacific Ocean Margin. *Proceedings of the National Academy of Sciences of the USA*, 103pp.2815-2820.
Inagaki, F., Suzuki, M., Takai, K., Oida, H., Sakamoto, T., Aoki, K., Nealson, K.H. and Horikoshi, K. 2003. Microbial communities associated with geological horizons in coastal subseafloor sediments from the Sea of Okhotsk. *Applied and Environmental Microbiology*, 69pp.7224-7235.
Jensen, P., Aagaard, I., Burke, R.A., Dando, P.R., Jorgensen, N.O., Kuijpers, A., Laier, T., O' Hara, S.C.M. and Schmaljohann, R. 1992. 'Bubbling reefs' at the Kattegat: submarine landscapes of carbonate-cemented rocks support a diverse ecosystem at methane seeps. *Marine Ecology Progress Series*, 83pp.103-112.
Jorgensen, B.B. 2006. Bacteria and marine biogeochemistry *IN:* Schulz, H.D. and Zabel, M. (eds.) *Marine Geochemistry.* 2nd ed. Berlin Heidelberg Springer, pp.169-206.
Jorgensen, B.B. and Boetius, A. 2007. Feast or famine- microbial life in the seabed. *Nature*, 5pp.770-781.
Judd, A.G. and Hovland, M. 2007a. Introduction to seabed fluid flow *IN:* Anonymous*Seabed fluid flow: the impact on geology, biology and the marine environment.* 1st ed. Cambridge, UK Cambridge University Press, pp.1-44.
Judd, A.G. and Hovland, M. 2007b. *Seabed fluid flow: the impact of geology, biology and the marine environment.* 2nd ed. Cambridge, UK: Cambridge University Press.
Judd, A.G. and Hovland, M. 1992. The evidence of shallow gas in marine sediments. *Continental Shelf Research*, 12pp.1231-1095.
Kaluzny, M.A., Duncan, L.A., Merrit, M.V. and Epps, D.E. 1985. Rapid separation of lipid classes in high yield and purity using bonded phase columns. *Journal of Lipid Research*, 26pp.135-140.
Karner, M.B., DeLong, E.F. and Karl, D.M. 2001. Archaeal dominance in the mesopelagic zone of the Pacific Ocean. *Nature*, 409pp.507-510.
Killops, S. and Killops, V. 2005. *Introduction to Organic Geochemistry.* 2nd ed. Oxford, UK: Blackwell Publishing.
Kim, H.Y. and Salem, N. 1990. Separation of lipid classes by solid phase extraction. *Journal of Lipid Research*, 31pp.2285-2289.
King, L.H. and MacLean, B. 1970. Pockmarks on the Scotian Shelf. *Geological Society of America Bulletin*, 81pp.3141-3148.
Knight, B.P., Chaudri, A.M., McGrath, S.P. and Giller, K.E. 1998. Determination of chemical availability of cadmium and zinc in soil using inert soil moisture samplers. *Environmental Pollution*, 99pp.293-298.
Knittel, K., Losekann, T., Boetius, A., Kort, R. and Amann, R. 2005. Diversity and distribution of mathantrophic acrhaea at cold seeps. *Applied and Environmental Microbiology*, 71pp.467-479.
Kowalchuck, G.A., Stephen, J.R., de Boer, W., Prosser, J.I., Embley, T.M. and Woldendorp, J.W. 1997. Analysis of ammonia oxidizing bacteria of the subdivision of the class Proteobacteria in coastal sand dunes by denaturing

gradient gel electrophoresis and sequencing of PCR amplified 16S ribosomal DNA fragments. *Applied and Environmental Microbiology*, 63pp.1489-1497.
Lipp, J.S., Morono, Y., Inagaki, F. and Hinrichs, K.-. 2008. Significant contribution of Archaea to extant biomass in marine subsurface sediments. *Nature*, 454pp.991-994.
Llyod, K.G., Lapham, L. and Teske, A. 2006. An anaerobic methane-oxidising community of ANME-1b archaea in hypersaline Gulf of Mexico sediments. *Applied and Environmental Microbiology*, 72pp.7218-7230.
Loh, A.N. and Bauer, A.E. 2004. Variable ageing and storage of dissolved organic components in the open ocean. *Nature*, 430pp.877-881.
Lovelock, J. 1979. *Gaia: A new look at life on Earth.* 1st ed. Oxford, UK: Oxford University Press.
Madigan, M.T., Martinko, J.M., Stahl, D.A. and Clark, D.P. 2012. *Brock Biology of Microborganisms.* 13th ed. San Francisco, CA: Pearson.
Manahan, S.E. 2005. *Environmental Chemistry.* 8th ed. Florida, USA: CRC Press.
Matthews, D.,E. and Hayes, J.,M. 1978. Isotope-ratio-monitoring gas chromatography-mass spectrometry. *Analytical Chemistry*, 50pp.1465-1473.
Merritt, D.A., Freeman, K.H., Ricci, M.P., Studley, S.A. and Hayes, J.,M. 1995. Performance and Optimization of a Combustion Interface for Isotope Ratio Monitoring Gas Chromatography/Mass Spectrometry. *Analytical Chemistry*, pp.2461-2473.
Merritt, D.A., Brand, W.A. and Hayes, J.M. 1994. Isotope-ratio-monitoring gas chromatography-mass spectrometry: methods for isotopic calibration. *Organic Geochemistry*, 21pp.573-583.
Merritt, D.A. and Hayes, J.M. 1994. Factors Controlling Precision and Accuracy in Isotope-Ratio-Monitoring Mass Spectrometry. *Analytical Chemistry*, (66), pp.2336-2347.
Milkov, . 2000. Worldwide distribution of submarine mud volcanoes and associated gas hydrates. *Marine Geology*, 167pp.29-42.
Murphey, B.F. and Nier, A.O. 1941. Variations in the relative abundance of carbon isotopes. *Physical Review*, 59pp.771-772.
Muyzer, G., de Waal, E.C. and Uitterlinden, A.G. 1993. Profiling of complex microbial populations by denaturing gradient gel electrophoresis analysis of polymerase chain reaction amplified genes coding for 16S rRNA. *Applied and Environmental Microbiology*, 59pp.695-700.
Muyzer, G. and Smalla, K. 1998. Application of denaturing gradient gel electrophoresis (DGGE) and temperature gradient gel electrophoresis (TGGE) in microbial ecology. *Antonie Van Leeuwenhoek*, 73pp.127-141.
Myers, R.M., Fischer, S.G., Lerman, L.S. and Maniatis, T. 1985. Nearly all single base substitutions in DNA fragments joined to a GC-clamp can be detected by denaturing gradient gel electrophoresis. *Nucleic Acids Res.*, 13pp.3131-3145.
Nier, A.O. 1939. Variations in the relative abundance of carbon istotopes. *Journal of the American Chemical Society*, 61pp.697.
Nübel, U., Engelen, B., Felske, A., Snaidr, J., Wieshuber, A., Amann, R.I., Ludwig, W. and Backhaus, H. 178. Sequence heterogeneities of genes encoding 16S rRNAs in Paenibacillus polymyxa detected by temperature gradient gel electrophoresis. *Journal of Bacteriology*, 5636(5643),
Pancost, R.D. and Boot, C.S. 2004. The paleoclimatic utility of terestrial biomarkers in marine sediments. *Marine Chemistry*, 92pp.239-261.
Pedersen, T.F. and Calvert, S.E. 1990. Anoxia versus productivity: What controls the formation of organic-rich sediments and sedimentary rocks. *Bulletin*, 74pp.454-466.
Peters, K.E., Walters, C.C. and Moldowan, J.M. 2005. Origin and preservation of organic matter *IN:* Anonymous*The biomarker guide volume 1: Biomarkers and isotopes in the environment and human history.* 2nd ed. New York Cambridge University Press, pp.3-17.
Pinkart, H.C., Devereux, R. and Chapman, P.J. 1998. Rapid separation of microbial lipids using solid phase extraction columns. *Journal of Microbiological Methods*, 34pp.9-15.
Primrose, S.B., Twyman, R.M. and Old, R.W. 2001. Basic techniques *IN:* Anonymous*Principles of Gene Manipulation.* 6th ed. Oxford, UK Blackwell Science, pp.8-25.
Redfield, A.C. 1958. The biological control of chemical factors in the environment. *American Scientist*, 4pp.205-221.
Reed, D., Fujita, Y., Delwiche, M.E., Blackwelder, D.B., Sheridan, P.P., Uchida, T. and Colwell, F.S. 2002. Microbial communities from methane-hydrate bearing deep marine sediments in a forearc basin. *Applied and Environmental Microbiology*, 68pp.3759-3770.
Reitner, J., Peckmann, J., Reimer, A., Schumann, P. and Thiel, V. 2005. Methane-derived carbonate build-ups and associated microbial communities at the cold seeps on the lower Crimean Shelf (Black Sea). *Facies*, 51pp.66-79.
Ricci, M.P., Merritt, D.A., Freeman, K.H. and Hayes, J.M. 1994. Acquisition and processing of data for isotope-ratio-monitoring mass spectrometry. *Organic Geochemistry*, 21pp.561-571.
Rieley, G. 1994. Derivitization of organic compounds prior to gas chromatographic-combustion-isotope-ratio mass spectrometric analysis: ldentification of isotope fractionation processes. *Analyst*, 119pp.915-919.
Rizov, I. and Doulis, A. 2001. Separation of plant membrane lipids by multiple solid-phase extraction. *Journal of Chromatography A*, 922pp.347-354.
Rothwell, R.G. and Rack, F.R. 2006. New techniques in Sediment Core Analysis: An Introduction *IN:* Anonymous*New techniques in Sediment Core Analysis.* 1st ed. London The Geological Society of London, pp.1-29.
Ruiz-Gutiérrez, V. and Pérez-Camino, M.C. 2000. Update on solid-phase extraction for the analysis of lipid classes and related compounds. *Journal of Chromatography A*, 885pp.321-341.

Rullkotter, J. 2006. Organic matter: the driving force for early diagenesis *IN:* Schulz, H.D. and Zabel, M. (eds.) *Marine Geochemistry.* 2nd ed. Berlin Springer, pp.125-168.
Sano, M., Yotsui, Y., Abe, H. and Sasaki, S. 1976. A new technique for the detection of metabolites labelled by the isotope 13C using mass fragmentography. *Biological Mass Spectrometry,* 3pp.1-3.
Schulz, H.D. 2006. Quantification of early diagenesis: Dissolved constituents in marine pore water *IN:* Schulz, H.D. and Zabel, M. (eds.) *Marine Geochemistry.* 2nd ed. Germany Springer, pp.124.
Seeberg-Everfeldt, J., Schluter, M., Feseker, T. and Kolling, M. 2005. Rhizon sampling of porewaters near the sediment water interface of aquatic systems. *Limnology and Oceanography: Methods,* 3pp.361-371.
Sessions, A.L. 2006. Isotope ratio detection for gas chromatography. *Journal of Separation Science,* 29pp.1946-1961.
Sheffield, V.C., Cox, D.R., Lerman, L.S. and Myers, R.M. 1989. Attachment of a 40bp G+C rich sequence (GCclamp) to genomic DNA fragments by polymerase chain reaction results in improved detection of single base changes. *Proceedings of the National Academy of Sciences of the USA,* 86pp.232-236.
Sorensen, K.B. and Lauer, A. 2006. Stratified communities of archaea in deep marine subsurface sediments. *Applied and Environmental Microbiology,* 72pp.4596-4603.
Sorensen, K.B., Lauer, A. and Teske, A. 2004. Archaeal phylotypes in cold metal-rich, low activity deep subsurface sediment off the Peru Basin, ODP Leg 201, Site 1231. *Geobiology,* 2pp.151-161.
Takai, K. and Horikoshi, K. 1999. Genetic diversity of archaea in deep=sea hydrothermal vent environments. *Genetics,* 152pp.1285-1297.
Takai, K., Moser, D.P., DeFlaun, M., Onstott, T.C. and Fredrickson, J.K. 2001. Archaeal diversity in waters from Deep South African gold mines. *Applied and Environmental Microbiology,* 67pp.5750-5760.
Teske, A. 2006. Microbial communities of deep marine subsurface sediments: molecular and cultivation surveys. *Geomicrobiology Journal,* 23pp.357-368.
Teske, A. and Sorensen, K.B. 2008. Uncultured archaea in deep marine subsurface sediments: have we caugth them all? *Internation Society for Microbial Ecology,* 2pp.3-18.
Valentine, D.L. and Reeburgh, W.S. 2000. New perspectives on anaerobic oxidation of methane. *Environmental Microbiology,* 2pp.477-484.
Vallaeys, T., Topp, E., Muyzer, G., Macheret, V., Laguerre, G. and Soulas, G. 1997. Evaluation of denaturing gradient gel electrophoresis in the detection of 16S rDNA sequence variation in rhizobia and methanotrophs. *FEMS Microbiology Ecology,* 24pp.279-285.
Vetriani, C., Jannasch, H.W., MacGregor, B.J., Stahl, D.A. and Reysenbach, A.L. 1999. Population structure and phylogenetic characterisation of marine benthic archaea in deep-sea sediments. *Applied and Environmental Microbiology,* 65pp.4375-4384.
Volk, T. and Hoffert, M.I. 1985. Global carbon pumps: analysis of relative strengths and efficiencies in ocean-driven atmospheric CO_2 changes *IN:* Sundquist, E.T. and Broecker, W.S. (eds.) *The Carbon Cycle and atmospheric CO_2: Natural variations Archaean to present.* Geophysical Monograph Vol. 32 ed. Washington DC, USA American Geophysical Union, pp.99-110.
Volkman, J.K. 2006. Lipid biomarkers for marine organic matter *IN:* Volkman, J.K. (ed.) *Marine organic matter: Biomarkers, isotopes and DNA.* 1st ed. Berlin Springer, pp.27-70.
White, D.C. 1983. Analysis of microrganisms in terms of quantity and activity in natural environments *IN:* Slater, J.H., Whittenbury, R. and Wimpenny, J.W.T. (eds.) *Microbes in their natural environments.* 1st ed. Cambridge, UK Cambridge University Press, pp.37-66.
White, D.C., Davis, W.M., Nickels, J.S., King, J.D. and Bobbie, R.J. 1979. Determination of the Sedimentary Microbial Biomass by Extractable Lipid Phosphate. *Oecologia,* 40pp.51-62.
White, D.C. and Ringelberg, D.B. 1998. Signature lipid biomarker analysis *IN:* Burlage, R.S., Atlas, R., Stahl, D., Geesey, G. and Sayler, G. (eds.) *Techniques in Microbial Ecology.* 1st ed. New York, Oxford University Press, pp.255-271.
Wickman, F.E. 1952. Variations in the relative abundance of the carbon isotopes in plants. *Geochimica Et Cosmochimica Acta,* 2(4), pp.243-254.
Woese, C.R. and Fox, G.E. 1977. Phylogenetic structure of the prokaryotic domain: The primary kingdoms. *Proceedings of the National Academy of Sciences of the USA,* 74pp.5088-5090.
Wuebbles, D.J. and Hayhoe, K. 2002. Atmospheric methane and global change. *Earth-Science Reviews,* 57pp.177-210.
Yuan, F. and Bennell, J.D. 1992. Acoustic and physical characteristics of gassy sediments in the Western Irish Sea. *Continental Shelf Research,* 12pp.1124-1134.

Chapter 3. Multidisciplinary investigation of gas seepage features in the western Irish Sea

Shane O' Reilly[1], Xavier Monteys[2], Michal Szpak[1], Brian Murphy[1], Sean Jordan[1], Brian Kelleher[1]

1. School of Chemical Sciences, Dublin City University, Dublin 9, Ireland
2. Geological Survey of Ireland, Beggar's Bush, Haddington Rd., Dublin 4., Ireland

Abstract

Gas seepage features, including pockmarks, a large mud diapir and methane-derived authigenic carbonate (MDAC) mounds, in the Irish Designated Seabed Zone (IDSZ) of the Irish Sea, were investigated by a combined acoustic, underwater video and geochemical approach. This study comprises the first report of pockmarks in the IDSZ of the Irish Sea. Ten circular-elongate shallow pockmarks, with an average diameter of 100m are described. Interstitial CH_4, SO_4^{2-}, HS^-, NH_4^+, PO_4^{3-} and Fe^{2+} profiles of cores sampled from these features and control cores outside these features and in the surrounding region, combined with seismic and underwater video investigations suggest that at present pockmarks and the Lambay Deep area are not actively seeping to surface sediments or the water column. However seismic evidence indicates significant sub-surface gas fronts characterizing deeper sediments at these features, which suggests likely periodic activity and temporal complexity. Previous reports that MDAC mounds at the Codling Fault Zone are sites of enhanced active seepage are supported in this study. Gas plumes to the water column and an extensive region dominated by MDAC slabs, concretions and seabed anoxia in this region are reported. Redox profiling, and electron microscopy of the sampled MDAC indicates anaerobic oxidation of methane (AOM) is a major process at investigated sites.

Abbreviations

IDSZ – Irish Designated Seabed Zone, MDAC – methane-derived authigenic carbonate, CFZ - Codling Fault Zone, AOM – anaerobic oxidation of methane, LD – Lambay Deep, LDMD – Lambay Deep mud diapir, KBB - Kish Bank Basin, SWI – sediment/water interface

3.1 Introduction

Seepage of methane and other fluids from the ocean's seafloor is a global occurrence, yet one which is poorly quantified and understood (Fleisher, et al. 2001). Since methane is an important trace gas in the atmosphere and is a potent greenhouse gas (IPCC 2007), seabed seepage is important in the global carbon cycle and consequently for global warming (Weissert 2000). One result of gas seepage to the seabed is the formation of gas seepage structures on the ocean's seafloor, such as pockmarks, mud diapirs, mud volcanoes and methane-derived authigenic carbonates (MDAC). Pockmarks (King and MacLean 1970) are globally ubiquitous shallow seabed depressions, thought to be formed due to rapid gas expulsion from gas accumulations underneath impermeable sediment layers. They are predominantly found in soft fine-grained sediments and are on average tens of metres across and a few metres deep, but morphology and size varies considerably (Hovland, Gardner and Judd 2002). Soft silty clays seem to provide the ideal sediment grain size for pockmark formation, and pockmarks are thus mostly found in regions with fine sediments. Mud diapirs occur when gas-charged mud or clay sediments rise, due to buoyancy effects through other sedimentary layers,. These structures can be tens to hundreds of metres in diameter and their size and morphology depends on the depth and size of the gas accumulation that triggers their formation. They are found worldwide, often in areas of known hydrocarbon potential (Judd and Hovland 2007).

Authigenic carbonate crusts, which may form dramatic pavements or mound structures, are a sink for methane seeping from sub-seabed or released from gas-hydrates (Bohrmann, et al. 1998) and hence are important components for regulation of ocean-atmosphere carbon fluxes (Aloisi, et al. 2002). It is now accepted that anaerobic oxidation of methane (AOM) to carbonate (and reduction of SO_4^{2-} to HS^-) is microbially mediated and of global significance, serving as an important control on the flux to the atmosphere, estimated to be in the vicinity of 5-20% of net modern atmospheric CH_4 flux (20-100 $x10^{12}$ g a^{-1}) (Valentine and Reeburgh 2000). The current leading theory is that a consortium of sulphate-reducing bacteria and methanogenic archaea mediate AOM (Boetius, et al. 2000). Furthermore sites of active methane seepage have been shown to support unique macro- and micro-faunal biodiversity (Dando, et al. 1991, Jensen, et al. 1992, Sibuet and Olu 1998), to be

important in relation to marine industrial and petroleum safety (Hovland, Gardner and Judd 2002) and also in petroleum and gas prospecting (Judd and Hovland 2007).

Numerous reports in recent years have highlighted the presence of gas seepage features in Irish waters: in the Irish Sea (Jones, Floodgate and Bennell 1986, Yuan and Bennell 1992, Croker, Kozachenko and Wheeler 2005, Judd, Croker and Tizzard 2007), in the Malin Sea (Monteys et al. 2008a, Monteys et al. 2008b, Szpak, et al. 2012), at the Porcupine Bank (Games 2001) and in Dunmanus Bay (unpublished). Croker et al. (1995, 2005) conducted substantial work mapping and performing seismic investigations of gas seepage structures in the Irish Sea. One area of interest is the Lambay Deep (LD), which is an isolated linear basin approximately 30km NE of Dublin. Its associated mud diapir (LDMD) is the only documented mud diapir in the Irish Designated Seabed Zone (ISDZ) of the Irish Sea (Croker, Kozachenko and Wheeler 2005). Gas seepage in the Kish Bank Basin (KBB) has also facilitated the formation of carbonate mound structures. Circa 30 mounds haven been recently identified along the Codling Fault Zone (CFZ) in the east perimeter of the Kish Bank Basin. This location has been suggested to be the most active site of gas migration in the IDSZ of the Irish Sea (Croker, Kozachenko and Wheeler 2005). However in comparison to other areas such as the North Sea and off the Norwegian coast (Dando, et al. 1991, Bøe, Rise and Ottesen 1998, Hovland, et al. 2005), off the coast of Congo (Gay, et al. 2006, Gay, et al. 2007), and in the Black Sea (Peckmann, et al. 2001, Stadnitskaia, et al. 2005) relatively little is known about these seepage features.

In this paper we present a multidisciplinary investigation of gas seepage features in the Irish Sea ISDZ pockmarks in the northern mudbelt region, the Lambay Deep mud diapir and MDAC mounds at the Codling Fault Zone. Sub-bottom seismic profiling and multibeam echosounder (MBES) mapping was combined with underwater video investigations and interstitial methane and pore water geochemical analysis of retrieved cores. The main objectives of this study was to investigate previously unreported pockmarks in the Irish Sea IDSZ, the LDMD and the CFZ mounds by a combination of sub-bottom seismic profiling to investigate shallow gas occurrence and accumulations below these features, and underwater video, pore water and gas analysis of surface sediment cores to investigate current seepage activity.

3.2 Materials & Methods

3.2.1 Environmental & geological setting

The Irish Sea (approximately 260km long and 190km wide) lies between Great Britain on the east and Ireland on the west, and is connected with the Atlantic Ocean by the North Channel on the north and St. George's Channel on the south. The Irish/UK median line effectively bisects the Irish Sea into the Irish sector, here termed the Irish designated seabed zone (IDSZ), and the UK sector. Water depths range from 0-20m in the coastal areas and bays and at the Ireland/UK median line are on average 100m, with localized depressions of 130-180m. The IDSZ encompasses two Mezozoic sedimentary basins, namely the Kish Bank Basin and the SW section of the Central Irish Basin, and is primarily underlain with Permian and Carboniferous rocks. Quaternary sediment thickness is between 50-150m, but with the presence of thinner and even absent Quaternary cover also occurring (Croker, Kozachenko and Wheeler 2005).

The northern section (north of $53^0$10'N) of the Irish Sea IDSZ is characterized by weaker hydrodynamic conditions, allowing deposition of fine-grained particles and resulting in the region being a smooth muddy seabed. This is in contrast to the southern region (south of $53^0$10'N), which is subject to comparatively high-energy currents and is characterized by gravelly sands and cobbles and high energy bedforms such as sand streaks, sand ribbons, gravel furrows and sand waves. The CFZ is a major NW-SE trending strike-slip fault making up the eastern edge of the KBB and consists of a complex fault zone several kilometers wide (Jackson, et al. 1995). This fault has been extensively surveyed by the Petroleum Affairs Division (PAD) and others (Croker, Kozachenko and Wheeler 2005, Judd, Croker and Tizzard 2007). Water depth here is 50-60m at the west of the fault and 80-120m to its east. Croker et al. (2005) divided the fault into three zones: the northern muddy zone containing the LD and its associated mud diapir (Lat $53^0$26.391'N, Lon $5^0$48.143'W); the central sandy zone characterized by sand waves; and the southern zone characterized by current-swept seabed and patches of coarse sediments. 23 mounds have been identified in the central zone and have a relief of 5-10m, a length of typically greater than 250m and a width of about 80m. The LD is a linear trench-like feature 50-60m lower than the surrounding seabed, with a maximum depth of 110m (Judd, Croker and Tizzard 2007, Croker 1995). In this study IDSZ mudbelt pockmarks (MP1 and MP2),

the LD and the LDMD, and the MDAC mounds at the Colding Fault Zone were investigated in June 2010 aboard the R.V. *Celtic Voyager* (Cruise Leg CV10_28).

3.2.2 Bathymetry

Bathymetry data was collected as part of the INFOMAR (Integrated Mapping for the Sustainable Development of Ireland's Marine Resources) program. Data acquired was acquired onboard the *RV* Celtic Voyager using a Kongsberg SIMRAD EM1002 multibeam echosounder with an operational frequency of 93-98kHz and a pulse length of 0.7ms. Bathymetric terrain models were then gridded at 5x5m.

3.2.3 Sub-bottom acoustic profiling

Sub-bottom data was acquired using a heave-corrected SES Probe 5000 3.5 kHz transceiver in conjunction with a hull-mounted 4^0x4^0 transducer array. Acquisition parameters, data logging and interpretation were carried out using the CODA Geokit suite.

3.2.4 Drop camera

A Kongsberg Simrad OE14-208 digital camera and video system, housed in a Seatronics frame was used to obtain video and image stills of the features. 6 videolines were deployed, collecting over 12 hours of footage. 4 videolines were deployed at the CFZ MDAC targets, with 1 videoline each deployed in and around the LD/LDMD and MP2.

3.2.5 Coring and sediment sub-sampling

Seepage features were sampled in June 2010 aboard the R.V. *Celtic Voyager* (Cruise Leg CV10_28). In addition two 3m vibrocores were also obtained from an Irish Sea Marine Assessment (ISMA) expedition in 2009 aboard the *Celtic Voyager* also. Site locations are shown in Fig. 1 and a description of samples taken is given in Table 1. Cores of up to 3m were taken using a 1m gravity corer and GeoResources3000 vibrocorer. In some cases due to weather constraints gravity coring had to be performed instead of vibrocoring. Core-liners were sectioned and sealed prior to opening and processing. Sediment sub-samples were stored at -20^0C onboard and at -80^0C back in the lab. Three MDAC mound targets were chosen in the Codling Fault Zone based on a previous expedition on R.V. *Lough Beltra* in 1997 (Croker,

Kozachenko and Wheeler 2005). The locations for the target sites and the sampling locations are given in Figure 1 and Table 1 also. MDAC hard grounds were sampled using Shipek and Van Veen grabs samples. Attempts to sample the grounds using gravity and vibrocore were unsuccessful.

3.2.6 Methane analysis

Interstitial gas sampling was carried out immediately upon core retrieval according to established methods (Gal'chenko, Lein and Ivanov 2004). Windows were cut in the core liner and 10mL sediment plugs were sampled, transferred to a 20mL headspace vial and 1.2M NaCl solution containing 67ppm thimerosal (Sigma Aldrich T5125) was then added to the vial leaving a 3mL headspace. Sealed vials were stored in the dark at 4^0C prior to analysis. Methane analysis was performed by standard methods (Kolling and Feseker 2009) on an Agilent 7820A GC-FID with a 30m HP-PLOTQ column. Methane was quantified using calibration standards prepared from 99.995% methane (Sigma Aldrich 02391-1EA). Core GC75 was used as a positive method control to track the effect of sampling and storage on methane profiles. Replicate standards were run periodically during analysis and reproducibility was monitored by replicate analysis of standards and selected samples. Relative standard deviation $\leq$8%.

3.2.7 Pore water analysis

Sediment pore water was sub-sampled from core liner windows using Rhizon samplers (Rhizosphere Research Products, Wageningen, NL) and aliquots immediately transferred to vials prior to preservation and storage at 4^0C in the dark. 1mL aliquots for sulphide (HS^-) analysis were preserved by addition of 400µL 50mM zinc acetate. Aliquots for phosphate (PO_4^{3-}) and ammonium (NH_4^+) analysis were preserved with 1-2 drops of chloroform and PO_4^{3-} samples were stored in glass vials. Aliquots for iron (II) (Fe^{2+}) analysis were preserved by acidification with 1% ascorbic acid. HS^-, Fe^{2+} and PO_4^{3-} analysis was performed by established complexometric UV/Vis spectrophotometric methods for marine pore waters (Kolling and Feseker 2009); by leucomethylene blue, Ferrospectral® and phosphomolybdate complexation respectively. Analysis was conducted on a BIOTEK Powerwave HT plate reader and calibration standards were prepared in artificial seawater prepared from commercially available sea salts (Sigma Aldrich, Dorset, UK - S9883). NH_4^+ analysis was performed using a SCHOTT NH1100 ion selective electrode and using NH_3 ISE ion

strength adjustment buffer (Reagecon, Clare, Irl. - ISANH5) and NH_3 ISE calibration solution (Reagecon, Clare, Irl - ISENH5). Quantification was performed according to manufacturer guidelines. Sulphate (SO_4^{2--}) analysis was performed using $BaCl_2$ turbidimetry stabilized with glycerol, to allow quantitative measurement, according to established IODP methods (Gieskes, Gamo and Brumsack 1991). Again core GC75 served as a positive control for sulphate depletion and sulphide accumulation at anoxic zones and relative standard deviations were ≤5%.

3.2.8 Redox potential (E_h) analysis

The redox potential (E_h) of sample sediments was assessed by using a Ag/Cl redox probe (Bradley James Corp. ORP ProcessProbe). The accuracy of the probe was monitored by testing with quinhydrone (Sigma Aldrich, Dorset, UK - 28,296-O) and E_h was calculated from measured potential readings according to manufacturer guidelines. High resolution down core E_h profiling was not performed due to reported problems with this analysis (Schulz 2006)

3.2.9 Scanning electron microscopy (SEM)

MDAC nodules, cemented shells and concretions were washed in deionized water and subsequently etched with 1% HCl for 1min. Samples were oven-dried at 70^0C and subsequently sputter-coated with 30nm gold. SEM imaging was performed using a Hitachi S3400-N scanning electron microscope at an accelerating voltage of 15.0kV and a working distance of 10cm.

3.3 Results

2.3.1 Mapping and sub-bottom acoustic profiling

Figure 1. shows seabed multibeam echosounder topographic maps of seepage features in the IDSZ of the Irish Sea. The mapped mudbelt region north of $53^{0}30$ ranges from less than 10m to about 50m water depth, and overall displays a very smooth and homogenous seabed. Mapping in this area resulted in the detection of ten shallow pockmarks, four of which are shown in Figure 16 (white broken circles). These are largely circular to elongate unit pockmarks occurring at an average water depth of 43m, with depressions ranging in depth from 0.3 – 1.6m and diameters ranging (based on longest axis) from about 50-250m and with an average diameter of about 100m. Figure 17. shows sub-bottom seismic profiling of one of the mud belt pockmarks. The profile and shallow gradient of the pockmark can be clearly distinguished, whereby the southern edge has a relatively steeper gradient compared to the northern edge of the depression. Numerous zones of acoustically turbid sediment and possible gas occurrence can be observed (Figure 2. Zone C). At approximately 8mbsf and below potential gas fronts were observed at and in the vicinity of the pockmark feature. However there was no clear indication of gas migration to overlying sediment layers or into the water column at the time of data collection.

Figure 16. shows the LD and its associated mud diapir (LDMD) on its eastern edge. As previously reported by Croker et al. (2005) the LD can be described as an elongate NW – SE facing depression that displays very sharp gradients rapidly reaching water depths of about 120m, compared to an average water depth of 50-60m surrounding the feature. The LDMD is a large elongate feature that is considerably higher than the surrounding seabed. It has an approximate E-W trending and appears to emerge from within the LD and ends at about 70m water depth, with a total length of approximately 600m and width of about 200m at its widest point. Croker et al. 2005 previously reported that the region is influenced by sub-surface gas fronts. However as for MP2 there was no clear indication of gas presence of migration to overlying surface layers or into the water column.

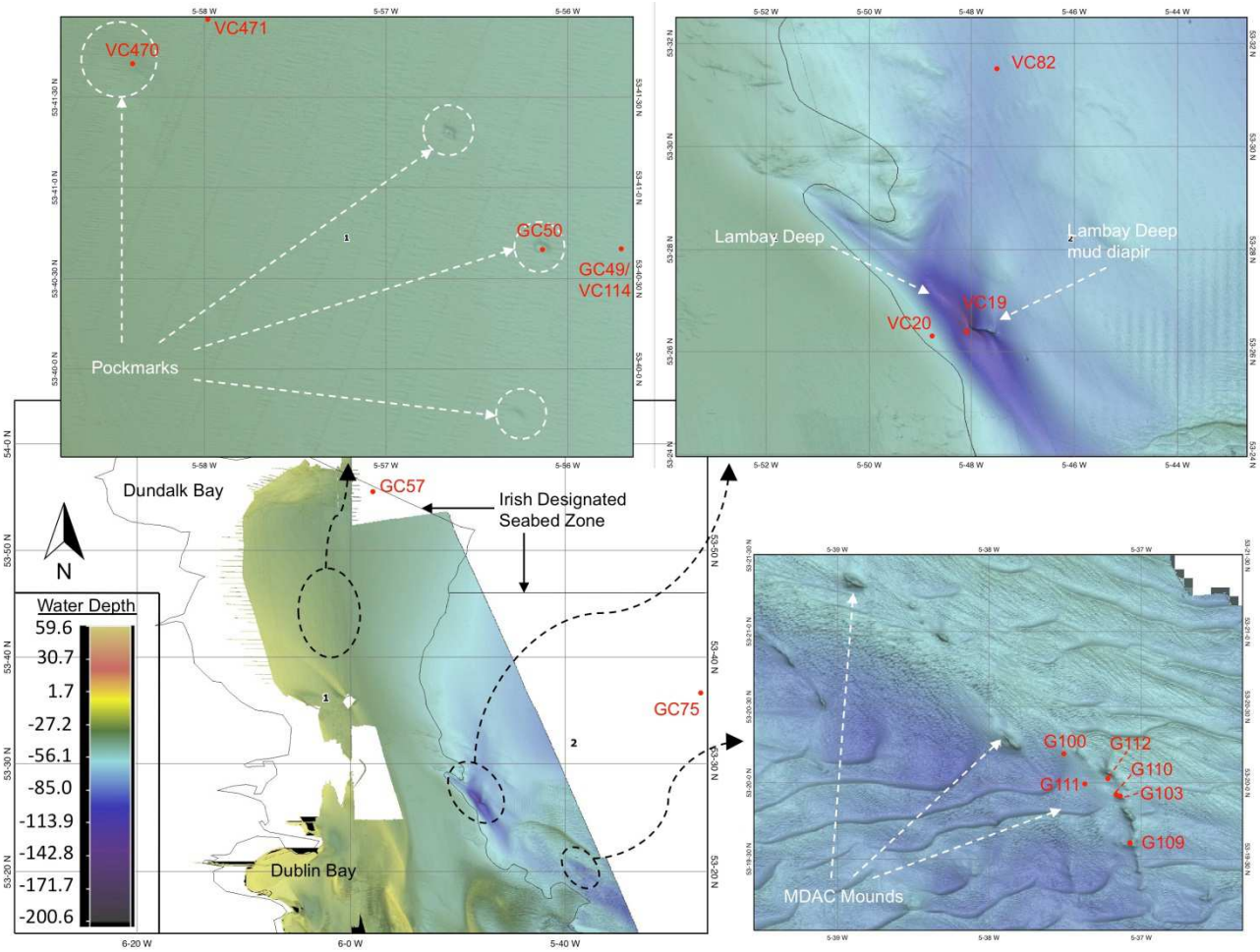

Figure 16: Locations of mapped Irish Sea pockmarks, Lambay Deep with its associated mud diapir , and the target methane-derived authigenic carbonate (MDAC) mounds in the Codling Fault Zone. Sampling stations as outlined in Table 1. are highlighted in red. Bathymetric water depth scale bar is shown. (Data and maps courtesy of INFOMAR).

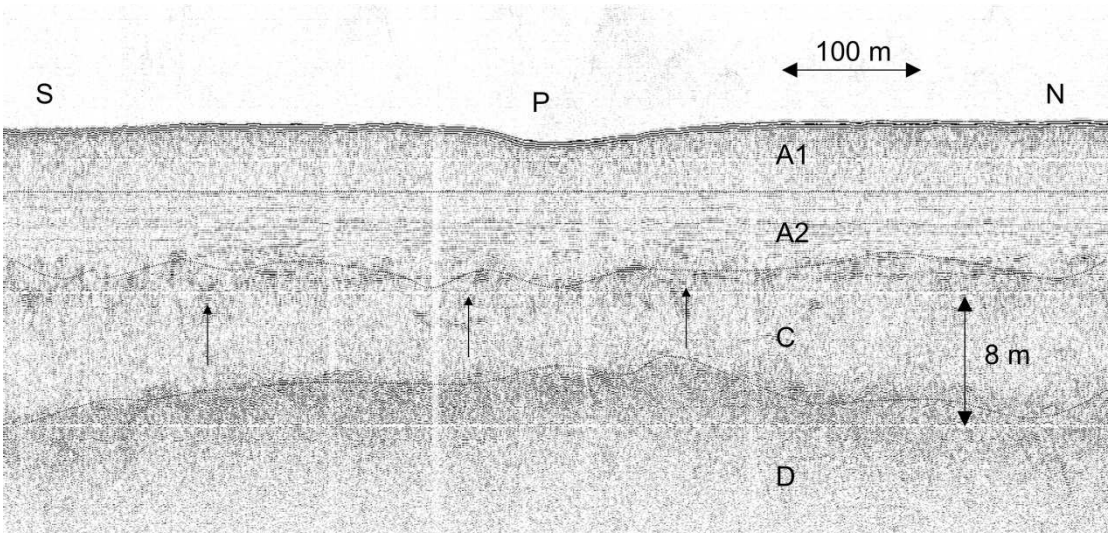

Figure 17: Sub-bottom sparker profile through a pockmark in the mudbelt region.

3.3.2 Sampling and underwater video investigation

Figure 16. and Table 2. give details for the sampling station locations for this study, types of samples taken and water depth. A 3m vibrocore, VC470, was sampled from within MP1 in 2009 along with a 2.3m control core, here named VC471. On the 2010 R.V. *Celtic Voyager* expedition a 1m gravity core was taken from within MP2 (GC50) and also a 3m vibrocore taken from within the LD (VC19). It was intended to take a vibrocore directly from the LDMD itself but unfortunately this was not completed. Control cores were also taken in the vicinity of the features and in the mudbelt region for comparison (See Table 2.). Further control cores were also taken at stations in the greater mudbelt region to the north (GC57) and to the south (VC82). GC75 was a short gravity core, which when sampled exhibited unambiguous geochemical zonation from oxic to anoxic conditions and served as a positive methodological control for this study. Upon opening and logging of sampled cores it was observed that overall, the sampled sediments consisted of homogenous Holocene sandy muds and there were no indication of geochemical zonation or distinct sub-surface anoxia, either visually or using the redox probe. E_h readings for cores ranged +128 - +42mV indicating suboxic conditions, while for the anoxic zone in GC75 measured values ranged from -140 - -194mV. Comparative descriptions of cores with corresponding controls showed high similarity in terms of sediment type, infauna and shell content. There was a higher proportion of sand and shell in the LD region compared to the mudbelt to the north.

Underwater video investigations collected extensive footage of the MP2 and the LDMD features along with the surrounding seabed. Figure 18. shows selected underwater still images of MP2 and also of the surrounding seabed environment, with video trace-lines shown in white. Fine-grained muds dominate the seabed inside and outside this feature and are characteristic throughout this mudbelt region. *Nephrops norvegicus* and their associated burrows are abundant in the region and no distinct macrobenthic (e.g. vestimentiferans) or microbial mats (e.g. *Beggiatoa* sp.), commonly reported at active seepage sites (Fisher, et al. 1997, Jorgensen and Boetius 2007) were present inside or in the vicinity of the pockmark. Figure 19. shows representative underwater still images from the LD and the LDMD and surrounding seabed. In comparison to the mudbelt region, the LD region, which lies at the edge of the mudbelt and the sandy region to the south, and its surrounding seabed is characterized by a higher proportion of sand and a greater abundance and diversity of

marine flora and fauna. Image stills 1 to 3 (Figure 5.) are representative images from within the LD, along its slope and at the edge and shows similar sediment type, but with the shell fragments component increasing considerably in the shallower depths. Sediment type across the LDMD was similar to surrounding sediment but there was an apparent increase in the proportion of shell fragments (Image 4), large cobbles (Image 6), benthic macrofauna, in particular brittle starfish (Image 5) and hermit crabs (Images 6), and benthic flora (Image 6).

MBES topographic maps of some of the MDAC mound structures in the CFZ are shown in Figure 20., as well as representative underwater still images, which were successively taken at the mound target sites. Video trace-lines are shown in white and numbers represent corresponding numbered underwater still images. As has been reported previously (Croker, Kozachenko and Wheeler 2005, Judd, Croker and Tizzard 2007), and due to the dynamic erosional environment, the region is dominated by extensive sand waves and the mound features, with reliefs of up to 10m, which follow a NW-SE trend along the Codling Fault appear to be eroded and/or covered by sand. As can be seen in the images the sediment in the region is dominated by medium to coarse sands and extensive sand waves are apparent (e.g. Figure 20 Image [2], [5] and [6]). Video investigation of the mounds confirmed that these features are largely covered by sand but extensive carbonate crusts and nodules of diverse morphologies can be observed in all images, as well as areas of black reduced surface sediments (Image [7]). Figure 20. [1] shows an underwater still image of exposed MDAC slabs, which was taken in close proximity to a mound feature. These are large and thick (10-20cm thick slabs as observed here) structures and are likely present throughout the region in the sub-seabed. Figure 20 [7] shows a high abundance of seabed benthic flora and fauna, which does not appear to be as abundant in the region surrounding the mounds. Figure 21. exhibits a close-up of one of the mound structures (circled in the inset) with a single beam echo sounder profile overlain on the mound. Extensive gas bubbling was observed coming from this mound and into the water column. Gas bubbles were clearly large and the plume was detected reaching tens of metres into the water column.

Mound structures could not be cored using the vibrocorer but were successfully ground-truthed using Shipek and Van Veen grabs. Three vibrocores were retrieved from the region but no MDAC was retrieved from these cores. Seabed in the region of the CFZ was found to be primarily well-sorted olive brown medium sand

with significant shell hash (generally 10% or less). A high percentage (>60%) of grab samples taken at the target sites yielded significant amounts of nodules and concretions of diverse morphologies and sizes, fossilized tubeworms, benthic flora and black sediment (Figure 22. A-C). No live tubeworms were retrieved. Surface anoxia was confirmed by redox potential measurements in black sediment, which exhibited E_h readings of -177mV. SEM images of the MDAC showed that quartz grains were cemented by various polymorphs of precipitated carbonate, in particular well-developed prisms of aragonite (Figure 23. A, B and D), and were also characterized by extensive amorphous to well developed framboidal pyrite (Figure 23. B, C and D). Sub 3µm rod-, cocci- and filamentous microbial structures and distinct structures, which appear to be microalgal were also observed (Figure 23. C). SEM analysis also highlighted extensive cratering and channeling in one hard carbonate nodule (Figure 9. E).

Table 2: Sampling station locations and descriptions

Name	Abbrev.	Type	Latitude		Longitude		Date	Water Depth (m)	Core length (m)	Brief Description
ISMA-V-470	VC470	Vibrocore	53^0	41.5970	5^0	58.3665	17/10/09	41	3	Mudbelt pockmark (MP1)
ISMA-V-471	VC471	Vibrocore	53^0	41.4692	5^0	57.9566	17/10/09	42	2.3	MP1 control
CV10_28_019 VC	VC19	Vibrocore	53^0	26.4068	5^0	48.1412	3/6/10	118	3	Lambay Deep
CV10_28_020 VC	VC20	Vibrocore	53^0	26.4404	5^0	48.5529	3/6/10	79	3	Lambay Deep control
CV10_28_049 GC	GC49	Gravity	53^0	40.6765	5^0	55.6449	4/6/10	50	1	MP2 control
CV10_28_050 GC	GC50	Gravity	53^0	40.6722	5^0	56.1720	4/6/10	43	1	Mudbelt pockmark (MP2)
CV10_28_057 VC	GC57	Gravity	53^0	54.9778	5^0	57.0370	4/6/10	42	1	North mudbelt
CV10_28_075 VC	CG75	Gravity	53^0	36.9934	5^0	25.4455	5/6/10	100	0.85	East mudbelt. Positive method control
CV10_28_82 VC	VC82	Vibrocore	53^0	31.6471	5^0	47.5960	5/6/10	71	3	South mudbelt
CV10_28_114 VC	VC114	Vibrocore	53^0	40.6399	5^0	55.6957	7/6/10	47	3	Central mudbelt
CV10_28_100 SG	G100	Shipek grab	53^0	20.1889	5^0	37.5058	6/6/10	68	n/a	Codling Fault MDAC
CV10_28_103 SG	G103	Shipek grab	53^0	19.9154	5^0	37.1514	6/6/10	58	n/a	Codling Fault MDAC
CV10_28_109 SG	G109	Shipek grab	53^0	19.5904	5^0	37.0692	6/6/10	67	n/a	Codling Fault MDAC
CV10_28_110 SG	G110	Shipek grab	53^0	19.9238	5^0	37.1634	6/6/10	67	n/a	Codling Fault MDAC
CV10_28_111 VV	G111	Van Veen g	53^0	19.9749	5^0	37.3612	6/6/10	65	n/a	Codling Fault
CV10_28_112 VV	112G	Van Veen g	53^0	20.0283	5^0	37.2291	6/6/10	65	n/a	Codling Fault

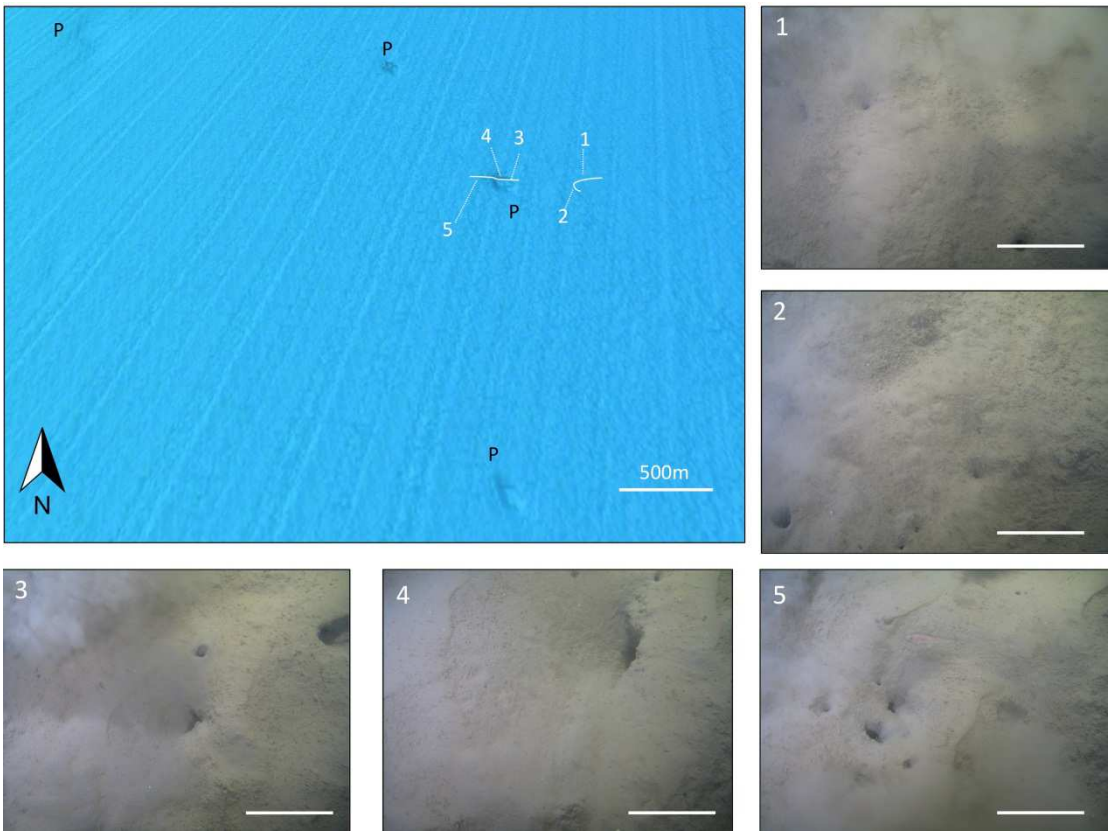

Figure 18: Underwater still images taken from within mudbelt pockmark (MP2) and from surrounding seabed. P – pockmarks, and numbers correspond to representative numbered underwater still images.

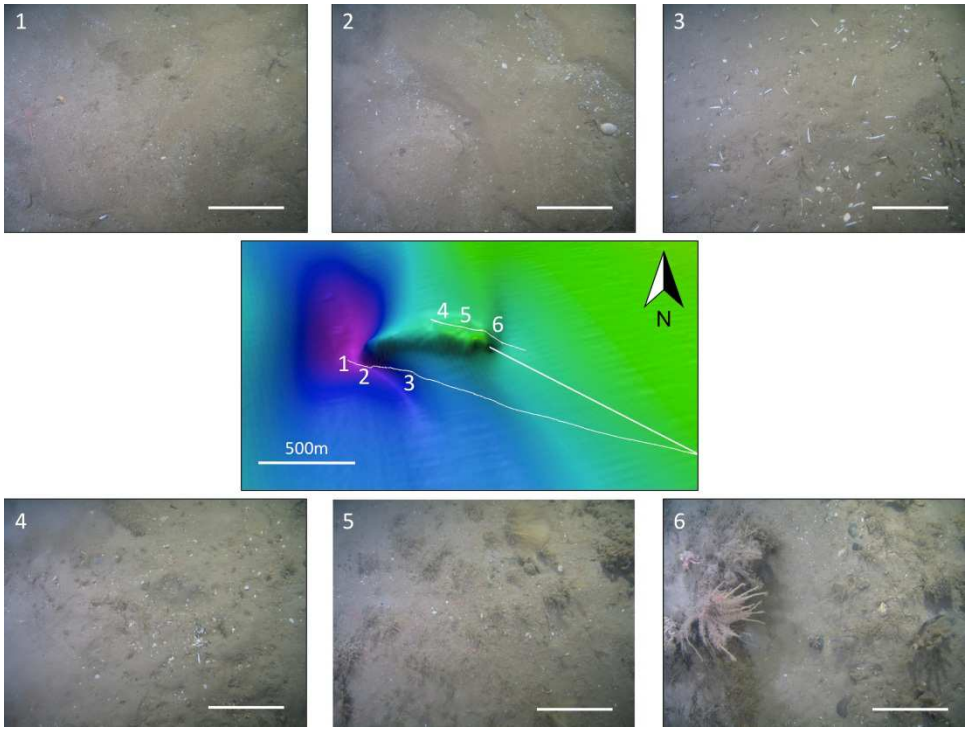

Figure 19: Underwater still images taken from within the Lambay Deep area, its associated mud diapir and surrounding seabed. Numbers correspond to representative numbered underwater still images.

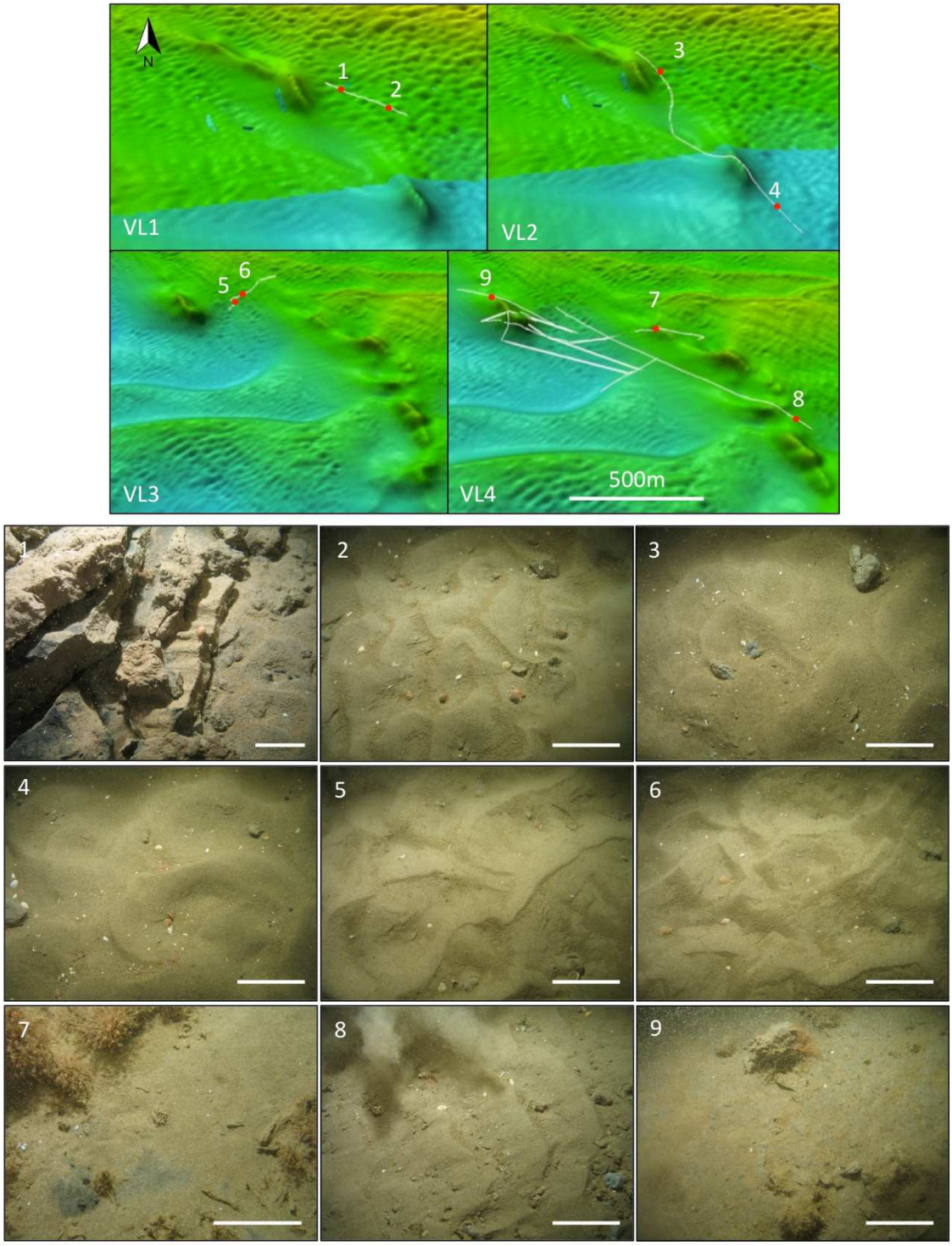

Figure 20: Multibeam echosounder mapping of MDAC mounds in Codling Fault Zone. Videolines 1, 2, 3 and 4 (VL1, etc.) are shown with underwater video deployment traces shown in white. Representative images are numbered and shown. Scale bars on images represent 25cm

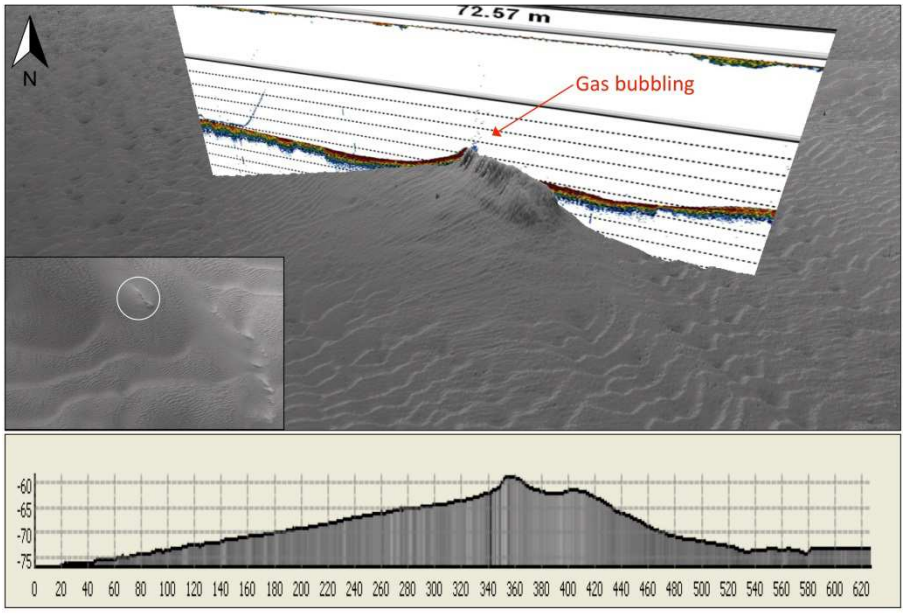

Figure 21: Mound structure (circled mound inset) showing active bubbling to the water column

Figure 22: Grab-sampling of MDAC mound targets. (A), (B) and (C) Black anoxic sediment with high abundance of cemented fossil tube worms and MDAC (D) Large 7cm diameter carbonate nodule.

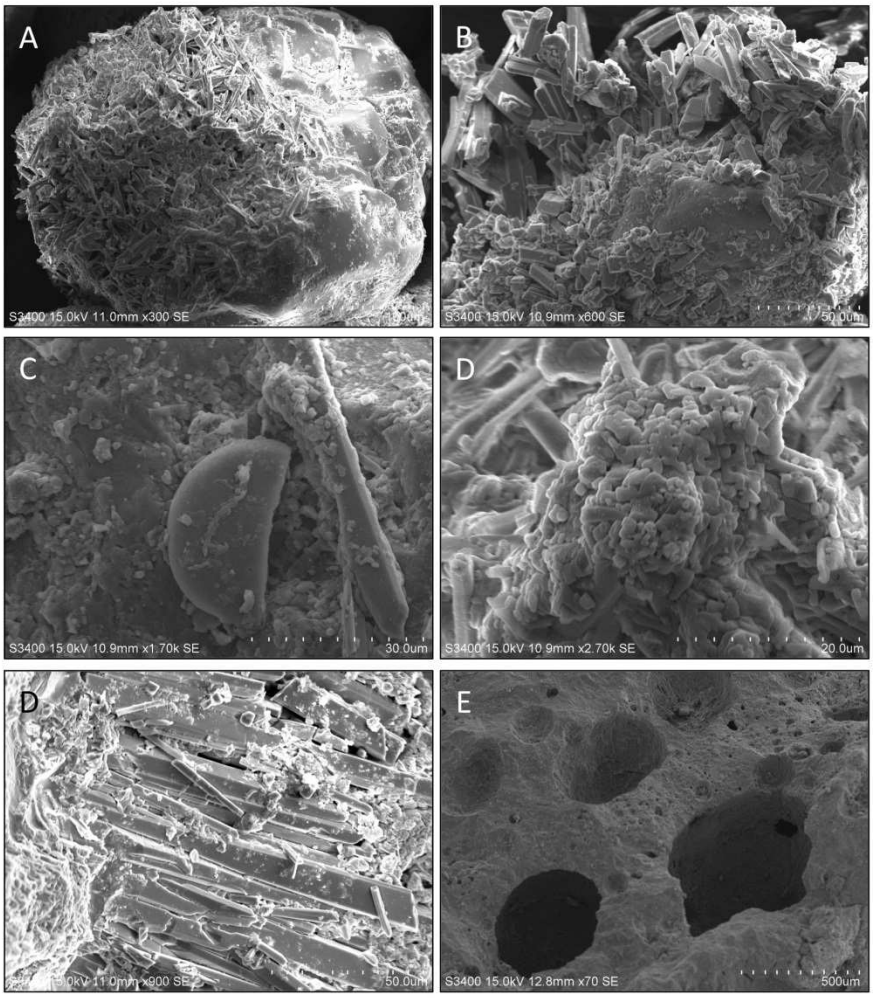

Figure 23: Scanning electron microscopy images of (A) Carbonate encrusted quartz grain, (B) Close-up of quartz grain cemented by aragonite crystals and also framboidal pyrite, (C) image showing apparent rod, cocci and filamentous microbial structures, (D) close-up of framboidal pyrite, (D) close-up of well-developed aragonite crystals and (E) image of nodule showing high density of craters and pores.

3.3.3 Methane and pore water analysis

Figure 24. shows down-core profiles for interstitial CH_4, SO_4^{2-} and HS^- for cores taken from MP2 (GC50) and the LD (VC19) compared with corresponding controls GC49/VC114 and VC20. Profiles for regional controls GC57 and VC82 are also shown, in addition to the GC75 positive control. Studies of pore water geochemistry and modelling of benthic fluxes in marine sediments provide a good indication of early diagenetic processes, rates and paths of organic matter remineralization, links with regional patterns of water column productivity, microbial process rates, and CH_4 flux rates at seepage sites (Schulz 2006, Borowski, Paull and Ussler III 1996,

Grandel, et al. 2000). CH_4 is expressed here in μmol mL^{-1} wet sediment, while SO_4^{2-} and HS^- are expressed in mM. It must be noted that degassing effects during core retrieval preclude the measurement of representative *in-situ* CH_4 levels and it is the overall variation in profiles which are utilized (Schulz 2006). 1m gravity cores display maximum concentrations in the range of 0.2μmol mL^{-1} or less. 3m cores display slightly increasing concentrations of CH_4 at deeper sediment depth, generally reaching maximum concentrations at 0.5μmol mL^{-1} at about 3mbsf. There was observed increases in CH_4 trends in 3m cores but no significant differences between sample cores and controls.

SO_4^{2-} concentrations, range from 19-25mM and no clear reduction (typical $[SO_4^{2-}]$ in seawater is about 28.9mM) or depletion is observed in cores within the features or in controls. There are slightly decreasing trends of SO_4^{2-} apparent in the 3m cores and are in line with increasing CH_4 concentrations. In addition HS^- is absent or negligible in both samples and controls. On the other hand the positive control GC75 exhibits distinct SO_4^{2-} reduction after 0.5mbsf to a measured minimum of 11mM, and shows a gradient of complete depletion within the first 1mbsf. With SO_4^{2-} reduction there is a concurrent increase in HS^- and CH_4, reaching maximum concentrations of 0.15mM and 1.7μmol mL^{-1} respectively. Comparison of cores taken within features and the controls, and comparison with the positive control GC75, indicates that the cores taken from the MP2 and LD do not possess enhanced interstitial methane and seepage to the SWI is not occurring. CH_4 analysis of three vibrocore core catchers sampled from sand in the CFZ region yielded 13.4, 29.7 and 51.3μmol CH_4 mL^{-1} and in comparison to GC75 the latter two core catchers appear to be elevated in CH_4.

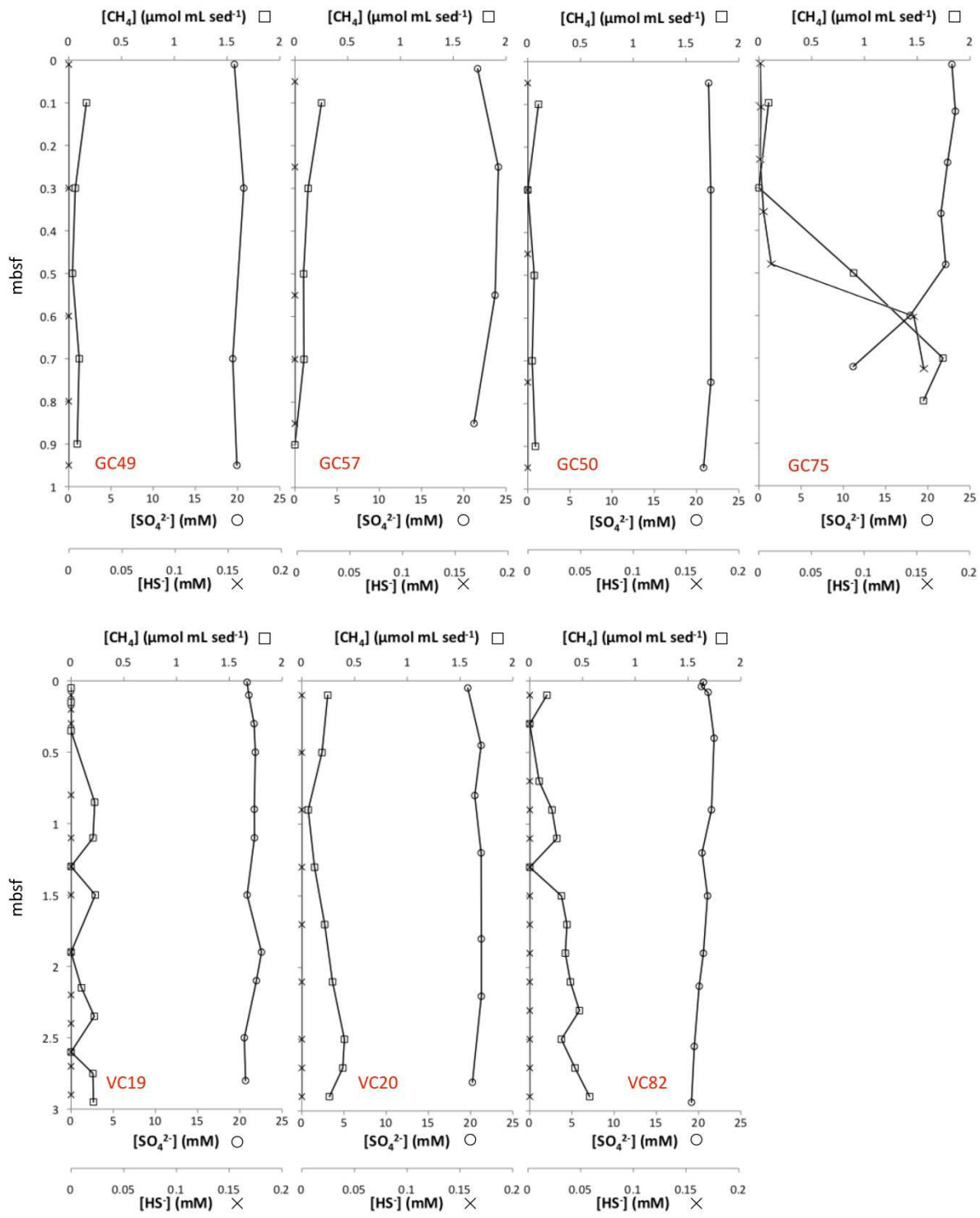

Figure 24: Down-core interstitial CH_4 and pore water SO_4^{2-} and HS^- concentrations from an Irish Sea pockmark (GC50) and the Lambay Deep (VC19) cores, with control cores in close proximity to the features - GC49 and VC20 respectively. GC57 is an additional control core taken in the N.E. and GC75 is a positive control.

Figure 25. shows pore water profiles for PO_4^{3-}, NH_4^+ and Fe^{2+} for sampled cores from features and controls. A PO_4^{3-} profile is not available for GC75, while Fe^{2+} profiles

were not measured for VC470 and VC471. Note the scales for PO_4^{3-} are 0 -60μM, while the scales for NH_4^+ are 0 – 0.2mM for gravity cores (apart from GC75 which is 0 – 8mM) and is 0 – 2mM for vibrocores. Scales for Fe^{2+} are 0 - 3μM apart from GC75 and VC82, which have scales of 0 - 20μM. Pore water PO_4^{3-} profiles were generally quite variable in terms of absolute values and gradients but cores generally displayed a peak in concentrations in the upper 0.3mbsf before depletion and a gradual increasing trend at depth, which is clearly observed in 3m cores. Maximum Fe^{2+} concentration were typically observed in the upper 0.1mbsf, and ranged from 0.8 – 19.5μM, before levels were depleted to low concentrations of less than about 0.4μM. A maximum concentration of 18μM was observed at 0.24mbsf in the positive control (GC75). General trends for NH_4^+ were gently increasing linear gradients with $[NH_4^+]_{min}$ observed closest to the SWI and $[NH_4^+]_{max}$ at the deepest sediment layers. $[NH_4^+]_{min}$ ranged from 0.02 – 0.3mM at the shallowest depths to 0.6 - 1.4mM (for 3m cores).

Core GC50 from the vicinity of the pockmark MP2, shows a peak in PO_4^{3-} from between 0.15 – 0.3mbsf and follows a general decreasing trend with $[PO_4^{3-}]_{min}$ of 7μM at 0.95mbsf . The NH_4^+ profile is relatively constant down-core with $[NH_4^+]$ between 0.01mM and 0.03mM, and also for Fe^{2+} with values generally around 1μM from 0 – 0.95mbsf. In comparison GC49, from within MP2 displays $[PO_4^{3-}]$ and $[NH_4^+]$ peak at 19μM and 0.06mM at 0.15mbsf. The PO_4^{3-} profile shows an apparent decreasing trend to 0.7mbsf but is variable, while the NH_4^+ profiles displays a very gradual decreasing trend until 0.7mbsf before increasing again. Fe^{2+} concentrations deplete from maximum levels of 1.4μM at 0.02mbsf. GC50 and GC49 shows relatively similar profiles.

The MP1 core VC470 and its corresponding control VC471 display an overall high similarity in down-core PO_4^{3-} and NH_4^+ profiles. PO_4^{3-} trends are similar, whereby $[PO_4^{3-}]_{max}$ is observed between at 0.07mbsf (40.9μM) and 0.15mbsf (52.4μM) for VC470 and VC471 respectively. There is a sharp rate of decrease until $[PO_4^{3-}]_{min}$ is reached between 0.65 - 0.75mbsf at about 4μM for both cores, followed by a subsequent linear increase to 1.7mbsf, with values of 28.5μM and 35.1μM for VC470 and VC471 respectively. $[NH_4^+]$ displays a gentle decreasing trend until about 0.3mbsf before linearly increasing from about 1mbsf until maximum depths, where $[NH_4^+]_{max}$ also occurs (1.5mM and 0.5mM for VC470 and VC471 respectively). However there is clearly a steeper gradient for NH_4^+ in VC470 compared to VC471.

LD core VC19 displays an overall linear increasing trend of PO_4^{3-}, measuring 10.22µM at the SWI and 33.7µM at 2.4mbsf, but there is also an apparent slight concave-up trend from the SWI to 0.4mbsf. A distinct linear increasing trend for NH_4^+ from the SWI (0.10mM) to 2.9mbsf (0.59mM) is also observed. Fe^{2+} was not detected in significant amounts in this core. VC20 shows a slight concave-up profile for PO_4^{3-}, whereby a steeper gradient is observed from 0.05mbsf to 0.65mbsf, before remaining relatively constant down-core. [PO_4^{3-}] are double (20.3µM) that of VC19 at the top depths and consistently higher along the core. This core has a Fe^{2+} peak at 0.93µM at 0.2mbsf, followed by a rapid depletion at depth.

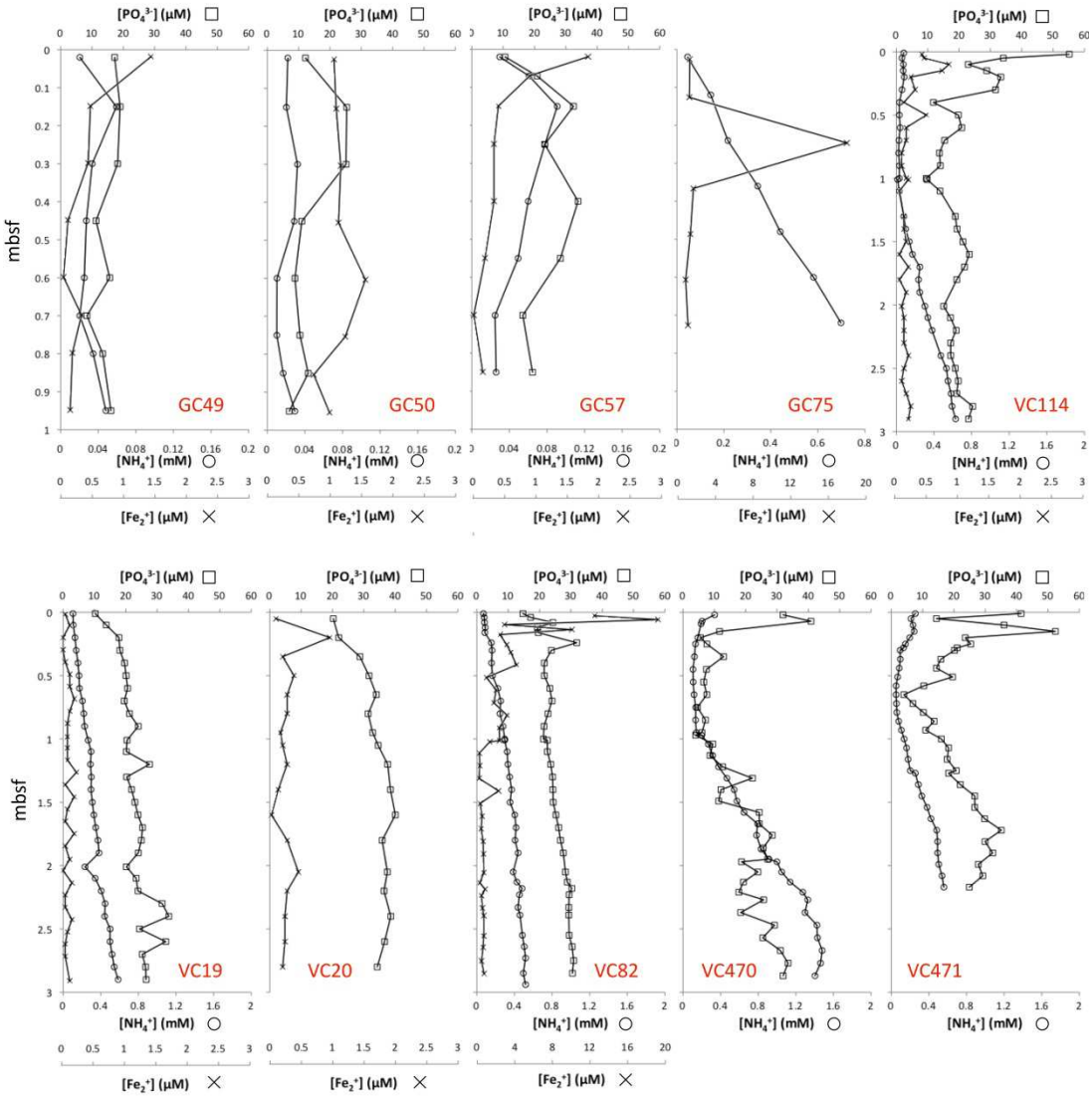

Figure 25: Down-core pore water profiles of PO_4^{3-}, NH_4^+ and Fe^{2+} of Irish Sea pockmarks – GC50 and VC470 and the Lambay Deep mud diapir, VC19. These are compared with proximal control cores – GC49 (and VC114), VC471 and VC20 respectively. Additional regional controls are also given – GC57 (North mudbelt),and VC82 (south mudbelt) as well as the GC75 positive control core.

3.4 Discussion

3.4.1 Description and distribution of pockmarks in the Irish Designated Seabed Zone (IDSZ) of the Irish Sea

This study enhances knowledge regarding the occurrence and distribution of pockmarks in Irish waters. Pockmarks are found globally, primarily in fine-grained sediment regions (Judd and Hovland 2007) and it is this fine-grained particle size that is thought to form a cap on fluid (primarily gas) migration from deeper sedimentary layers due to its relative impermeability. In this study bathymetric mapping revealed ten unit pockmarks occurring at an average water depth of about 43m, which run along an approximate NNW line from approximately $53^0$41'N to $53^0$48'N. These pockmarks are similar in size and morphology to the most commonly described pockmarks, in that they are of average diameter, shallow circular or slightly elongate features (Judd and Hovland 2007). They are characterized by a gradual slope, with likely significant infilling and sedimentation since the time of formation of the depressions. Extensive mapping and processing of datasets from the Irish Sea IDSZ is ongoing and will likely reveal more pockmarks in this mudbelt region. In particular there may be a significant number of undiscovered pockmarks in yet to be mapped regions of the Irish Sea IDSZ lying east of about $5^0$51'W.

3.4.2 Seabed geochemistry of the Irish Sea mudbelt and Lambay Deep areas: A preliminary assessment

While pore water O_2 was not measured in this study results from redox measurements indicate that O_2, which is thermodynamically the most favourable electron acceptor (-3190kJ mol^{-1}) (Schulz 2006), is depleted in the first few centimeters. Thus other electron acceptors are responsible for organic matter remineralization below these depths. Fe^{2+} profiles indicate that Fe^{2+} is essentially depleted in the first 20cm. Fe^{2+} is an end product of organic matter degradation with Fe (III)-oxides as electron acceptors. The energy yield from this reaction is -1410 kJ mol^{-1} and is thermodynamically less favourable to oxidation by Mn-oxides (-3090kJ mol^{-1}) and NO_3^- (-2750kJ mol^{-1}) (Schulz 2006), which indicates that these electron acceptors are consumed within the first 20cm. The next favourable electron acceptor, which is quantitatively the most important in marine sediments, is SO_4^{2-}. SO_4^{2-} depletion in is pore water is primarily related to utilization by sulphate-reducing bacteria for organic

matter remineralization (Whiticar 2002). The products of this reaction are HS^- and CO_3^{2-}, which thus increase in pore water as a consequence of SO_4^{2-} reduction.

Reduction of Fe (III)-oxides is a significant process in this environment by virtue of the distinct Fe^{2+} reactive layers observed in most cores. In addition Fe^{2+} profiles generally display steep gradients, which suggests that it is rapidly oxidized as it diffuses to overlying layers or bound to the solid phase at depth. Essentially constant or slight decreasing trends in SO_4^{2-} are observed in most of these cores, with negligible HS^- levels throughout (apart from GC75). This suggests that SO_4^{2-} is not a significant electron acceptor in these cores, or there is a resupply of SO_4^{2-} for utilization in organic matter remineralization. The fact that negligible levels of HS^- were observed in most cores indicates that either SO_4^{2-} reduction to HS^- is not occurring or that it is rapidly reoxidized. Sediments in the mudbelt region are extensively populated by *Nephrops Norvegicus* and other species, and high densities of burrows were observed in the mudbelt regions (Fig. 5). Sediments up to about 1mbsf are subject to bioturbation and bioirrigation by benthic organisms, which results in enhanced exchange between pore waters and overlying seawater (Berner 1980). This would have the effect of increasing the penetration depth of O_2 and other electron acceptors, in particular SO_4^2, which otherwise would be depleted at shallower depths. It is known that in certain circumstances burrowing fauna can influence transport processes to the degree that advection and bioirrigation dominate over molecular diffusion (Jorgensen 2006). Therefore it may be a significant factor affecting pore water geochemistry in the mudbelt, and may account for resupply of SO_4^{2-}rich seawater into the sediments.

NH_4^+ pore water profiles here generally show linearly increasing trends with depth and are probably related to degradation of organic matter. PO_4^{3-} is not utilized as an electron acceptor and in most cases its consumption is either due to biological uptake and formation of new biomass, the adsorption onto particulate surfaces or co-precipitation with *in-situ* formed minerals or in the formation of authigenic fluorapatite (Hensen, Zabel and Schulz 2006). In these sediments the main release of both Fe^{2+} and PO_4^{3-} into sediments occur at different depths, in the top 5cm for Fe^{2+} and 20-30cm for PO_4^{3-}. This indicates that most PO_4^{3-} released into pore water in these sediments is not from *in-situ* Fe minerals, but that PO_4^{3-} production is primarily as a result of bacterial activity in organic matter degradation. The subsequent observed decreasing trend followed by an increase to depth may be due to co-

precipitation or authigenic mineral formation in the former case and re-release of bound PO_4^{3-}. In the central and north mudbelt region two distinct reactive zones were observed in 3m vibrocores (VC114, 470 and 471), at depths of between 0.05 - 0.4mbsf and from about 1mbsf to depth. These zones were not apparent in cores to the south (VC82, 19 or 20) and indicate overall lower rates of PO_4^{3-} cycling to the south. Diffusive fluxes to the SWI were also generally greater to the north, as high as 4.6 mmol $m^{-2}a^{-1}$ to the north and generally 0.28 mmol $m^{-2}a^{-1}$ or less to the south.

Thus from NH_4^+ and PO_4^{3-} pore water profiles is a clear that there is a higher rate of organic matter remineralization and cycling in the mudbelt compared to south. This would be expected due to the higher rate of deposition and smaller particle size in the north. The sedimentary environment of the mudbelt in the Irish Sea IDSZ has appears to be suboxic at the investigated depths. It is proposed that based on the lack of observable SO_4^{2-} reduction in SO_4^{2-} and HS^- pore water profiles, in conjunction with the zone of Fe^{2+} production in the range of 0.02 – 0.5mbsf for sampled cores, that microbial remineralization of organic matter using Fe (III)-oxides as an electron acceptor is the primary process occurring in the top 1m of sediment. It is likely that SO_4^{2-} reduction is occurring at greater depths, which is apparent in 3m vibrocores, but that it may not be the primary process. The possible resupply of SO_4^{2-} rich water by *Nephrops norvegicus* in the mudbelt is one hypothesis for the low levels of SO_4^{2-} reduction. Overall the pore water geochemistry and thus geochemical processes in the mudbelt surface sediments are similar regionally. For example for GC57 (northern region), GC49 (central region) and VC82 (southern region) displayed very similar SO_4^{2-} and CH_4 profiles and profiles for PO_4^{3-}, NH_4^+ and Fe^{2+} were generally similar with similar overall values (apart from Fe^{2+} at SWI for VC82) and reactive zones occurring at the same sedimentary depths. However it must be noted that a significant region of the mudbelt was not investigated in this study i.e. very shallow waters <30mbsf and comparatively deeper waters. Indeed the deepest core sampled at 100m water depth (GC75) displayed markedly different geochemical zonation and processes.

3.4.3 Inference about present seepage and distinct processes at mudbelt pockmarks and the Lambay Deep mud diapir.

Floodgate et al. (1984) sampled acoustically turbid surface sediments in the W. Irish Sea at 100m water depth (now in the UK sector). They noted significant levels of CH_4

in 1.2m cores, which increased with depth up to concentrations in the range of 10,000μmol kg^{-1}. Further studies highlighted a substantial shallow gas zone in the W. Irish Sea and numerous gas plumes and gas fronts were identified (Yuan and Bennell 1992). Yuan et al. (1992) is the only other study, to our knowledge, which has identified pockmarks in the W. Irish Sea. These were found to be largely associated with but also present outside acoustically turbid zones in the mudbelt. These studies however focused on the mudbelt region, lying to the east of this current study, which are in deeper waters and now are part of the UK sector.

Sub-bottom seismic profiling of selected mud-belt pockmarks and the LDMD, followed by subsequent underwater video investigations of these features and surrounding seabed, indicated that at present there is no significant active seepage reaching the SWI and that there are not distinct macrobenthic communities or microbial masts associated with these features. This conclusion is supported by interstitial gas and pore-water geochemistry of cores taken from these features and compared with numerous controls. The geochemical results presented here are considered robust considering that the core GC75, which exhibited a distinct oxic/anoxic chemical zonation, served as a positive control for SO_4^{2-} depletion and methanogenesis. GC75 displayed a characteristic oxic/anoxic geochemical zonation whereby successive electron acceptors are depleted, leading to utilization and depletion of SO_4^{2-}, with the concurrent production of HS^-. The high concentration of CH_4 observed below 0.5mbsf results from enhanced methanogenesis fueled by organic matter supply or CH_4 migration from depth (Martens, Albert and Alperin 1998). In addition, steep gradients of NH_4^+ and Fe^{2+} were observed indicating high levels of organic matter remineralization and microbial activity. Thus this core provides an important reference for what may be considered enhanced processes and microbial activity at target seepage sites. This profile exhibits a distinct and characteristic sulphate-methane transition zone (SMTZ) where the CH_4 is being anaerobically oxidized, most likely by the sulphate-reducing bacteria (SRB)/ANME microbial consortia (Boetius, et al. 2000). Uniform CH_4 and SO_4^{2-} profiles and the lack of clear SMTZs' in any cores taken from within any of the features, or from the control cores indicates strongly that AOM and CH_4 seepage to the SWI is not an ongoing process at present in either the mudbelt pockmarks or the Lambay Deep mud diapir. This study however was limited to the upper 3mbsf and conclusions cannot be drawn as to geochemical processes occurring deeper in the sediment. It is noteworthy

that high densities of *Nephrop norvegicus* burrows were observed (Figure 18.) and as discussed above due to bioturbation may having a significant impact on pore water geochemistry and may account for the distinct pore-water profiles whereby reduction of SO_4^{2-} is not evident. It is therefore also possible that some level of seepage is occurring but that CH_4 is being aerobically oxidized.

As regards the differences in pore water nutrients and electron acceptors between sample cores and controls, there are no clear conclusions to be drawn about possible variation in processes and microbial activity at the pockmarks or Lambay Deep. There were interesting trends observed between GC50 and its control GC49 for MP2. Fe^{2+} is consistently higher in GC50 compared to GC49 and does not display appreciable depletion at depth. This suggests that there are increased rates of incorporation of Fe^{2+} into the solid phase outside the pockmark and/or that GC50 is more reducing. However no indication of this was observed by E_h measurements. Levels of PO_4^{3-} were consistently higher in GC49 also. Comparison of PO_4^{3-} profiles for VC470 and VC471 do indicate that PO_4^{3-} concentrations are substantially higher for the control core VC471 at the SWI and the PO_4^{3-} release in the reactive zone is greater, which suggests a greater microbial activity outside the pockmark. A steeper increasing gradient is also observed in VC471. Similarly NH_4^+ profiles show a steeper increasing gradient at depth for VC470 compared to VC471.

While results here indicate that active seepage to the water column and in the upper 3mbsf is not occurring, sub-bottom seismic profiling does indicate that these features are influenced by gas fronts in deeper sediment layers. Yuan et al. (1986) mapped an extensive lateral shallow gas zone in the mudbelt region to the west of the Isle of Man but could not provide conclusive evidence of the vertical extent of gas due to acoustic blanking. A further sampling expedition using longer coring instruments is required to address questions raised in this study, in particular regarding the temporal activity of these features. Recent research has shown that pockmarks in the Lower Congo Fan are currently dormant but were periodically active in the past (Gay, et al. 2007).

3.4.4 The Codling Fault MDAC mounds: a site of active and enhanced current gas seepage to the water column.

The study provides a comprehensive ground-truthing study of the Codling Fault MDAC mounds and enhances previous findings by Croker et al. (1995, 2005) and Judd et al. (2007). Extensive gas seepage from one of the mounds was recorded (Figure 21.). The unambiguous extent and height of the plume highlights the considerable, but as yet unquantified, seepage occurring in the region. Moreover the height of the gas plume, rising tens of metres into the water column, combined with the shallow location of these features (<100m water depth) emphasizes the potential for possible atmospheric flux and impact on regional climate. CH_4 release from the oceans has been linked to rapid climate change events (e.g. Hesselbo, et al. 2000). CH_4 analysis of vibrocore core catchers (up to 51.3µmol mL^{-1}) suggests that seabed CH_4 levels are elevated, at least in comparison to surface sediments in the mudbelt and the Lambay Deep area to the north. The size and thickness of slabs and pavements indicates considerable seepage over geological timescales and the periodic stacking nature suggests variation in seepage over geological timescales (Figure 7 [1]). It has been shown that the region is characterized by; a considerable abundance of carbonate nodules and crusts (Figure 20 [2] – [9]), patches of anoxia at the SWI (Figure 21 [7] and Figure 22B) and a substantial proportion of cemented fossil worm tubules (Figure 22A-D). This indicates a significant area in this region is currently influenced or has been influenced by seepage. The presence of extensive MDAC nodules of relatively small sizes also highlights the high-energy erosional environment in this region (Croker, Kozachenko and Wheeler 2005).

CH_4 is oxidized in an oxic environment to CO_2 and H_2O and is a well documented process (Higgins and Quale 1970), but the extensive presence of authigenic pyrite with authigenic carbonate demonstrated by underwater video investigation, ground truthing and SEM indicates that the primary process here is anaerobic oxidation of methane (AOM). As previously reported (Judd, Croker and Tizzard 2007) SEM analysis confirmed AOM on the micro scale with the presence of quartz grains cemented by various carbonate polymorphs and the simultaneous presence of framboidal pyrite (Figure 23). AOM is known to be mediated by a consortium of sulphate-reducing bacteria and methanothrophic archaea (Boetius, et al. 2000) and the possible presence of microbes in the MDAC was indicated also with the presence of rod-, cocci- and filamentous-like structures in SEM images (Figure 23C).

Previous measurements of bulk $\delta^{13}C$ carbonate nodules at a site nearby the CFZ, named Texel 11, ranged from -41 - -46‰ (Judd, Croker and Tizzard 2007), indicating that carbonate was formed by microbial oxidation of CH_4 (Peckmann, et al. 2001).

3.4.5 Sources of seepage at Irish Sea gas seepage features

In the Irish Sea the source of thermogenic CH_4 is thought to be from coal-bearing Carboniferous rocks. The source of biogenic CH_4 is from tertiary lignites and modern silts and clays. Conditions for biogenic CH_4 are provided by fine-grained mudbelt regions, where pockmarks have been found to occur, as reported here and previously by Yuan et al. (1992). Migration pathways of CH_4 from sub-seabed to the SWI are thought to be primarily along faults, faults associated with salt structures (e.g. mud diapirs) and regions where Carboniferous source rocks sub-crop beneath Quaternary sediments. Yuan et al. (1992) noted in their study that due to the extent and distribution of gas in the mudbelt that the seepage is likely of biogenic rather than thermogenic origin. They argue that in contrast to present day conditions whereby sedimentation is controlled by prevailing oceanographic conditions, in the early Holocene after ice retreat, Atlantic waters would have controlled sedimentation in the Irish Sea and that an east-west trending glacial sediment ridge and a rock ridge may have formed a barrier to northerly movement up the Irish Sea. This influx of warm waters and sediment traps would have facilitated rapid accumulation of fine-grained organic matter-rich sediments. Several other studies have argued that a frontal trough on the southern boundary of the muddy region, marks the boundary between low-energy stratified waters and high-energy well-mixed waters (north and south respectively), whereby enhanced biological productivity and biomass accumulation and deposition in the low-energy region, has led to a large expanse of gas-bearing sediments in this area (Belderson 1964, Simpson and Bowers 1979, Rees and Brander 1986).

Subsequent studies in the Irish Sea have shown the presence of significant shallow gas accumulations in sandy regions and also extensive ^{13}C-depleted methane-derived authigenic carbonates, which indicate that the primary source of gas in the Irish Sea is thermogenic in origin and probably derived from underlying Westphalian Coal Measures or the Dinantian/Namurian Holywell Shale (Croker 1995, Judd 2005). The MDAC mounds form along the Codling Fault on the eastern border of the Kish Bank Basin and hence it is most likely that seepage is of thermogenic origin migrating

from significant depth from Permo-Triassic and Carboniferous rocks. However Judd et al. (2007) suggest that active migration occurs along the fault and seeping gas may be from Tertiary sediments or underlying Carboniferous rocks, or that both may be contributing sources of gas. At present distinct conclusions regarding the source of seepage can only be hypothesized. Stable carbon isotope analysis of gas samples may provide information as to the source of seepage (Floodgate and Judd 1992).

3.5 Conclusion

In comparison to previously reported pockmarks in the UK sector of the Irish Sea, the pockmarks reported here in the Irish sector appear to not be actively seeping to the SWI and surface sediments at present. Underwater video investigation indicates that there are not distinct ecological niches within these features, compared to the surrounding seabed. Investigation of the Lambay Deep and its mud diapir suggests that this is also dormant feature at present. In contrast to the pockmarks the mud diapir does appear to host an increased abundance and diversity of benthos but it is not clear if this is related to seepage or the apparent increase in hard surface lithology. Pore water and interstitial CH_4 analysis supports the inference that these investigated features are not active seepage sites at present. However seismic profiling has shown that the investigated pockmarks and the Lambay deep region are characterized by sub-surface gas fronts and other gas signatures in deeper sedimentary layers. It must be noted also that this study limited geochemical investigations to 3mbsf of less, and that a core sample was not retrieved directly from the mud diapir itself. Thus conclusions regarding the geochemical processes at deeper sediment depths cannot be drawn and questions regarding the temporal activity of these features remain largely unknown, and are likely complex. In terms of overall seabed it was noted that there appears to a higher level of organic matter remineralization and cycling in the central and northern part of the mudbelt, compared to the sandier region in the south, which is likely related to the lower energy conditions to the north allowing deposition of fine grain sediments.

This study highlighted an extensive abundance of sand-covered and exposed carbonate nodules and crusts, surface anoxia and cemented worm tubules characterizing the seabed at and in the vicinity of the Codling Fault mounds. Active seepage into the water column and bubbling plumes tens of metres in height was

observed and, though unquantified is clearly substantial and due to the shallow nature and size of the plume may escape the water column to the atmosphere. SEM and redox profiling of sampled MDAC and sediments indicate the process of anaerobic oxidation of methane (AOM) is occuring at this site and as found elsewhere is likely to be a significant sink and control on methane seepage. This study thus supports previous inferences that the CFZ is the region of greatest seepage in the Irish Sea. The extensive seepage highlights the commercial potential in terms of energy resources and that further investigation to consider the distinct and unique biodiversity at this site should be investigated in terms of conservation under the EU Habitat's Directive.

Acknowledgements

The authors would like to thank the captain and the crew of R.V. *Celtic Voyager*. Peter Croker (PAD) is thanked for sharing invaluable advice and data for the cruise preparation. The Irish Marine Institute is thanked for funding the ship time through the RTDI funding scheme. Eamonn Kelly (Dept. of the Environment, Heritage and Local Government) is also thanked for his assistance and input. Brendan Twamley and technical staff in Dublin City University are also thanked for training and advice regarding SEM analysis. This work was carried out within the framework of an INFOMAR research project (2009) and with the collaboration of the Geoloigcal Survey of Ireland (GSI).

References

Aloisi, G., Bouloubassi, I., Heijs, S.K., Pancost, R.D., Pierre, C., Sinninghe Damsté, J.S., Gottschal, J.C., Forney, L.J. and Rouchy, J. (2002). CH4-consuming microorganisms and the formation of carbonate crusts at cold seeps. *Earth and Planetary Science Letters,* 203(1), pp.195-203.

Belderson, R.H. 1964. Holocene sedimentation in the western half of the Irish Sea. *Marine Geology,* 2pp.147-163.

Berner, R.A. 1980. *Early diagenesis: A theoretical approach.* 1st ed. Princeton, New Jersey: Princeton University Press.

Bligh, E.G. and Dyer, W.J. 1959. A rapid method of total lipid extraction and purification. *Canadian Journal of Biochemistry and Physiology,* 37(911), pp.917.

Bøe, R., Rise, L. and Ottesen, D. 1998. Elongate depressions on the southern slope of the Norwegian Trench (Skagerrak): morphology and evolution. *Marine Geology,* 146(1-4), pp.191-203.

Boetius, A., Ravenschlag, K., Schubert, C.J., Rickert, D., Widdel, F., Gieseke, A., Amann, R., Jorgensen, B.B., Witte, U. and Pfannkuche, O. 2000. A marine microbial consortium mediating anaerobic oxidation of methane. *Nature,* 407pp.623-626.

Bohrmann, G., Greinert, J., Suess, E. and Torres, M.E. 1998. Authigenic carbonates from the cascadia subduction zone and their relation to gas hydrate stability. *Geology,* 26pp.647-650.

Borowski, W.S., Paull, C.K. and Ussler III, W. 1996. Marine pore water sulphate profiles indicate in situ methane flux from underlying gas hydrate. *Geology,* 24pp.655-658.

Boudreau, B.P. 1997. *Diagenetic models and their implementation: modelling transport and reactions in aquatic sediments.* 1st ed. Berlin: Springer.

Bouloubassi, I., Aloisi, G., Pancost, R.D., Hopmans, E., Pierre, C. and Sinninghe Damsté, J.S. 2006. Archaeal and bacterial lipids in authigenic carbonate crusts from eastern Mediterranean mud volcanoes. *Organic Geochemistry,* 37(4), pp.484-500.

Croker, P.F. 1995. Shallow gas accumulation and migration on the western Irish Sea. *Geol Soc Lon Spec Publ,* 93pp.41-58.
Croker, P.F., Kozachenko, M. and Wheeler, A.J. 2005. *Gas-related structures in the Western Irish Sea (IRL-SEA6).* Dublin: Petroleum Affairs Division.
Dando, P.R., Austen, M.C., Burke Jr, R.A., Kendall, M.A., Kennicutt II, M.C., Judd, A.G., Moore, D.C., O' Hara, S.C.M., Schmaljohann, R. and Southward, A.J. 1991. Ecology of a North Sea pockmark with an active methane seep. *Marine Ecology Progress Series,* 70pp.49-63.
Elvert, M., Boetius, A., Knittel, K. and Jorgensen, B.B. 2003. Characterization of specific membrane fatty acids as chemotaxonomic markers of sulphate-reducing bacteria involved in anaerobic oxidation of methane. *Geomicrobiology Journal,* 20pp.403-419.
Fang, J., Chan, O., Joeckel, R.M., Huang, Y., Wang, Y., Bazylinski, D.A., Moorman, T.B. and Ang Clement, B.J. 2006. Biomarker analysis of microbial diversity in sediments of a saline groundwater seep of Salt Basin, Nebraska. *Organic Geochemistry,* (37), pp.912-931.
Fisher, C.R., Urcuyo, I.A., Simpkins, M.A. and Nix, E. 1997. Life in the slow lane: Growth and longetivity of of cold seep vestimentiferans. *Marine Ecology,* 18pp.83-94.
Fleisher, P., Orsi, T.H., Richardson, M.D. and Anderson, A.L. 2001. Distribution of free gas in marine sediments: a global overview. *Geo-Marine Letters,* 21pp.103-122.
Floodgate, G.D. and Judd, A.G. 1992. The origins of shallow gas. *Continental Shelf Research,* (12), pp.1145-1156.
Gal'chenko, V.F., Lein, A.Y. and Ivanov, M.V. 2004. Methane content in the bottom sediments and water column of the Black Sea. *Microbiology,* 73pp.211-223.
Games, K.P. 2001. Evidence of shallow gas above the Connemara oil accumulation, Block 26/28, Porcupine Basin *IN:* Shannon, P.M., Haugthon, P.D.W. and Corcoran, D.V. (eds.) *The petroleum exploration of Ireland's offshore basins.* Special Publication No. 188 ed. London, UK Geological Society of London, pp.361-374.
Gay, A., Lopez, M., Berndt, C. and Séranne, M. 2007. Geological controls on focused fluid flow associated with seafloor seeps in the Lower Congo Basin. *Marine Geology,* 244(1-4), pp.68-92.
Gay, A., Lopez, M., Cochonat, P., Séranne, M., Levaché, D. and Sermondadaz, G. 2006. Isolated seafloor pockmarks linked to BSRs, fluid chimneys, polygonal faults and stacked Oligocene–Miocene turbiditic palaeochannels in the Lower Congo Basin. *Marine Geology,* 226(1-2), pp.25-40.
Gieskes, J.M., Gamo, T. and Brumsack, H. 1991. *Chemical methods for interstitial analysis aboard JOIDES Resolution: Technical note 15.* Texas: Ocean Drilling Program.
Grandel, S., Rickert, D., Schluter, M. and Wallman, K. 2000. Pore water distribution and and quantification of diffusive benthic fluxes of silicic acid, nitrate and phosphate in surface sediments from the deep Arabian Sea. *Deep-Sea Research II,* 47pp.2707-2734.
Hensen, C., Zabel, M. and Schulz, H.N. 2006. Benthic cycling of oxygen, nitrogen and phosphorus *IN:* Schulz, H.D. and Zabel, M. (eds.) *Marine Geochemistry.* 2nd ed. Berlin Springer, pp.205-240.
Hesselbo, S.P., Grocke, D.R., Jenkyns, H.C., Bjerrum, C.J., Farrimond, P., Morgans Bell, H.S. and Green, O.R. 2000. Massive dissociation of gas hydrate during a Jurassic oceanic anoxic event. *Nature,* 406pp.392-395.
Higgins, I.J. and Quale, J.R. 1970. Oxygenation of methane by methane-grown *Pseudomonas methanica* and *Methanomonas methanooxidans*. *Biochemical Journal,* 118pp.201-208.
Hovland, M., Gardner, J.V. and Judd, A.G. 2002. The significance of pockmarks to understanding fluid flow processes and geohazards. *Geofluids,* 2pp.127-136.
Hovland, M., Svensen, H., Forsberg, C.F., Johansen, H., Fichler, C., Fosså, J.H., Jonsson, R. and Rueslåtten, H. 2005. Complex pockmarks with carbonate-ridges off mid-Norway: Products of sediment degassing. *Marine Geology,* 218(1-4), pp.191-206.
IPCC 2007. *Contribution of Working Group 1 to the Fourth Assessment Report of the Intergovernmental Working Group on Climate Change.* Cambridge, USA: Cambridge University press.
Jackson, D.I., Jackson, A.A., Evans, D., Wingfield, R.T.R., Barnes, R.P. and Arthur, M.J. 1995. The geology of the Irish Sea. *BGS UK Offshore Regional Rep, HMSO, London,*
Jensen, P., Aagaard, I., Burke, R.A., Dando, P.R., Jorgensen, N.O., Kuijpers, A., Laier, T., O' Hara, S.C.M. and Schmaljohann, R. 1992. 'Bubbling reefs' at the Kattegat: submarine landscapes of carbonate-cemented rocks support a diverse ecosystem at methane seeps. *Marine Ecology Progress Series,* 83pp.103-112.
Jones, G.B., Floodgate, G.D. and Bennell, J.D. 1986. Chemical and microbiological aspects of acoustically turbid sediments: preliminary investigations. *Marine Biotechnology,* 6pp.315-332.
Jorgensen, B.B. 2006. Bacteria and marine biogeochemistry *IN:* Schulz, H.D. and Zabel, M. (eds.) *Marine Geochemistry.* 2nd ed. Berlin Heidelberg Springer, pp.169-206.
Jorgensen, B.B. and Boetius, A. 2007. Feast or famine- microbial life in the seabed. *Nature,* 5pp.770-781.
Judd, A.G. 2005. *The distribution and extent of methane-derived authigenic carbonate. Technical report produced for Strategic Environmental Assessment SEA6.* UK: Department of Trade and Industry.
Judd, A.G., Croker, P. and Tizzard, L. 2007. Extensive methane-derived authigenic carbonates in the Irish Sea. *Geo-Marine Letters,* 27pp.259-267.
Judd, A.G. and Hovland, M. 2007. *Seabed fluid flow: the impact of geology, biology and the marine environment.* 2nd ed. Cambridge, UK: Cambridge University Press.
Kaluzny, M.A., Duncan, L.A., Merrit, M.V. and Epps, D.E. 1985. Rapid separation of lipid classes in high yield and purity using bonded phase columns. *Journal of Lipid Research,* 26pp.135-140.
Kenig, F., Simons, D.H., Crich, D., Cowen, J.P., ventura, G.T. and Rehbein-Khalily, T. 2005. Structure and distribution of of branched aliphatic alkanes with quaternary carbon atoms in Cenomanian and Turonian black shales of Pasquia Hills (Saskatchewan, Canada). *Organic Geochemistry,* 36pp.117-138.

King, L.H. and MacLean, B. 1970. Pockmarks on the Scotian Shelf. *Geological Society of America Bulletin*, 81pp.3141-3148.
Kolling, M. and Feseker, T. *Marine sediment onboard and in-lab analysis methods* [Online]. Available from: http://www.geochemie.uni-bremen.de/koelling/inlab.html [Accessed 06/10 2009].
Martens, C.S., Albert, D.B. and Alperin, M.J. 1998. Biogeochemical processes controlling methane in gassy sediments - Part 1: A model coupling organic matter flux to gas production, oxidation and transport. *Continental Shelf Research*, 18pp.1741-1770.
Monteys, X., Garcia, X., Szpak, M., Garcia-Gil, S. and Kelleher, B. 2008a. Multidisciplinary approach to the study and environmental implications of two large pockmarks on the Malin Shelf, Ireland. *IN: 9th International Conference on Gas in Marine Sediments*. Bremen Germany: ICSG 2008 Abstract Volume.
Monteys, X., Hardy, D., Doyle, E. and Garcia-Gil, S. 2008b. Distribution, morphology and acoustic characterisation of a gas pockmark field on the Malin Shelf, NW Ireland. *IN: Symposium OSP-01, 33rd International Geological Congress*. Oslo, Norway:
Nichols, P.D., Guckert, G.B. and White, D.C. 1986. Determination of monounsaturated double bond fatty acid position and geometry for mcirobial cultures and complex consortia by capillary GC-MS of the dimetyl disulphide adducts. *Journal of Microbiological Methods*, 5pp.49-55.
Pancost, R.D. and Boot, C.S. 2004. The paleoclimatic utility of terestrial biomarkers in marine sediments. *Marine Chemistry*, 92pp.239-261.
Pancost, R.D., Hopmans, E.C. and Sinninghe Damsté, J.S. 2001. Archaeal lipids in Mediterranean cold seeps: molecular proxies for anaerobic methane oxidation. *Geochimica Et Cosmochimica Acta*, 65(10), pp.1611-1627.
Peckmann, J., Reimer, A., Luth, U., Luth, C., Hansen, B.T., Heinicke, C. and Hoefs, J. 2001. Methane-derived carbonates and authigenic pyrite from the northwestern Black Sea. *Marine Geology*, 177pp.129-150.
Rees, I.S. and Brander, K. 1986. Patterns of acoustic scattering in the vincity of shelf-sea fronts. *Challenge Society Newsletter*, 22pp.13-14.
Schulz, H.D. 2006. Quantification of early diagenesis: Dissolved constituents in marine pore water *IN:* Schulz, H.D. and Zabel, M. (eds.) *Marine Geochemistry.* 2nd ed. Germany Springer, pp.124.
Sibuet, M. and Olu, K. 1998. Biogeography, biodiversity and fluid dependence of deep-sea cold-seep communities at active and passive margins. *Deep Sea Research Part II: Topical Studies in Oceanography*, 45pp.517-567.
Simpson, J.H. and Bowers, D. 1979. Shelf sea fronts' adjustments revealed by satellite IR imagery. *Nature*, 280pp.648-651.
Stadnitskaia, A., Ivanov, M.K. and Sinninghe Damsté, J.S. 2008. Application of lipid biomarkers to detect sources of organic matter in mud volcano deposits and post-eruptional methanotrophic processes in the Gulf of Cadiz, NE Atlantic. *Marine Geology*, 255(1-2), pp.1-14.
Stadnitskaia, A., Muyzer, G., Abbas, B., Coolen, M.J.L., Hopmans, E.C., Baas, M., van Weering, T.C.E., Ivanov, M.K., Poludetkina, E. and Sinninghe Damste, J.S. 2005. Biomarker and 16s rRNA evidence for anaerobic oxidation of methane and related carbonate precipitation in deep sea mud volcanoes of the Sorokin Trough, Black Sea. *Marine Geology*, 217pp.67-96.
Szpak, M., Monteys, X., O'Reilly, S., Simpson, A., Garcia, X., Evans, R., Allen, C., McNally, D., Courtier-Murias, D. and Kelleher, B. 2012. Geophysical and geochemical survey of a large pockmark on the Malin Shelf, Ireland. *Geochemistry, Geophysics, Geosystems*, In press
Valentine, D.L. and Reeburgh, W.S. 2000. New perspectives on anaerobic oxidation of methane. *Environmental Microbiology*, 2pp.477-484.
van der Meer, M.T.J., Schouten, S., Sinninghe Damste, J.S., de Leeuw, J.W. and Ward, D.M. 2003. Compound specific isotopic fractionation patterns suggest different carbon metabolisms among *Chloroflexus*-like bacteria in hot spring microbial mats. *Applied and Environmental Microbiology*, 69pp.6000-6006.
Volkman, J.K., Barrett, S.M., Blackburn, S.I., Mansour, M.P., Sikes, E.L. and Gelin, F. 1998. Microalgal Biomarkers: A review of recent research developments. *Organic Geochemistry*, 29pp.1163-1179.
Volkman, J.K. 2005. Sterols and other triterpenoids: source specificity and evolution of biosynthetic pathways. *Organic Geochemistry*, 36(2), pp.139-159.
Weissert, H. 2000. Deciphering methane's fingerprint. *Nature*, 406pp.356-357.
White, D.C. and Ringelberg, D.B. 1998. Signature lipid biomarker analysis *IN:* Burlage, R.S., Atlas, D., Stahl, D., Geesey, G. and Sayler, G. (eds.) *Techniques in microbial ecology.* 1st ed. New York Oxford University Press, pp.255-272.
Whiticar, M.J. 2002. Diagenetic relationships of methanogenesis, nutrients, acoustic turbidity, pockmarks and freshwater seepages in Eckenforde Bay. *Marine Geology*, 182pp.29-53.
Yuan, F. and Bennell, J.D. 1992. Acoustic and physical characteristics of gassy sediments in the Western Irish Sea. *Continental Shelf Research*, 12pp.1124-1134.
Zelles, L. 1999. Fatty acid patterns of phospholipids and liposaccharides in the characterisation of microbial communities in soil: A review. *Biology and Fertility of Soil*, 29pp.111-129.

Chapter 4. Microbial population diversity at a large pockmark on the Malin Shelf, N.W. Ireland

Shane S. O' Reilly[1], Paul V. Flanagan[2], Anna Kulakov[2],
Michal T. Szpak[1], Xavier Monteys[3], Paul, Kelly[2],
Leonid Kulakov[2], Chrostopher C.R. Allen[2], Brian P. Kelleher[1]

1. School of Chemical Sciences, Dublin City University, Dublin 9, Ireland
2. Queen's University Belfast, University Road, Belfast, N. Ireland BT7 1NN
3. Geological Survey of Ireland, Beggar's Bush, Haddington Rd., Dublin 4., Ireland

Abstract

This study reports novel findings relating to microbial community composition at a large pockmark on the Malin Shelf, off the N.W. coast of Ireland. We used denaturing gradient gel electrophoresis (DGGE) profiling and phylogenetic analysis of 16S rDNA bacterial clone libraries to elucidate the changes occurring in eubacterial populations at varying depths. Results show that the predominant bacterial populations belong to the phyla γ- and α-proteobacteria, in particular the genera *Psychrobacter* and *Sulfitobacter*, which have been reported widely previously in cold marine water column and sedimentary environments. Both of these major groups were observed to display distinct changes in population structure with depth due to geochemical zonation in the sediment and data also indicates evolutionary distinct populations. The ubiquity of these genera in cold marine environments indicates that the major bacterial groups are not associated with fluid seepage processes. Archaeal and bacterial populations were observed, which have been previously reported in active cold seep environments and sites with abundant hydrocarbons, and may imply a proportion of microbial community is supported by minor seepage. Interestingly no known cultured sulphate reducers were found but certain bacterial groups were relatively distantly matched with sulphate reducing δ-proteobacteria, and were found above the sulphate-methane transition zone and not below. This suggests a previously undescribed population is mediating sulphate reduction at the pockmark.

Abbreviations

ANME – anaerobic methanotrophs, AOM – Anaerobic oxidation of methane, DGGE – denaturing gradient gel electrophoresis, MDAC – methane-derived authigenic carbonate, OTU – operational taxonomic unit, SMTZ – sulphate-methane transition zone, SRB – sulphate-reducing bacteria

4.1 Introduction

Scientific and technological advances in mapping, observing and sampling of the seafloor over the past number of decades has brought to light the fact that the global seafloor is a highly dynamic geo- and biosphere (Jorgensen and Boetius 2007). Dramatic and diverse landscapes and geological features include cold seeps, deep-water coral reefs, mud volcanoes, mud diapirs, methane-derived authigenic carbonate (MDAC) mounds, hydrothermal, seamounts, ridges, trenches and pockmarks. Many of these features are formed as a result of seeping fluids, which can often exhibit exciting and unique ecosystems (Judd and Hovland 2007). Sites of active seepage are often colonized by thiotrophic bacterial mats and chemosynthetic benthic fauna (Jorgensen and Boetius 2007). Current estimates suggest that marine seabed and subsurface represents the major prokaryotic biomass pool (Whitman, Coleman and Wiebe 1998), but while research and interest has increased significantly in the past decade in deep ocean and shelf sediments (Vetriani, et al. 1999, Webster, Parkes and Fry 2004, Inagaki, et al. 2006) and also in coastal environments (Musselwhite, et al. 2003, Kopke, et al. 2005, Wilms, et al. 2006), it is also true that the identity and physiological properties of marine microorganisms remains distinctly uncertain as most have not yet been cultivated (Pace 1997, Fry, et al. 2008). At active seepage environments consortia of methanotrophic archaea (ANME) and sulphate-reducing bacteria (SRB) in the class δ-proteobacteria have recently been shown to mediate the process of anaerobic oxidation of methane (AOM) in these environments (Boetius, et al. 2000). However more recent studies have shown that alternative oxidants are utilized as electron acceptors during AOM, for example nitrate, nitrite (Ettwig, et al. 2008), iron and manganese (Beal, House and Orphan 2009).

In this study the microbial diversity of a low activity large composite pockmark off the N.W. coast of Ireland was investigated. Marine pockmarks are seafloor surface expressions of sub-seabed fluid expulsion, first described in the 1970's (King and MacLean 1970). Pockmark formation has never been observed and most mapped pockmarks are relict or dormant features. Thus there remains active debate as to how these features evolve, form, persist and become extinct. The leading formation mechanism is that they are formed by rapid upward expulsion of overpressurised hydrocarbon gas, hydrothermal gas or groundwater springs from below relatively impermeable fine-grained sedimentary seabed layers (Judd and

Hovland 2007). From a microbiological perspective there have been relatively few studies investigating the microbial diversity of pockmarks and very little is known about the possible role they play in the formation and evolution of pockmarks. Active pockmarks in the North Sea have been shown to be characterized by gas flares to the water column, carbonate crusts and giant sulphur-oxidising bacterial mats (Dando, et al. 1991, Wegener, et al. 2008). Microbial diversity from samples at these sites associated with regions of gas ebullition was dominated with ANME-2 archaea and SRB of the δ-proteobacteria (Wegener, et al. 2008). Another prime example of an active pockmark system is the giant REGAB pockmark on the Gabon continental margin, which is characterized by massive carbonate crusts and seep associated fauna such as Vesicomyidae and Mytilidae bivales families, and Siboglinidae (Vestimentifera) tube worms (Ondreas, et al. 2005, Olu-Le Roy, et al. 2007).

Acoustic and electromagnetic investigation of the Malin pockmark highlighted the presence of a shallow subsurface gas pocket below the pockmark and gas signatures in and around the feature, but with a lack of migration pathways and active seepage to the surface within the feature (Szpak, et al. 2012). Video investigations of the region did not record any MDAC crusts or mounds, bacterial mats, increased megafaunal abundance or gas ebullition but there is some acoustic and pore water evidence to suggest minor gas migration to the surface. (Szpak, et al. 2012). We wished to text the hypothesis that: (i) specific changes in chemical parameters will lead to changes in eubacterial community composition (ii) that analysis of diversity would suggest, which might be the conclusion that see little environmental change over a protracted time period.

4.2 Materials and Methods

4.2.1 Environmental and geological setting

The Malin Deep pockmark field is situated on the Irish continental shelf, 70km N.W. of Ireland (Figure 26.). This region is structurally complex, bordered by the Stanton Banks fault to the north and the Malin Terrace to the south. The Skerryvore fault, a major normal fault, divides the region into the Donegal Basin and the West Malin Basin (Dobson and Whittington 1992). Quaternary sediment thickness ranges from 125-175m in a general south to north direction (Evans, Whittington and Dobson 1986). While the Malin Deep seafloor is characterized by a complex seabed geology

with a variety of sediment facies, which include recent sand bedforms, gravel lags and coarser clasts, the seafloor in the vicinity of the pockmark is smooth and soft, ranging from fine-grained sand to silt (Monteys et al. 2008b). A detailed description of the setting and pockmark field has been previously reported (Szpak, et al. 2012, Monteys et al. 2008b, Monteys et al. 2008a).

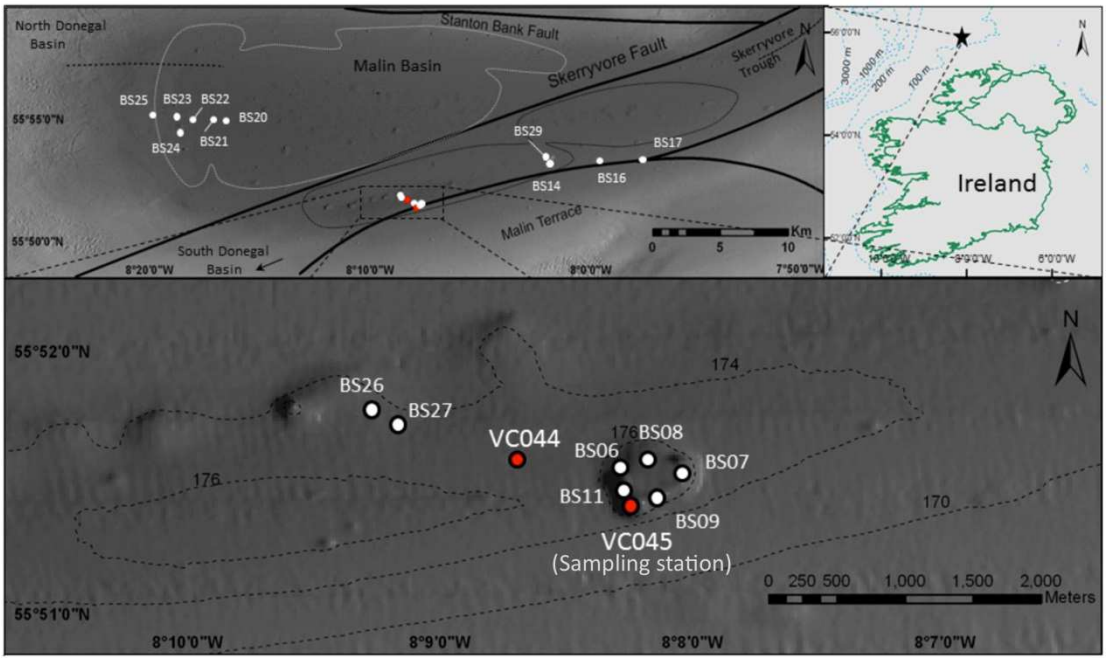

Figure 26: Multibeam shaded relief bathymetry with major structural features: Skerryvore Fault and Stanton Bank Fault and index map with site location (top panel). Linear pockmark clusters are visible in the Malin Deep micro basin south of Skerryvore Fault are marked a with black dotted line and several minor unit pockmarks in the Malin Deep area marked with a dotted light grey line. Detailed sampling site are shown and the site in the study, VC045, taken from within the pockmark cluster is shown. Figure adapted from Szpak et al. (2012)

4.2.2 Sampling

A 6m vibrocore, VC045, was sampled at a water depth of 180m in 2008 from inside a large pockmark (55.85680^{o}N Lat., -8.13720^{o}E Long.) during the CE_08 expedition aboard the RV *Celtic Explorer* using a Geo-Resources 6000 vibrocorer. The core was cut into 1m sections, wax-sealed to preserve anoxia and refrigerated for the duration of the cruise prior to sub-sampling and freezing at -80^{0}C back in the lab. Sub-samples were taken under sterile conditions and from freshly exposed sediment to minimize contamination risk from sampling equipment and alteration of sediment characteristics.

4.2.3 DNA extraction and purification

DNA was extracted from three depths from core VC045, at 0.2mbsf, 2.1mbsf and 5.9mbsf according to a modified method from Zhou et al (1996). Briefly 5g wet sediment was vortexed briefly with 13.5 mL of DNA extraction buffer (100mM Tris-HCl [pH 8.0], 100mM Na-EDTA [pH 8.0], 100mM Na_2HSO_4 [pH 8.0], 1.5M NaCl and 1% hexadecylmethylammonium bromide [CTAB]) and sterile glass beads. 100µL 10mg/mL proteinase K was added and the mixture was incubated on a reciprocating shaker at 37^0C for 30 min at 225rpm. 1.5mL 20% sodium dodecyl sulphate (SDS) was then added and the samples were incubated at 65^0C for 4 hours at 100rpm. Supernatant was transferred to fresh 50mL sterile tubes after centrifugation at 6000g for 10 min at room temperature. The sediment residues were then extracted twice more with 4.5mL extraction buffer and 500µL 20% SDS at 65^0C for 10min as before. Combined supernatants were extracted for approx 5 min with equal volumes of 24:1 (vol/vol) chloroform/isoamyl alcohol. The upper aqueous phase was recovered after centrifugation at 6000g for 10min. Crude DNA was precipitated overnight at -20^0C with 0.6 volume isopropanol. The DNA pellet was collected by centrifugation at 15,000rpm for 20min and dissolved in minimal volume 1X TE buffer. Crude DNA concentration and purity was estimated spectrophotometrically. The crude total DNA was further purified on a 1% low-melting point agarose gel electrophoresis and DNA bands were purified from the agarose gel using the Illustra GFX^{TM} PCR and gel band purification kit (GE Healthcare).

4.2.4 PCR amplification of 16S rRNA genes

16S bacterial and archaeal rDNA polymerase chain reactions were carried out using DNA Engine DYAD^{TM} Peltier Thermal Cycler. 16S bacterial rRNA sequences were amplified from purified genomic DNA using universal 63f (5'-CAGGCCTAACACATGCAAGTC-3') forward primer and 1387r (5'-GGGCGGWGTGTACAAGGC-3') reverse primer (Marchesi, et al. 1998). PCR was performed as follows: denaturation step of 95^0C for 5min; followed by 33 cycles of 94^0C for 30s, 55^0C for 30s and finally 72^0C for 1min 30s. 16S archaeal rRNA gene sequences were amplified from the purified genomic DNA by PCR using S-D-Arch-0025-a-S-17 (5'-CTGGTTGATCCTGCCAG-3') forward primer and S-*-Univ-0907-a-A-20 (5'-CCGTCAATTCMTTTRAGTTT-3') reverse primer (Vetriani, et al. 1999).

PCR was performed as follows: denaturation step of 94^0C for 3min; followed by 40 cycles of 94^0C for 30s, 48^0C for 30 s, and 72^0C for 30s; and finally an elongation step of 72^0C for 5min.

4.2.5 Denaturing gradient gel electrophoresis (DGGE)

The 16S bacterial rRNA amplified PCR products from each three depths were used as templates for nested PCR to re-amplify the variable V3 region for DGGE analysis using DGGE primer 2 (5'-ATTACCGCGGCTGCTGG-3') and DGGE primer 3 (5'-CGCCCGCCGCGCGCGGCGGGCGGGGCGGGGGCACGGGGGGCCTACGGGAGGCAGCAG-3'). (Muyzer, de Waal and Uitterlinden 1993). The 16s archaeal PCR products were amplified as above but replacing DGGE primer 3 with 344f(GC) (5'-CGCCCGCCGCGCCCCGCGCCCGTCCCGCCGCCCCCGCCACGGGGCGCAGCAGGCGCGA-3'). DGGE was performed using the CBS Scientific^{TM} DGGE 2401 system as described previously (Muyzer, de Waal and Uitterlinden 1993, Myers, et al. 1985). PCR samples were added directly to 8% w/v polyacrylamide gels (40% v/v stock acrylamide, 0.5x TAE (40mM Tris acetate [pH 7.4], 20mM sodium acetate, and 1mM EDTA) with denaturing gradients from 20-100% (100% denaturant consisted of 7M urea and 40% v/v formamide). Electrophoresis was performed at constant voltage and temperature of 90V and 60^0C repectively, for 16 hrs. The gels were then stained using 1X SYBRGold^{TM} nucleic acid stain (Invitrogen) for 45mins and imaged by transillumination (BIO RAD^{TM} VERSA DOC 1000).

4.2.6 DGGE Band sequencing and statistical image analysis

DGGE band sequencing was performed as described previously (Muyzer, de Waal and Uitterlinden 1993). Prominent bands on the DGGE gels were excised and DNA was eluted by placing the gel fragment in 30μL TE buffer overnight at 4^0C. 1μL of eluted DNA was used as PCR templates using non-GC clamp DGGE primer 1 (5'-CCTACGGGAGGCAGCAG-3') instead of DGGE primer 3 and P2 primers, and previously mentioned PCR conditions. Amplified products were sequencing in the forward direction by DNA Sequencing & Services (University of Dundee, Scotland). 16S rRNA sequences were subjected to NCBI BLAST search to identify sequences with highest similarity. DGGE profiles were subjected to statistical image analysis using Phoretix 1D v10.3 (TotalLab) software package. Cluster analysis was performed using UPGMA and Ochiai coefficient based similarities.

4.2.7 16S rRNA bacterial clone library construction and restriction clustering of operational taxonomic units (OTUs)

16S bacterial rRNA amplified sequences from 2.1mbsf and 5.9mbsf were chosen for clone library preparation based on DGGE results. Cloning was performed sing the CloneJET^{TM} PCR cloning kit (Fermentas) according to manufacturer's guidelines. 16S rRNA clone inserts were reamplified from colony PCR reactions using 63f and 1387r primers and operational taxonomic units (OTUs) were grouped by restriction analysis. Fastdigest^{TM} RSaI and HaeIII (Fermentas) restriction enzymes were used with Fastdigest^{TM} 10X Green Buffer and was carried out using a PCR block at 37^0C for 45 mins. Restriction profiles were analysed on 1.4% agarose gel and each gel was standardized to allow comparison between gels. Clones showing identical restriction profiles were assigned to the same OTU group. Initially at least 30% of clones from each group were sequenced in full using pJET1.2 forward and reverse sequencing primers. Sequencing was performed as per 1.2.6 above.

4.2.8 Phylogenetic analysis

Sequencing results were checked using FinchTV and nucleotide sequence similarities were analysed by NCBI GenBank BLAST search (MEGA BLAST algorithm). Sequences found to be 98% or greater in similarity were considered the same and grouped as a phylotype. Sequence anomalies were checked using Pintail (v1.0) (Ashelford, et al. 1994). Sequence alignment was performed by ClustalW algorithm (Thompson, Higgins and Gibson 1994) using the MEGA5 software package (Tamura, et al. 2011). Neighbour-joining phylogenetic trees were constructed using the maximum composite likelihood model also using the MEGA5 software package. 16S rRNA bacterial reference sequences were included and obtained from GenBank. Trees were checked using other models and were similar. Trees were subjected to bootstrap analysis (n = 1000) to assess confidence levels and bootstrap values of 50 or higher are reported here. The nucleotide sequence data reported in this study were deposited in the GenBank nucleotide sequence database under the accession numbers JQ349446 to JQ349503.

4.3 Results

DGGE profiles for bacterial and archaeal 16S rRNA sequences for 0.2, 2.1 and 5,9 mbsf from the pockmark are shown in Figure 27. Bacterial community structure appeared to be complex and distinct variations between community composition is evident at the different depths. Overall however, DGGE profiles indicate that the major bacterial community composition was similar from the surface to the bottom 6mbsf. In contrast to the bacterial community, the archaeal community was less diverse, with the presence of fewer than ten distinct bands in each DGGE lane. However there was also a distinct variation in archaeal community composition at the different depths investigated (data not shown). Digitized bacterial DGGE images were subjected to cluster analysis to statistically compare similarity between samples. Results are given in Figure 28. and compared to control marine sediment samples - GC04, GC04, GC09 and GC10 (taken from 1mbsf sediment from Dunmanus Bay, Ireland). This analysis indicates that the Malin site has a distinct bacterial population compared to the control site. Figure 28. also indicates that between the three investigated depths in the core, the bacterial community at 2.1mbsf and 5.9mbsf are statistically the most similar to each other compared to the top sample at 0.2mbsf.

Table 3. shows results for sequencing of some successfully excised and amplified bands and BLAST searches for nucleotide sequences of highest similarity. The type of environment and publication reference for closest phylotypes is also given. Table 3. indicates that there is a clear dominance of the phylum proteobacteria at this site, in particular the γ-proteobacteria and α-proteobateria. Specifically BLAST searches suggest species belonging to the genus *Psychrobacter, Sulfitobacter, Alcanivorax, Halomonas* and *Thiomicrospira* are the dominant bacterial members of this community. DGGE sequencing results for excised bands from the archaeal 16S rRNA DGGE profiles indicate an the archaeal community is phylogenetically similar to archaeal 16S rRNA sequences from clones from turbidites in the Gulf of Mexico, from deep sea sediments in the Sea of Ohkotsk, from cold-water coral mounds in the Porcupine Seabight off the Irish coast (Hoshino, et al. 2011), and also at marine active methane seepage environments at the Pacific Ocean margin and Eel River Basin. Cluster analysis of digitized archaeal 16S rRNA profiles indicates the archaeal community changes significantly over the 6m core (data not shown).

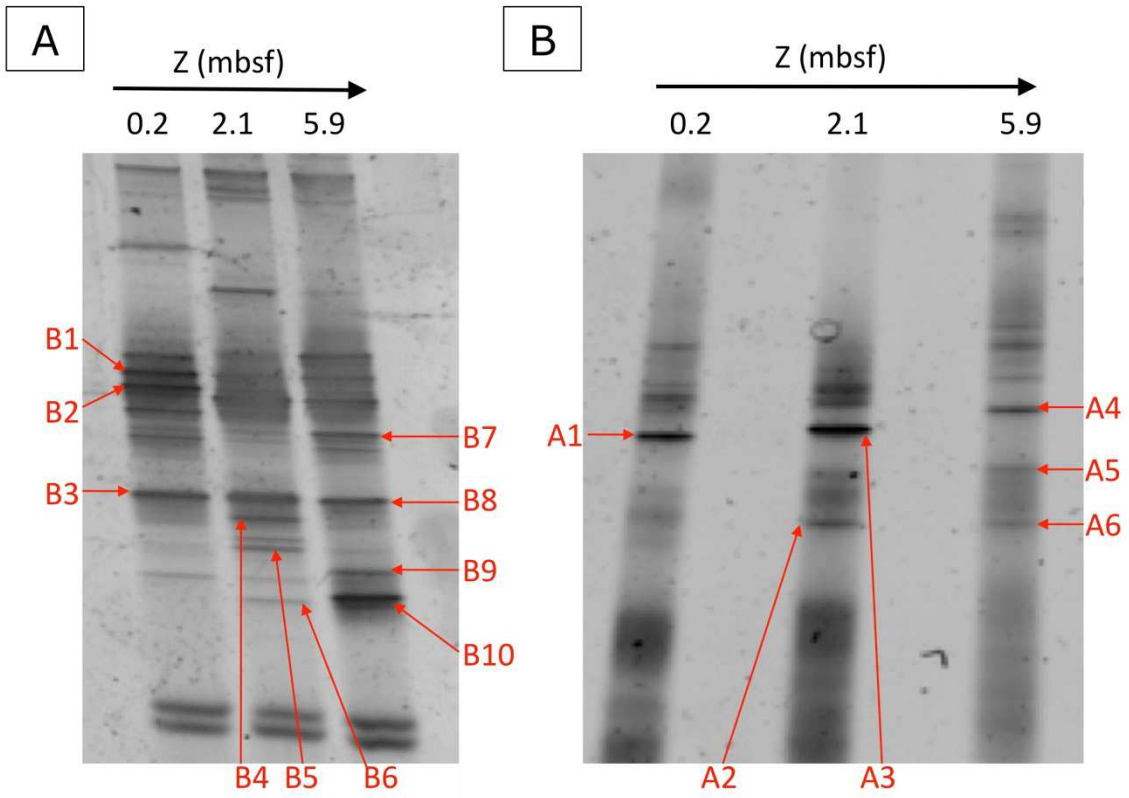

Figure 27: DGGE vertical profiles of bacterial (A) and archaeal (B) community composition of the pockmark at 0.2, 2.1 and 5.9mbsf

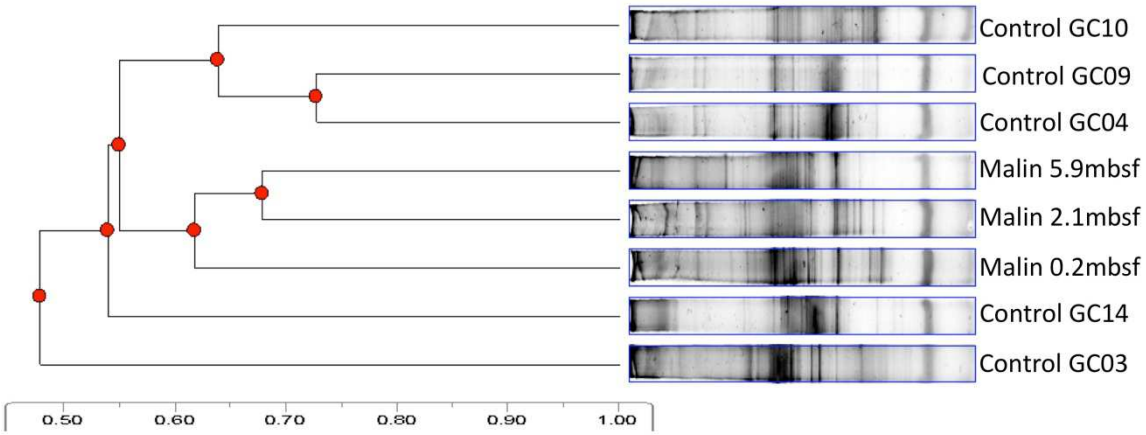

Figure 28: Cluster analysis of 16S rRNA bacterial DGGE profiles. Analysis was performed by UPGMA clustering and and Ochiai coefficient-based similarities. The distance scale indicates Euclidean distance.

Table 3: Bacterial and archaeal DGGE band sequencing and BLAST similarities.

DGGE band	Depth (mbsf)	Organism (Accession No.)	% match[1]	Environment	Reference
B1	0.2	*Alcanivorax* sp. ANT-2400 S4 (GQ153640.1)	96	Deep sea sediments, Meditterranean Sea	Tapilatu et al. (2009)
B2	0.2	*Psychrobacter* sp. KOPRI 25504 (GU062550.1)	98	Arctic marine sediments	Kim et al. (2010)
B3	0.2	*Sulfitobacter* sp. COL-20 (HQ534315.1)	100	Antarctic seawater	Giudice et al. (2011)
B4	2.1	*Psychrobacter* sp. KOPRI 25504 (GU062550.1)	98	Arctic marine sediments	Kim et al. (2010)
B5	2.1	*Psychrobacter* sp. C11 (DQ831958.1)	96	Antarctic seawater	Giudice et al. (2007)
B6	2.1	*Psychrobacter* sp. KOPRI 25504 (GU062550.1)	100	Arctic marine sediments	Kim et al. (2010)
B7	5.9	*Halomonas* sp. DPB4_(MB)_50.2mbsf (DQ344858.1)	100	Deep sea sediments	Biddle et al. (2005)
B8	5.9	*Sulfitobacter* sp. COL-20 (HQ534315.1)	95	Antarctic seawater	Giudice et al. (2011)
B9	5.9	*Pseudoalteromonas* sp. TB27 (JF273878.1)	99	Antarctic sponge	Papaleo et al. (2011)
B10	5.9	*Thiomicrospira* sp. Milos-T2 (AJ237758.1)	95	Shallow hydrothermal vent, Aegean Sea	Brinkhoff et al (1999)
A1	0.2	Uncultured ANME-1 euryarchaeote clone slm_arc_110 (HQ700669.1)	99	Sediment turbidites, Gulf of Mexico	Nunoura et al. (2009)
A2	2.1	Uncultured archaeon clone OHKA2.13 (AB094530)	99	Deep sea sediments, Sea of Ohkotsk	Inagaki et al. (2003)
A3	2.1	Uncultured archaeon clone FeSO4_A_116 (GQ356853.1)	99	Methane seepage sediment, Eel River Basin	Beal et al. (2009)
A4	5.9	Uncultured euryarchaeote clone: ODP1251AQ1.19 (AB364330.1)	93	Deep Sea methane hydrate-bearing sediments	Nunoura et al. (2008)
A5	5.9	Uncultured archaeon clone 3H3M_ARC63 (JN229818.1)	98	Cold water coral mounds, Porcupine Seabight	Hoshino et al. (2011)
A6	5.9	Uncultured archaeon clone: OHKA2.13 (AB094530.1)	99	Deep sea sediments, Sea of Ohkotsk	Inagaki et al. (2003)

Note 1: % match based on NCBI MegaBLAST search algorithm.

Bacterial 16S rRNA clone libraries were prepared and operational taxonomic units were grouped together based on RFLP clustering. An overview of the composition of the 2.1mbsf and 5.9mbsf bacterial communities is given in Figure 29., with pore water SO_4^{2-} and Cl^- profiles (adapted from Szpak et al., 2012). Similar to the results from DGGE, resulting cloning libraries indicate that the proteobacteria is the major phylum in both libraries, representing 93.4 and 98.1% of the bacterial population at 2.1 and 5.9mbsf respectively. The proteobacteria present at this site are from γ, α and β classes, whereby respectively they represent the 73.8, 18.0 and 1.6% of the population at 2.1mbsf and 54.7, 37.7 and 5.7% of the population at 5.9mbsf. Clones related to unclassified actinobacteria are also present, representing 4.9 and 1.9% of the respective clone libraries. Clones phylogenetically related to the phylum acidobacteria are also present at 2.1mbsf, representing 1.6% of the clone library.

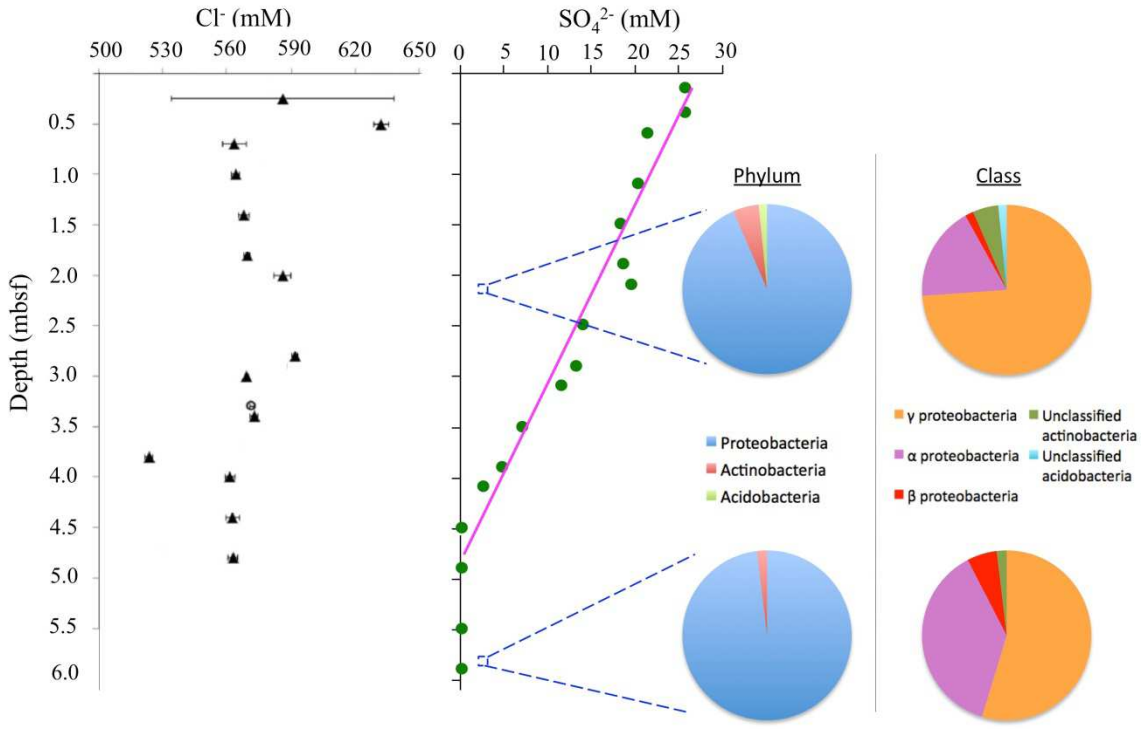

Figure 29: Percentage composition of bacterial clone libraries from 2.1mbsf and 5.9mbsf in terms of phylum and class. Pore water sulphate and chloride profiles are also shown. Porewater data adapted from Szpak et al. (2012).

A complete OTU table for the clone libraries is given in Table 4. and shows accession numbers for representatives from each OTU group, the closest phylotype percentage match in the NCBI database (MegaBLAST algorithm), the percentage composition of

the total library and the environment of the closest phylotype. A neighbour-joining bacterial 16S rRNA phylogenetic tree showing positions of clones from this study is given in Figure 5. As can be seen in Table 4. and Figure 30. the major OTU groups are phylogenetically closely related to the *Psychrobacter* and *Sulfitobacter* species. At 2.1mbsf clones closely related to the *Psychrobacter* represent 59.0% of the clone library and those related to the *Sulfitobacter* represent 18.0% of the library. The percentages for each of the aforementioned OTU's at 5.9mbsf are both about 37.7% Other major phylotypes found at 2.1mbsf are those closely related to *Alcanivorax Borkumensis* SK2 (6.7% of total) (Yakimov, et al. 1998), related to uncultured actinobacteria, previously reported at low-activity cold seeps in the Weddell Sea, Antarctica, (4.9% of total) (Niemann, et al. 2009) and *Pseudoalteromonas arctica* (3.3%). Less significant groups, representing less than 2% of the library each, are those closely related to uncultured bacteria reported in cold-water corals at the Porcupine Seabight (Hoshino, et al. 2011), uncultured bacteria reported at hydrocarbon seeps off the Coast of Santa Barbara (Redmond, Valentine and Sessions 2010), *Pseudomonas tetradonis*, an uncultured *Pseudomonas* reported associated with marine sponge off the Irish coast (Kennedy, et al. 2009) and denitrifying bacteria somewhat related (96% BLAST similarity) to those commonly found in the activated sludge process (Heylen, et al. 2006).

The bacterial clone library at 5.9mbsf is similar in composition to the 2.1mbsf but there are distinct differences in the relative proportions. The two major OTU groups related to the *Psychrobacter* and *Sulfitobacter* represent about 37.7% of the total library in both cases. The next most abundant group at this depth is represented by uncultured *Pseudomonas* reported associated with marine sponge off the Irish coast (9.4%), followed by groups closely related to *Pseudoalteromonas arctica* and somewhat related (95% BLAST similarity) to an uncultured β-proteobacterium previously reported in contaminated soil (Martin, et al. 2012) (both about 3.8% of the total library). Similar to the 2.1mbsf clone library clones closely matching uncultured actinobacteria found at low-activity cold seeps in the Weddell Sea, Antarctica, and to uncultured bacteria reported at hydrocarbon seeps off the Coast of Santa Barbara are also present at 5.9mbsf but in lower proportions in the case of the former group (1.9% vs. 4.9%). In contrast to the 2.1mbsf clone library minor clone groups closely related to *Colwellia aestuarii* and *Variovorax paradoxus* are present in the 5.9mbsf clone library (both about 2% of total).

Table 4: Operational taxonomic unit (OTU) table of 16S rRNA bacterial clone 2.1 and 5.9mbsf libraries from the pockmark.

OTU	Accession Number	Closest Phylotype (Accession No.)	% Match	% Total library	Environment	Reference
		2.1mbsf clone library				
1	JQ349463	*Psychrobacter nivimaris* strain 88/2-7 (NR_028948.1)	≥97	59.0	Particulate organic matter, Antarctica	Heuchert et al. (2004)
2	JQ349486	*Sulfitobacter pontiacus* ChLG-10 (NR_026418.1)	≥97	18.0	Marine sediments, Black Sea	Sorokin et al. (1995)
3	JQ349489	*Alcanivorax borkumensis* SK2 (NR_029340.1)	98	6.7	Seawater/sediment North Sea	Yakimov et al. (1998)
4	JQ349490	Uncultured actinobacterium clone ANTXXIII_706-4_Bac69 (FN429805.1)[2]	98	4.9	Cold seep, Weddell Sea, Antarctica	Niemann et al. (2009)
5	JQ349494	*Pseudoalteromonas arctica* strain C53q-3a (JN681829.1)	98	3.3	Seawater, Danish Coast	Bernbom et al. (2011)
6	JQ349491	Uncultured bacterium clone 3H3M_69 (JN230300.1)[3]	98	1.6	Marine sediments, Porcupine Seabight	Hoshino et al. (2011)
7	JQ349492	Uncultured bacterium clone Propane SIP20-4-09 (GU584779.1)	98	1.6	Marine hydrocarbon seeps, offshore Santa Barbara	Redmond et al. (2010)
8	JQ349493	*Thauera* sp. R-28312 (AM084110.1)	96	1.6	Activated sludge	Heylen et al. (2006)
9	JQ349496	Pseudoalteromonas tetraodonis strain IAM 14160 (NR_041787.1)	99	1.6	Coastal seawater, Antartica	Ivanova et al (2001)
10	JQ349497	Pseudomonas sp. PM1 16S (EU768833.1)	99	1.6	Marine sponge, Irish coastal waters	Kennedy et al. (2009)
		5.9mbsf clone library				
1	JQ349448	*Psychrobacter marincola* strain KMM 277 (NR_025458.1)[1]	≥97	37.7	Marine sediments, W. Pacific Ocean	Romanenko et al. (2002)
2	JQ349479	*Sulfitobacter litoralis* strain Iso 3 (NR_043547.1)	≥92	37.7	Seawater, East Korea	Park et al. (2007)
3	JQ349498	Pseudomonas sp. PM1 16S (EU768833.1)	99	9.4	Marine sponge, Irish coastal waters	Kennedy et al. (2009)
4	JQ349503	Uncultured bacterium 16S rRNA gene clone D3DH031 (FQ660126.1)	95	3.8	Contaminated soil	Martin et al (2012)
5	JQ349497	*Pseudoalteromonas arctica* strain C53q-3a (JN681829.1)	98	3.8	Seawater, Danish Coast	Bernbom et al. (2011)
6	JQ349500	Uncultured bacterium clone Propane SIP20-4-09 (GU584779.1)	99	1.9	Marine hydrocarbon seeps, offshore Santa Barbara	Redmond et al. (2010)
7	JQ349499	Uncultured actinobacterium clone ANTXXIII_706-4_Bac69 (FN429805.1)[2]	98	1.9	Cold seep, Weddell Sea, Antarctica	Niemann et al. (2009)
8	JQ349501	*Variovorax paradoxus* EPS (CP002417.1)	99	1.9	Ubiquitous	Lucas et al. (2010)
9	JQ349502	*Colwellia aestuarii* strain SMK-10 (NR_043509.1)	98	1.9	Tidal flat sediment, Korea	Jung et al. (2006)

Note 1: OTU group dominated by clones most closely affiliated to *Psychrobacter marincola* but clones with closest phylogeny to *Psychrobacter celer* strain SW-238 (NR_043225.1), *Psychrobacter pacifisensis* strain NIBH P2K6 (NR_027187.1) are also present.

Note 2: Closest cultured relatives are distantly related (~82% match) to sulphate reducing δ-proteobacteria *S. palmitis*, *S. svalbardensis*

Note 3: Closest cultured relatives are distantly related (82-84% match) to the sulphate reducing δ-proteobacteria *Dessulfobacca acetoxidans*, *Desulfobacterium anilini* and *Desulfacinum subterraneum*

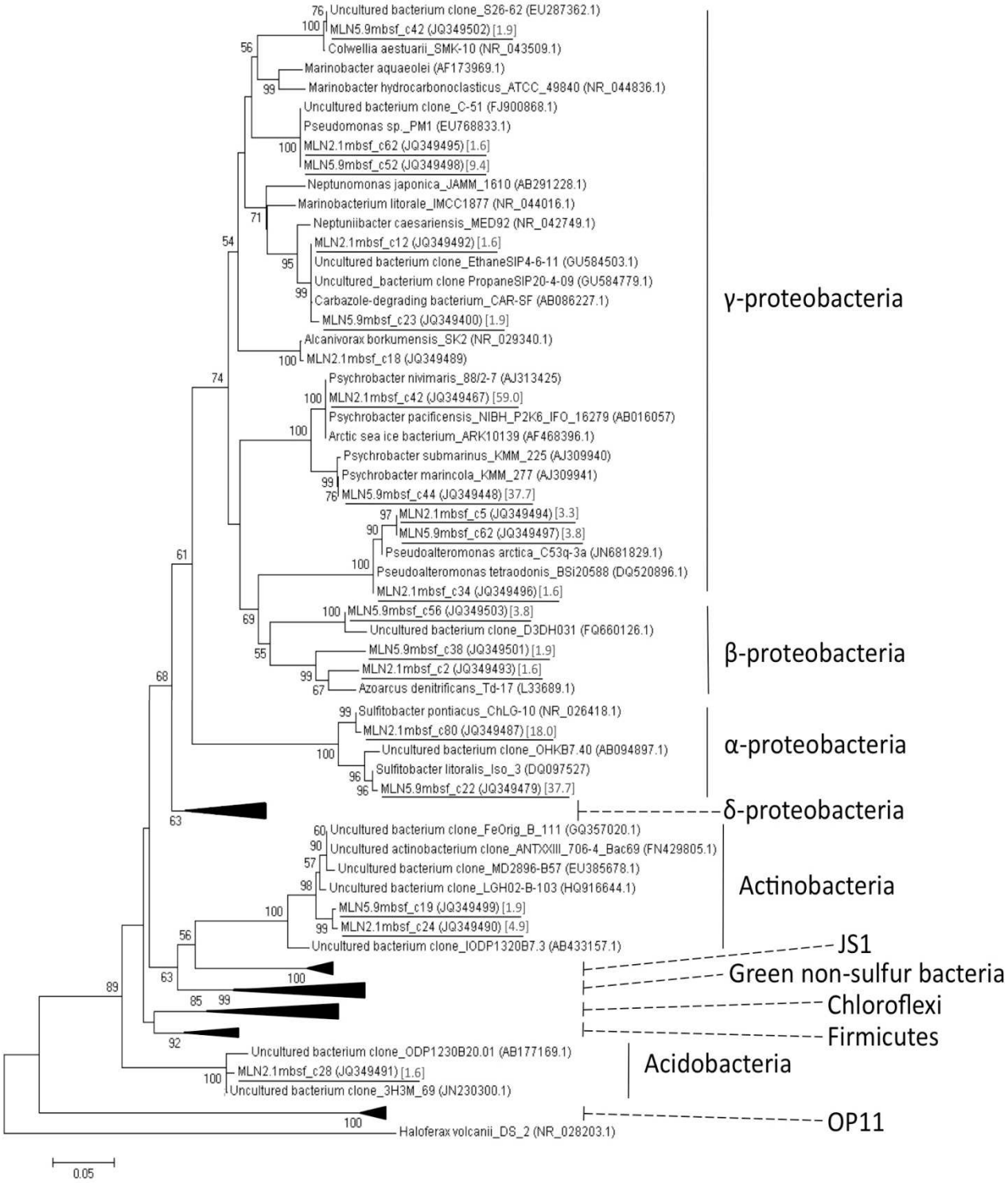

Figure 30: Neighbour-joining phylogenetic tree of bacterial 16S rRNA 2.1mbsf and 5.9 mbsf clone libraries from the pockmark. Nucleotide sequences from this study are underlined. Accession numbers are in brackets, while values for percentage of total library for each clone is given in square brackets. The tree was subjected to bootstrap analysis (n = 1000) to assess confidence intervals and bootstrap values >50 are reported.

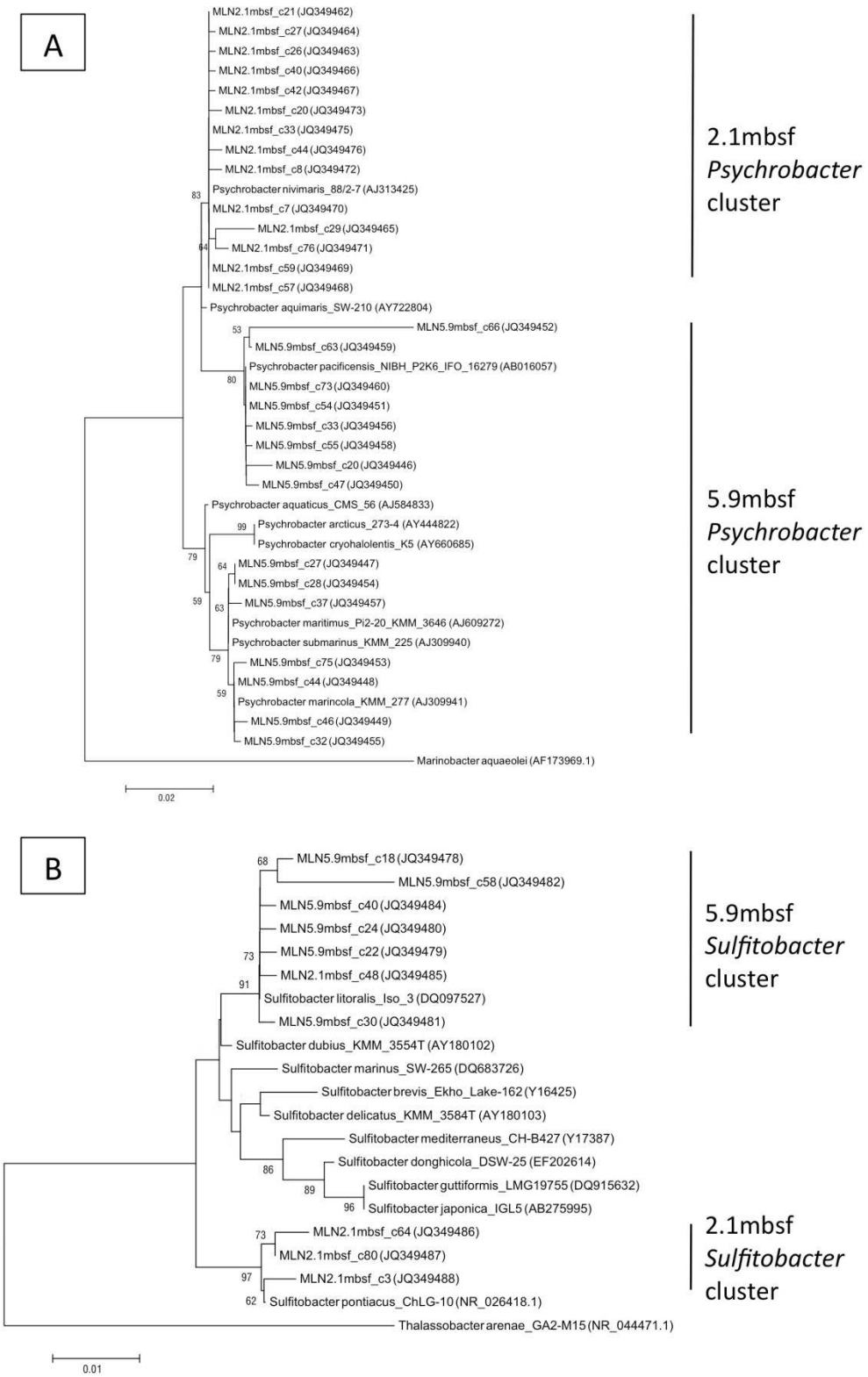

Figure 31: Neighbour-joining phylogenetic tree for selected clones from the *Psychrobacter* (A) and *Sulfitobacter* (B) OTU's from the 2.2mbsf and 5.9mbsf clone libraries. Nucleotide sequences from this study are underlined. Accession numbers are in brackets. The tree was subjected to bootstrap analysis (n = 1000) to assess confidence intervals bootstrap values >50 are reported.

Figure 31. shows constructed neighbour-joining phylogenetic trees from a selection of clones from the *Psychrobacter* (Figure 31.A) and *Sulfitobacter* (Figure 31.B) major OTU groups from the 2.1mbsf and 5.9mbsf clone libraries. Figure 31. shows distinct clustering of both bacterial populations based on depth. As shown here and given in Table 4. are representative clones from OTU group 1 at 2.1mbsf (n = 14) are phylogenetically most closely related to *Psyhrobacter nivimaris*, while at 5.9mbsf (n = 14) are most related to *Psychrobacter marincola*. In addition clones from OTU group 2 at 2.1mbsf (n = 3) are phylogenetically most closely related to *Sulfitobacter pontiacus*, while at 5.9mbsf (n = 6) are most related to *Sulfitobacter litoralis*. Thus it is evident there are distinct and shifting major populations with depth in the core.

4.4 Discussion

4.4.1 *Psychrobacter* and *Sulfitobacter* sp., the dominant bacterial populations in the Malin Shelf pockmark.

Several studies have shown that the dominant bacterial members of the seafloor belong to previously undescribed lineages (Inagaki, et al. 2006, Fry, et al. 2008, Teske and Sorensen 2008), thus limiting inferences about their physiology and metabolisms. However in this study the dominant members of clone libraries from this site were closely related (generally greater than 99% BLAST match) to *Psychrobacter* and *Sulfitobacter* sp., of which many species have been cultivated and described in the laboratory. *Psychrobacter* are a genus of non-motile gram-negative rods or coccibacilli, currently in the *Moraxellaceae* family (Juni and Heym 1986). These bacteria differ from the related genera *Moraxella* and *Acinetobacter* in that they are psychrotolerant or psychrophillic and halotolerant (Bowman, Cavanagh and Austin 1996). A number of distinct species have been isolated from a wide variety of cold marine environments, such as marine sediments, Antarctic ornithogenic soils (Bowman, Cavanagh and Austin 1996), sea ice (Bowman, et al. 1997), coastal seawater (Yumoto, et al. 2003), deep sea trench environments (Maruyama, et al. 2000), and these environments are an apparent ecological niche for these bacteria. *Sulfitobacter* are a genus of bacteria belonging to the class α-proteobacteria, and members of this genus were first isolated from the Black Sea (Sorokin 1995), but have since been shown to be ubiquitous in the marine environment (Park, et al. 2007). They are gram-negative obligate heterotrophs, which are motile and generate

metabolic energy through sulfite oxidation. Thus they are found to be particularly abundant in environments with abundant inorganic sulphur, such as marine sediments (Sorokin 1995).

To the authors knowledge these genera have not been reported in temperate marine environments such as off the Irish coast, have not been reported at seabed seepage features, and have not been reported at these depths in the sediment column previously. Thus this study extends the already diverse range of habitats in which they exist and raises questions as to their metabolic capabilities in the environment. It is clear that there are geographic controls on the distribution of marine seabed microbes, for example archaea belonging to the Deep Sea Archaeal Group (DSAG) and bacteria in the JS1 group are predominantly observed in the methane-hydrate bearing sediments along the Pacific margins (Inagaki, et al. 2006, Nunoura, et al. 2008), while at ODP site 1227, the South Africa Gold Mine Euryarchaeotic Group (SAGMEG) dominate archaeal communities and members of the *Chloroflexi* were the dominant bacteria (Webster, et al. 2006), but the consequence and importance of the widespread geographical range of both the *Psychrobacter* and *Sulfitobacter* genera is unknown. In a previous study comparing bacterial populations present in Antarctic seawater and seawater contaminated with hydrocarbons, it was shown that both *Psychrobacter* and *Sulfitobacter* were among the major genera present (Prabagaran, et al. 2007). Specifically they reported that *Sulfitobacter* were present in greater abundance uncontaminated seawater while *Psychrobacter* were only present in hydrocarbon-containing seawater. However it must also be noted that the clones in the study by Prabagaran et al. (2007) were not the same species in this study.

Results in this study have also shown that there is a shift in population abundance between these two genera with depth and also that there are two distinct populations of both between the two clone libraries (Table 4. and Figure 31.). The major OTU group in the 2.1mbsf clone library was phylognetically most related (generally 99% BLAST similarity or higher) to *P. nivimaris*. This bacterium was first isolated from organic particles in seawater and was found to have optimal growth temperature of between 10-15^{o}C and maximum NaCl growth concentrations of 0-9% (w/v). The major OTU group in the 5.9mbsf clone library was more diverse and contained clones phylognetically most related to *P. marincola, P. submarinus* and *P. celer*. Laboratory investigation of cultures of *P. marincola* and *P. submarinus* have shown that these species require salt concentration of between 0.5 – 15.5 % (w/v), do

not engage in nitrate reduction and do not produce H_2S, while *P. celer* is also not capable of nitrate reduction but in contrast to *P. marincola* and *P. submarinus* is capable of anaerobic growth and does not require salt for growth (grows at 0-16% NaCl and with optimal growth at 2-3% NaCl). As mentioned above all of these species are non-motile. At 2.1mbsf clones closely related to *Sulfitobacter pontiacus* was the dominant bacteria in the sulphate-forming population of the Black Sea (Sorokin 1995). On the other hand at 5.9mbsf clones from this OTU group most closely matched *Sulfitobacter litoralis.* These bacteria were first isolated and described from seawater in the East Sea, Korea (Park, et al. 2007). *Sulfitobacter pontiacus* DSM 10014^T was found to perform nitrate reduction while in contrast *Sulfitobacter litoralis* has been shown not to perform nitrate reduction to nitrite (Park, et al. 2007).

It is unclear whether the inverse shift in abundance between these OTU's is related to depth, geochemical zonation or some other process. Generally microbial biomass correlates with metabolic activities, which are estimated by supply of electron donors and acceptors (Parkes, Cragg and Wellsbury 2000, Inagaki, et al. 2003, Nunoura, et al. 2009), and therefore geochemical zonation in sediments is a consequence and controlling factor for microbial communities in sedimentary environments. For example the abundance of populations of SRB in marine sediments is linked with the reduction and depletion of sulphate (Schulz 2006). In addition there can be clear lithological control on microbial community composition, for example in the Sea of Okhotsk, the DSAG archaeal and bacterial J1 communities dominated pelagic clay layers, while in adjacent volcanic ash layers the Miscellaneous Crenarchaeotic Group (MCG) and γ-proteobacteria were dominant (Inagaki, et al. 2003). It is hypothesized here that the population shift in abundance is as a result of geochemical zonation, since lithologically the 6m core was homogenous consisting of Holocene sandy mud throughout. The increased proportion of *Sulfitobacter* sp. may be related to a greater abundance of reduced sulphur species at 5.9mbsf, due to complete conversion of sulphate to sulphide from about 3.8mbsf. However most studied *Sulfitobacter* species are specialized in the oxidation of sulphite and not sulphide (Park, et al. 2007). In addition as mentioned *S. pontiacus*, in constrast to *S. litoralis*, is capable of nitrate reduction, which suggests that the utilization and depletion of nitrate as an electron acceptor in this environment may in some part be mediated by *S. pontiacus*. We also hypothesize that the decrease in *Psychrobacter*

abundance with depth could be related to decreasing availability of organic matter with depth. *P. nivimaris* was originally isolated associated with organic matter particles in seawater and it is possible that this species requires a threshold organic matter concentrations. As mentioned above *P. celer* was able to grow under anaerobic conditions and may account for its presence at 5.9mbsf and not 2.1mbsf.

β-proteobacteria are typically present in very low frequency in polar/temperate environments and our study indicates this also. Clones relatively distantly related to *Thauera* sp. (96% similarity) were present at 2.1mbsf (OTU group 8). *Thauera* and *Azoarcus* genera are denitrifiers, which have been extensively reported to engage in degradation of aromatic compounds (Heylen, et al. 2006, Zhou, et al. 1995). This group was not present in 5.9mbsf, which suggests that this group is engaged in the denitrification process in the upper 2mbsf of sediment. Clones matching *Variovorax paradoxus* were also present in less than 2% at 5.9mbsf and previous studies have reported *Variovorax* strains in anaerobic sediments with abundant reduced sulphur (Scholten 2000, Wang 2006). One species of this genus, *V. ginsengisoli* has been shown to be a facultative anaerobe (Im, et al. 2010). Scholten et al. (2000) hypothesized that the strain ANRB-Zg may have a role to play in the oxidation of reduced sulphur to sulphate, although their possible role in sulphur cycling remains unknown. Results here do complement previous findings that *Variovorax* sp. may have a role in the sulphur cycle in marine sedimentary environments.

The genus *Pseudoalteromonas* plays an important role in marine environments due to their ability to survive in nutrient-poor settings by adjustment of their biochemical pathways and production of a wide variety of metabolites (Ivanova, et al. 2003). OTU group from both depths was closely matched to *Pseudoalteromonas arctica*. This bacteria was first isolated from Arctic sea ice and seawater, and they are aerobic gram-negative polar-flagellated rod-shaped bacteria, which exhibit growth at temperatures of 4-25^{o}C and 0-9% NaCl (w/v) (Al Khudary, et al. 2008). They are also strictly aerobic and thus their occurrence in sediments to a muddy to depth of 6mbsf is somewhat puzzling. However as mentioned this genus displays considerable metabolic variety and may be surviving or dormant at these depths with minimal oxygen. It is noteworthy that *Colwellia* and *Pseudoalteromonas* have also been reported in environments where *Psychrobacter* dominate (Bowman, et al. 1997). *Colwellia aestuarii* was first isolated from tidal flat sediment in Korea and is a gram-

negative motile bacterium that is capable of nitrate reduction, growth at temperatures down to 4^{o}C and under anaerobic conditions.

4.4.2 Evidence of microbial assemblages sustained by low activity or previous seepage

Active pockmarks are often characterized by massive carbonate crusts, giant sulphur-oxidising bacterial mats, seep associated fauna such as Vesicomyidae and Mytilidae bivales families, and Siboglinidae (Vestimentifera) tube worms (Dando, et al. 1991, Wegener, et al. 2008, Ondreas, et al. 2005, Olu-Le Roy, et al. 2007) and/or microbial consortia of ANME archaea and SRB of the δ-proteobacteria, which mediate AOM (Boetius, et al. 2000). However in contrast to other seepage environments the evolution and temporal variability in pockmark activity is still an area of active debate, made more complicated by the difficulty in observing and studying these seemingly transiently active features means there is still much unknown. For example pockmarks that were previously found to be sites of active seepage in the Skagerrak (Dando, et al. 1994) were subsequently found to be inactive (Wegener, et al. 2008) and demonstrates the periodic and temporal variability of pockmark activity.

Previous seismic investigations of the Malin pockmark have found a relatively large gas pocket at approximately 20m below the pockmark, and subtle vertical fluid flow and lateral gas accumulation signatures in subsurface sedimentary layers indicate that an active fluid system is present at these depths. However based on intensive video and seismic profiling this study concluded that at the time of sampling there was no direct evidence of seepage to the sediment/water interface and into the water column and that the pockmark was likely dormant (Szpak, et al. 2012). They investigated microbial activity in this pockmark using ^{1}H NMR, heteronuclear multiple quantum coherence (HMQC) NMR, and diffusion-edited (DE) NMR and results suggested microbial activity was greater outside the pockmark, whereby inside the pockmark microbial activity was reduced at depth. Towed electrical conductivity profiles across the pockmark also supported the conclusion that microbial activity and living biomass was greater in the vicinity of the pockmark compared to inside the pockmark. Thus they suggest that microbial cells are primarily non-living or dormant inside the pockmark.

The present study focused on the microbial diversity within the pockmark, but from the above discussion it is apparent that the genomic DNA extracted from

samples may not representative of active biomass, particularly in relation to the bacterial population. However this study presents evidence that at least the minor component of bacteria, and indeed the archaea based on DGGE findings, within this feature is or has previously been supported by seeping fluid. An OTU closely related to *Alcanivorax borkumensis* SK2 was found to be a significant component of the bacterial population at 2.1mbsf (approx. 7%). *A. borkumensis* SK2 is a gram negative aerobic non-motile heterotroph that displays optimal growth at 20-30^{o}C and 3-10% NaCl (w/v), is capable of nitrate reduction and displays a strict nutritional profile, whereby aliphatic hydrocarbons are used as sole of principle carbon source for growth (Yakimov, et al. 1998). This bacterium is often the dominant bacteria, up to 80 - 90% of the total population, in oil spills (Schneiker, et al. 2006), and its presence in a significant proportion suggests the presence of aliphatic hydrocarbons, which may be present above background levels as a result of seepage. This hypothesis is supported by OTU group 7 and group 6, from 2.1mbsf and 5.9mbsf respectively, whereby these groups are closely matched with novel uncultured propane-degrading bacteria associated with active hydrocarbon seeps off the coast of Santa Barbara (Redmond, Valentine and Sessions 2010) and also by the presence of OTU groups 4 (2.1mbsf) and 7 (5.9mbsf), which are closely matched to uncultured bacteria previously only reported in low activity cold seeps in Weddell Sea, Antarctica (Niemann, et al. 2009).

Microbial electron acceptors are usually depleted in order of maximum energy yield, with oxygen becoming depleted first, followed by nitrate, oxidized manganese, iron minerals and sulphate, whereby in the marine sedimentary setting sulphate is quantitatively the most important electron acceptor (Schulz 2006) Previously reported sulphate porewater profiles indicate that sulphate is depleted at about 3.8mbsf (Szpak, et al. 2012). In active seepage environments the sulphate-methane transition zone (SMTZ) is shifted closer to the surface and in many cases sulphate is completely depleted within centimeters of the surface where there is sufficient methane supply from depth to fuel AOM. This is not the case in this environment where surface anoxia and steep sulphate profiles were not observed (Szpak, et al. 2012). On the other hand Szpak et al. (2012) compared sulphate profiles with a control core and with diffusion flux rates of sulphate suggested that there was increased consumption of sulphate and possible higher rates of AOM, although differences were minor. SRB of the δ-proteobacteria such as *Desulfobulbus, Desulfosarcina* and *Desulfococcus* genera were not found in this study, which raises questions as to the process and

means of sulphate reduction from the surface to 3.8mbsf. It may be the case that the process is being carried out by another as yet unidentified process involving bacteria from a separate class, or it may be the case that quantitatively the SRB are of low abundance in the pockmark and clones were not selected for sequencing. Indeed a recent study reported that in deep Atlantic waters and in diffusive flow hydrothermal vent environments a relatively small number of bacterial species dominate but that thousands of low-abundance populations account for the major phylogenetic diversity (Sogin, et al. 2006). It is however worth noting also that the closest matching (82-84% similarity) cultured bacteria for OTU group 6 from 2.1mbsf include SRB such as *Dessulfobacca acetoxidans*, *Desulfobacterium anilini* and *Desulfacinum subterraneum*. Thus this group appears to be distantly related to these bacteria and may engage in sulphate reduction. Interestly this OTU group is not present at 5.9mbsf, below the SMTZ. Additionally the closest cultured bacteria to clones within OTU group 4 at 2.1mbsf and group 7 at 5.9mbsf include *Desulforomonas svalbardensis* and *palmitatis* (both 82% matches). This group composes almost 5% of the 2.1mbsf clone library and less than 2% of the 5.9mbsf clone library. Thus there is some evidence to support the inference that a distinct and as yet uncultured group is mediating sulphate reduction in this site.

Overall results from this study indicate that the Malin pockmark is not a site of enhanced methane seepage and a distinct and greater biological diversity such as has been reported previously (Wegener, et al. 2008, Ondreas, et al. 2005, Olu-Le Roy, et al. 2007). However results here and provided by Szpak et al. (2012) do show shallow gas accumulations, low or periodic seepage activity and that there is are distinct bacterial and archaeal populations, which have been previously associated with active methane and hydrocarbon seepage environments. However previous results suggesting microbial activity is reduced within the feature could also mean that the major portion of DNA extracted is detrital and indicative of previously active biomass. Indeed detrital DNA is considered to account for the major proportion (up to 90%) of total DNA in marine sediments (Dell'Anno, Bompadre and Danovaro 2002).

4.4.3 Evidence of genetic population divergence

In stark contrast to microbial growth and division in laboratory conditions, low growth rates, or intermittent periods of rapid growth interspersed by long periods of non-growth and starvation is the norm for microbes in nature, for which doubling

times can be as long as millennia (Price and Sowers 2004). It has been demonstrated that in methane-rich ocean-margin and sulphate-rich open-ocean marine sediments down to several hundreds metres depth, specific metabolic rates were three orders of magnitude lower at sulphate-rich sites than methane-rich sites, and that sub-seafloor microbial metabolic activity is greatly concentrated in relatively narrow ocean margin zones and most microbes in subseafloor sediments are adapted for extraordinary low metabolic activity (D'Hondt and Rutherford 2002). This is in stark contrast to metabolic activity and the rate of genetic divergence achieved in the lab (Korona 1996).

A previous study analysed 16S rRNA gene clustering of clones from the marine planktonic SAR11 cluster and phylogenetic clustering of populations was observed based on depth distribution and niche specialization, and resulted primarily from macroevolutionary divergence (Field, et al. 1997). Figure 31. displays clear clustering of both the *Psychrobacter* and *Sulfitobacter* OTU's, both the major OTU groups in clone libraries in this study, and indicates macroevolutionary divergence. While the primary factor or factors controlling this divergence are numerous and likely complex in nature, and include for example sediment depth, sulphate reduction, and availability of organic matter, we hypothesize that these populations have undergone niche specialization in the sedimentary column and become genetically divergent over geological timescales. While exact dating is not available within this core, the 6m core spans the Holocene era and the period between the surface and 6mbsf is likely 8000-10,000 years.

4.5 Conclusion

Both bacterial DGGE and clone library results show that the predominant bacterial populations belong to the phyla γ- and α-proteobacteria, in particular the genera *Psychrobacter* and *Sulfitobacter*, which have been extensively reported previously in polar marine water column and sedimentary environments. This study further extends the habitat range of these bacteria. Both of these major groups were observed to display distinct clustering based on depth and indicate a divergence of populations, likely due to niche specialization and sedimentary geochemical zonation. The findings that there were distinctly different populations of *Psychrobacter* and *Sulfitobacter* sp. above and below the SMTZ suggests these groups play a previously unreported role

in sedimentary geochemical cycling and may be demonstrating divergence of the populations over geological timescales based on diagenetic zonation.

DGGE and clone results indicate minor but significant populations of uncultured bacteria and archaea previously reported in active cold seep environments, which suggest that a proportion of the microbial community may currently be supported by minor seepage or have been periodic seepage in the past. Previous results, which indicated reduced microbial activity with the pockmark support the latter conclusion, and indicate that much of the DNA is representative of relict or dormant bacteria. Bacterial OTU groups found either only above the SMTZ or in greater abundance were distantly related to sulphate reducers, which suggest a previously undescribed population is mediating sulphate reduction at the pockmark.

Overall findings here agree with previous reports that currently the Malin pockmark is not characterized by enhanced fluid seepage to the surface and is not supporting distinct biological diversity as reported in previous active cold seep environments. However questions regarding the temporal activity of the pockmark and subsequent effect on microbial activity and community dynamics are a topic requiring further inquiry.

Acknowledgements

We wish to thank the Geological Survey of Ireland, the INtegrated Mapping FOr the Sustainable Development of Ireland's MArine Resource (INFOMAR) programme, the Irish Environmental Protection Agency, Science Foundation of Ireland, QUESTOR (Queens University Belfast) and the Irish Council for Science, engineering & technology (IRCSET) for funding this research. We would also like to thank NSERC, (Strategic and Discovery Programs), the Canada Foundation for Innovation (CFI), and the Ministry of Research and Innovation (MRI) for providing Canadian funding, and Prof. Øyvind Hammer.

References

Al Khudary, R., Stober, N.I., Ooura, F. and Antranikian, G. 2008. *Pseudoalteromona arctica* sp. nov., an aerobic, psychrotolerant, marine bacterium isolated from Spitzbergen. *International Journal of Systematic and Evolutionary Microbiology*, 58pp.2018-2024.

Ashelford, K.E., Chuzanova, N.A., Fry, J.C., Jones, A.J. and Weightman, A.J. 1994. At least 1 in 20 16S rRNA sequence records currently held in public repositories is estimated to contain substantial anomalies. *Applied and Environmental Microbiology*, 71pp.7724-7736.

Beal, E.J., House, C.H. and Orphan, V.J. 2009. Manganese- and iron-dependent marine methane oxidation. *Science*, 325pp.184-187.

Boetius, A., Ravenschlag, K., Schubert, C.J., Rickert, D., Widdel, F., Gieseke, A., Amann, R., Jorgensen, B.B., Witte, U. and Pfannkuche, O. 2000. A marine microbial consortium mediating anaerobic oxidation of methane. *Nature*, 407pp.623-626.
Bowman, J.P., Cavanagh, J. and Austin, J.J. 1996. Novel *Psychrobacter* species from Antarctic ornithogenic soils. *International Journal of Systemative Bacteriology*, 46pp.841-848.
Bowman, J.P., McCammon, S., Brown, M.V., Nichols, D.S. and McKeekin, T. 1997. Diversity and association of psychrophilic bacteria in antarctic sea ice. *Applied and Environmental Microbiology*, 63pp.3068-3078.
Dando, P.R., Austen, M.C., Burke Jr, R.A., Kendall, M.A., Kennicutt II, M.C., Judd, A.G., Moore, D.C., O' Hara, S.C.M., Schmaljohann, R. and Southward, A.J. 1991. Ecology of a North Sea pockmark with an active methane seep. *Marine Ecology Progress Series*, 70pp.49-63.
Dando, P.R., Bussmann, I., Niven, S.J., O' Hara, S.C.M. and Schmaljohann, R. 1994. A methane seep area in the Skaggerak, the habitat of the pognophore *Siboglinum poseidoni* and bivalve mollusc *Thyasira sarsi*. *Marine Ecology Progress Series*, 107pp.157-167.
Dell'Anno, A., Bompadre, S. and Danovaro, R. 2002. Quantification, base composition and fate of extracellular DNA in marine sediments. *Limnology and Oceanography*, 47pp.899-905.
D'Hondt, S. and Rutherford, S. 2002. Metabolic activity of subsurface life in deep sea sediments. *Science*, 295pp.2067-2070.
Dobson, M.M. and Whittington, R.J. 1992. Aspects of the geology of the Malin Sea area *IN:* Parnell, J. (ed.) *Basins on the Atlantic Seaboard: Petroleum Geology, Sedimentology and Basin Evolution.* 1st ed. London Geological Society Special Publications, pp.291-311.
Ettwig, K.F., Shima, S., van de Pas-Schoonen, K.T., Kahnt, J., Medema, M.H., op den Camp, H.J.M. and Jetten, M.S.M. 2008. Denitrifying bacteria anaerobically oxidise methane in the absence of archaea. *Environmental Microbiology*, 10pp.3164-3173.
Evans, D., Whittington, R.J. and Dobson, M.R. 1986. *Tiree. Sheet 56^{o}N 08^{o}W*. 1:250,000 series. Solid GeologyBritish Geological Survey
Field, K.G., Gordon, D., Wright, T., Rappe, M., Urback, E., Vergin, K. and Giovannoni, S.J. 1997. Diversity and depth-specific distribution of SAR11 cluster rRNA genes from marine planktonic bacteria. *Applied and Environmental Microbiology*, 63pp.63-70.
Fry, J.C., Parkes, J.R., Cragg, B.A., Weightman, A.J. and Webster, G. 2008. Prokaryotic biodiversity and activity in the deep subseafloor biosphere. *FEMS Microbiology Ecology*, 66pp.181-196.
Heylen, K., Vanparys, B., Wittebolle, L., Verstraete, W. and Boon, N. 2006. Cultivation of denitrifying bacteria: optimization of isolation conditions and diversity study. *Applied and Environmental Microbiology*, 72pp.2637-2643.
Hoshino, T., Morono, Y., Terada, T., Imachi, H., Ferdelman, T.G. and Inagaki, F. 2011. Comparative study of subseafloor community structures in deeply buried coral fossils and sediment matrices from the Challenger Mound in the Porcupine Seabight. *Frontiers in Microbiology*, 2pp.1-7.
Im, W.T., Liu, Q.M., Lee, K.J., Kim, S.Y., Lee, S.T. and Yi, T.H. 2010. *Variovorax ginsengisoli* sp. nov., a denitrifying bacteria isolated from soil in a ginseng field. *International Journal of Systematic and Evolutionary Microbiology*, 60pp.1565-1569.
Inagaki, F., Nunoura, T., Nakagawa, S., Teske, A., Lever, M.A., Lauer, A., Suzuki, M., Takai, K., Delwiche, M., Colwell, F.S., Nealson, K.H., Horikoshi, K., D'Hondt, S. and Jorgensen, B.B. 2006. Biogeographical distributions and diversity of microbes in methane hydrate-bearing deep marine sediments on the Pacific Ocean Margin. *Proceedings of the National Academy of Sciences of the USA*, 103pp.2815-2820.
Inagaki, F., Suzuki, M., Takai, K., Oida, H., Sakamoto, T., Aoki, K., Nealson, K.H. and Horikoshi, K. 2003. Microbial communities associated with geological horizons in coastal subseafloor sediments from the Sea of Okhotsk. *Applied and Environmental Microbiology*, 69pp.7224-7235.
Ivanova, E.P., Bakunina, I.Y., Nedashkovskaya, O.I., Gorshkova, N.M., Alexeeva, Y.V., Zelepuga, E.A., Zvaygintseva, T.N., Nicolau, D.V. and Mikhailov, V.V. 2003. Ecophysiological variabilities in ectohydrolytic enzyme activities of some *Pseudoalteromonas* species, *P. citrea, P. issachenkonii*, and *P. nigrifaciens*. *Current Microbiology*, 46pp.6-10.
Jorgensen, B.B. and Boetius, A. 2007. Feast or famine- microbial life in the seabed. *Nature*, 5pp.770-781.
Judd, A.G. and Hovland, M. 2007. *Seabed fluid flow: the impact of geology, biology and the marine environment.* 2nd ed. Cambridge, UK: Cambridge University Press.
Juni, E. and Heym, G.A. 1986. *Psychrobacter immobilis* gen. nov., sp. nov.: genospecies composed of gram-negative, aerobic, oxidase positive coccobacilli. *International Journal of Systematic Bacteriology*, 36pp.388-391.
Kennedy, J., Baker, B., Piper, C., Cotter, P.D., Walsh, M., Mooij, M.J., Bourke, M.B., Rea, M.C., O'Connor, P.M., Ross, R.P., Hill, C., O'Gara, F., Marchesi, J.R. and Dobson, A.J.W. 2009. Isolation and analysis of bacteria with antimicrobial activities from the marine sponge *Halicola simulans* collected from Irish waters. *Marine Biotechnology*, 11pp.384-396.
King, L.H. and MacLean, B. 1970. Pockmarks on the Scotian Shelf. *Geological Society of America Bulletin*, 81pp.3141-3148.
Kopke, B., Wilms, R., Engelen, B. and Cypionka, H. 2005. Microbial diversity in coastal subsurface sediments: a cultivation approach using various electron acceptors and substrates gradients. *Applied and Environmental Microbiology*, 71pp.7819-7830.
Korona, G. 1996. Genetic divergence and fitness convergence under unoform selection in experimental populations of bacteria. *Genetics*, 143pp.637-644.

Marchesi, J.R., Sato, T., Weightman, A.J., Martin, T.A., Fry, J.C., Hiom, S.J. and Wade, W.G. 1998. Design and evaluation of useful bacterium-specific pcr primers that amplify genes coding for 16S rRNA. *Applied and Environmental Microbiology,* 64pp.795-799.
Martin, F., Torelli, S., Le Paslier, D., Barbance, A., Martin-Laurent, F., Bru, D., Geremia, R., Blake, G. and Joueannou, Y. 2012. Betaproteobacteria dominance and diversity shifts in the bacterial community of PAH-contaminated soil exposed to phenanthrene. *Environmental Pollution,* 162pp.345-353.
Maruyama, A., Honda, D., Yamamoto, H., Kitamura, K. and Higashihara, T. 2000. Phylogenetic analysis of psychrophilic bacteria isolated from the Japan Trench, including a description of the deep-sea species Psychrobacter pacificensis sp. nov. *International Journal of Systematic and Evolutionary Microbiology,* 50(2), pp.835-846.
Monteys, X., Garcia, X., Szpak, M., Garcia-Gil, S. and Kelleher, B. 2008a. Multidisciplinary approach to the study and environmental implications of two large pockmarks on the Malin Shelf, Ireland. *IN: 9th International Conference on Gas in Marine Sediments.* Bremen Germany: ICSG 2008 Abstract Volume.
Monteys, X., Hardy, D., Doyle, E. and Garcia-Gil, S. 2008b. Distribution, morphology and acoustic characterisation of a gas pockmark field on the Malin Shelf, NW Ireland. *IN: Symposium OSP-01, 33rd International Geological Congress.* Oslo, Norway:
Musselwhite, C.L., McInerney, M.J., Dong, H., Onstott, T.C., Green-Blum, M., Swift, D., Macnaughton, S., White, D.C., Murray, C. and Chien, Y.J. 2003. The factors controlling microbial distribution and activity in the shallow subsurface. *Geomicrobiology Journal,* 20pp.245-261.
Muyzer, G., de Waal, E.C. and Uitterlinden, A.G. 1993. Profiling of complex microbial populations by denaturing gradient gel electrophoresis analysis of polymerase chain reaction amplified genes coding for 16S rRNA. *Applied and Environmental Microbiology,* 59pp.695-700.
Myers, R.M., Fischer, S.G., Lerman, L.S. and Maniatis, T. 1985. Nearly all single base substitutions in DNA fragments joined to a GC-clamp can be detected by denaturing gradient gel electrophoresis. *Nucleic Acids Res.,* 13pp.3131-3145.
Niemann, H., Fischer, D., Graffe, D., Knittel, K., Montial, A., Heilmeyer, O., Nothen, K., Pape, T., Kasten, S., Bohrmann, G. and Boetius, A. 2009. Biogeochemistry of a low-activity cold seep in the Larsen B area, western Weddell Sea, Antarctica. *Biogeosciences,* 6pp.2383-2395.
Nunoura, T., Inagaki, F., Delwiche, M.E., Colwell, F.S. and Takai, K. 2008. Subseafloor microbial communities in methane hydrate-bearing sediment at two distinct locations (ODP Leg 204) in the Cascadia Margin. *Microbes and Environment,* 23pp.317-325.
Nunoura, T., Soffiento, B., Blazejak, A., Kakuta, J., Oida, H., Schippers, A. and Takai, K. 2009. Subseafloor microbial communities associated with rapid turbidite deposition in the Gulf of Mexico continental slope. *FEMS Microbiology Ecology,* 69pp.410-424.
Olu-Le Roy, K., Caprais, J.-., Fifis, A., Fabri, M.-., Galeron, J., Budzinsky, H., Le Menach, K., Khripounoff, A. and Ondreas, H. 2007. Cold seep assemblages on a giant pockmark off West Africa: spatial patterns and environmental control. *Marine Ecology,* 28pp.115-130.
Ondreas, H., Olu, K., Fouquet, Y., Charlou, J.L., Gay, A., Dennielou, B., Donval, J.P., Fifis, A., Nadalig, T., Cochonat, P., Cauquil, E., Bourillet, J.F., Le Moigne, M. and Sibuet, M. 2005. ROV study of a giant pockmark on the Gabon continental margin. *Geo-Marine Letters,* 25pp.281-292.
Pace, N.R. 1997. A molecular view of microbial diversity and the biosphere. *Science,* 276pp.734-740.
Park, J.R., Bae, J.W., Nam, Y.D., Chang, H.W., Kwon, H.Y. and Quan, Z.X. 2007. *Sulfitobacter litoralis* sp. nov., a marine bacterium isolated from East Sea, Korea. *International Journal of Systematic and Evolutionary Microbiology,* 57pp.692-695.
Parkes, R.J., Cragg, B.A. and Wellsbury, P. 2000. Recent studies on bacterial populations and processes in subseafloor sediments: A review. *Hydrogeology Journal,* 8pp.11-28.
Prabagaran, S.R., Manorama, R., Delille, D. and Shivaji, S. 2007. Predominance of *Roseobacter*, *Sulfitobacter*, *Glaciecola* and *Psychrobacter* in seawater collected off Ushuaia, Argentina, Sub-Antarctica. *FEMS Microbiology Ecology,* 59pp.342-355.
Price, P.B. and Sowers, T. 2004. Temperature dependence of metabolic rates for microbial growth, maintenance and survival. *Proceedings of the National Academy of Sciences of the USA,* 101pp.4631-4636.
Redmond, M.C., Valentine, D.L. and Sessions, A.L. 2010. Identification of novel methane-, ethane, and propane-oxidising bacteria at marine hydrocarbon seeps by stable isotope probing. *Applied and Environmental Microbiology,* 76pp.6412-6422.
Schneiker, S., Martins dos Santos, V.A., Bartels, D., Bekel, T., Brecht, M., Buhrmester, J., Chernikova, T.N., Denaro, R., Ferrer, M., Gertler, C., Goesmann, A., Golyshina, O.V., Kaminski, F., Khachane, A.N., Lang, S., Linke, B., McHardy, A.C., Meyer, F., Nechitaylo, T., Pühler, A., Regenhardt, D., Rupp, O., Sabirova, J.S., Selbitschka, W., Yakimov, M.M., Timmis, K.N., Vorhölter, F.J., Weidner, S., Kaiser, O. and Golyshin, P.N. 2006. Genome sequence of the ubiquitous hydrocarbon-degrading marine bacterium *Alcanivorax borkumensis*. *Nature Biotechnology,* 24pp.997-1004.
Scholten, J.C.M. 2000. Isolation and characterisation of acetate-utilising anaerobes from a freshwater sediment. *Microbial Ecology,* 40pp.292-299.
Schulz, H.D. 2006. Quantification of early diagenesis: Dissolved constituents in marine pore water *IN:* Schulz, H.D. and Zabel, M. (eds.) *Marine Geochemistry.* 2nd ed. Germany Springer, pp.124.
Sogin, M.L., Morrison, H.G., Huber, J.A., Welch, D.M., Huse, S.M., Neal, P.R., Arrieta, J.M. and Herndl, G.J. 2006. Microbial diversity in the deep sea and the underexplored 'rare biosphere'. *Proceeding of the National Academy of Sciences of the USA,* 103pp.12115-12120.

Sorokin, D.Y. 1995. *Sulfitobacter pontiacus* gen. nov., sp. nov. - a new heterotrophic bacterium specialized on sulfite oxidation. *1995*, 64pp.295-305.
Szpak, M., Monteys, X., O'Reilly, S., Simpson, A., Garcia, X., Evans, R., Allen, C., McNally, D., Courtier-Murias, D. and Kelleher, B. 2012. Geophysical and geochemical survey of a large pockmark on the Malin Shelf, Ireland. *Geochemistry, Geophysics, Geosystems*, In press
Tamura, K., Peterson, D., Peterson, N., Stecher, G., Nei, M. and Kumar, S. 2011. MEGA5: Molecular Evolutionary Genetics Analysis using Maximum Likelihood, Evolutionary Distance, and Maximum Parsimony Methods. *Molecular Biology and Evolution*, 28pp.2731-2739.
Teske, A. and Sorensen, K.B. 2008. Uncultured archaea in deep marine subsurface sediments: have we caugth them all? *Internation Society for Microbial Ecology*, 2pp.3-18.
Thompson, J.D., Higgins, G. and Gibson, T.J. 1994. CLUSTAL W: improving the sensitivity of progressive multiple sequence alignment through sequence weighting, position-specific gap penalties and weight matrix choice. *Nucleic Acid Research*, 22pp.4673-4680.
Vetriani, C., Jannasch, H.W., MacGregor, B.J., Stahl, D.A. and Reysenbach, A.L. 1999. Population structure and phylogenetic characterisation of marine benthic archaea in deep-sea sediments. *Applied and Environmental Microbiology*, 65pp.4375-4384.
Wang, Y.P. 2006. Degradability of dimethyl terephthalate by *Variovorax paradoxus* T4 and *Sphingomonas yanoikuyae* DOS01 isolated from deep ocean sediments. *Ecotoxicology*, 15pp.549-557.
Webster, G., Parkes, R.J., Cragg, B.A., Newbury, C.J. and Weightman, A.J. 2006. Prokaryotic community composition and and biogeochemical processes in deep subseafloor sediments from the Peru margin. *FEMS Microbiology Ecology*, 58pp.65-85.
Webster, G., Parkes, R.J. and Fry, J.C. 2004. Widespread occurence of a novel division of bacteria identified in 16S rRNA gene sequences originally found in deep marine sediments. *Applied and Environmental Microbiology*, 70pp.5708-5713.
Wegener, G., Shovitri, M., Knittel, K. and Niemann, H. 2008. Biogeochemical processes and microbial diversity of the Gullfaks and Tommeliten methane seeps (Northern North Sea). *Biogeosciences*, 5pp.1127-1144.
Whitman, W.B., Coleman, D.C. and Wiebe, W.J. 1998. Prokaryotes: the unseen majority. *Proceedings of the National Academy of Sciences of the USA*, 95pp.6578-6583.
Wilms, R., Sass, H., Kopke, B., Koster, J., Cypionka, H. and Engelen, B. 2006. Specific bacterial, archaeal and eukaryotic communities in tidal flat sediments along a vertical profile of several metres. *Applied and Environmental Microbiology*, 72pp.2756-2764.
Yakimov, M.,M., Golyshin, P.N., Lang, S., Moore, E.R.B., Abraham, W.R., Lunsdorf, H. and Timmis, K.N. 1998. *Alcanivorax borkumensis* gen. nov., sp. nov., a new hydrocarbon-degrading and surfactant-producing marine bacterium. *International Journal of Systemative Bacteriology*, 48pp.339-348.
Yumoto, I., Hirota, K., Sogabe, Y., Nodasaka, Y., Yokota, Y. and Hoshino, T. 2003. Psychrobacter okhotskensis sp. nov., a lipase-producing facultative psychrophile isolated from the coast of the Okhotsk Sea. *International Journal of Systematic and Evolutionary Microbiology*, 53(6), pp.1985-1989.
Zhou, J., Fries, M.R., Chee-Sanford, J.C. and Tiedje, J.M. 1995. Phylogenetic analysis of a new group of denitrifiers capable of anaerobic growth of toluene and description of *Azoarcus tolulyticus* sp. non. *International Journal of Systematic and Evolutionary Microbiology*, 45pp.500-506.